AD_____

Award Number: DAMD17-98-1-8475

TITLE: Oncolytic Gene Therapy for Prostate Cancer

PRINCIPAL INVESTIGATOR: Theodore L. DeWeese, M.D.

CONTRACTING ORGANIZATION: Johns Hopkins University
Baltimore, Maryland 21205-2196

REPORT DATE: September 2001

TYPE OF REPORT: Annual

PREPARED FOR: U.S. Army Medical Research and Materiel Command
Fort Detrick, Maryland 21702-5012

DISTRIBUTION STATEMENT: Approved for Public Release;
Distribution Unlimited

REPORT DOCUMENTATION PAGE

Form Approved
OMB No. 074-0188

1. AGENCY USE ONLY (Leave blank)	2. REPORT DATE	3. REPORT TYPE AND DATES COVERED
	September 2001	Annual (1 Sep 99 - 31 Aug 01)

4. TITLE AND SUBTITLE
Oncolytic Gene Therapy for Prostate Cancer

5. FUNDING NUMBERS
DAMD17-98-1-8475

6. AUTHOR(S)
Theodore L. DeWeese, M.D.

7. PERFORMING ORGANIZATION NAME(S) AND ADDRESS(ES)
Johns Hopkins University
Baltimore, Maryland 21205-2196

E-Mail: deweete@jhmi.edu

8. PERFORMING ORGANIZATION REPORT NUMBER

9. SPONSORING / MONITORING AGENCY NAME(S) AND ADDRESS(ES)
U.S. Army Medical Research and Materiel Command
Fort Detrick, Maryland 21702-5012

10. SPONSORING / MONITORING AGENCY REPORT NUMBER

11. SUPPLEMENTARY NOTES

12a. DISTRIBUTION / AVAILABILITY STATEMENT
Approved for Public Release; Distribution Unlimited

12b. DISTRIBUTION CODE

13. ABSTRACT ***(Maximum 200 Words)***

The overall objective of this award was to define novel, clinically-translatable strategies of prostate cancer (PCa) treatment based on the use of adenoviral vectors. Areas of overall research accomplishment during the award period have included development of a replication-restricted, PSA-selective oncolytic Ad5 vector (CV706) by incorporation of a minimal promoter enhancer construct (PSE) from the human PSA gene 5' of E1A. Demonstration of *in vitro* and *in vivo* anti-PCa activity by CV706 via apoptosis was noted. Clear evidence of *in vitro* and *in vivo* synergy was seen when CV706 and ionizing radiation are combined. Identification of mechanisms of this synergy were studied and found to include radiation-induced enhancement of viral replication, augmentation of intratumoral apoptosis/necrosis and alteration in vascularization. Pre-clinical studies allowed translation of CV706 to the clinic in Phase I study in men with locally-recurrent PCa following radiation, providing validation of this approach, safety and toxicity assessment, identification of viral replication and anti-tumor activity. Subsequently, we are about to begin Phase I study of CV706 plus radiation in men with newly diagnosed clinically-localized PCa. Final experiments included exploration of Ad5 E4orf6 protein expression as a radiation sensitizer and identification of HIF-1 expression in PCa and its regulation by the PI3K/PTEN/AKT pathway providing rationale for design of gene therapy strategies based on HIF-1 transcription.

14. SUBJECT TERMS	15. NUMBER OF PAGES
Prostate Cancer	75
	16. PRICE CODE

17. SECURITY CLASSIFICATION OF REPORT	18. SECURITY CLASSIFICATION OF THIS PAGE	19. SECURITY CLASSIFICATION OF ABSTRACT	20. LIMITATION OF ABSTRACT
Unclassified	Unclassified	Unclassified	Unlimited

Table of Contents

Introduction

The overall objective of this award was to define novel and clinically-translatable strategies of prostate cancer (PCa) treatment based on the use of adenoviral vectors. Included in this objective were experiments to design/produce a replication-restricted adenovirus with prostate specificity. In addition, *in vitro* and *in vivo* studies were included to determine modes of PCa response to adenoviral infection that explain the potent anti-tumor effects seen as well as to determine novel aspects of adenoviral infection which can be modulated to increase tumor cell death. Ultimately, successful clinical translation of these adenoviruses alone and in combination with standard therapies was sought. Major findings during the award period have included: 1) development of a replication-restricted, PSA-selective oncolytic adenoviral vector (CV706), with prostate selectivity achieved through regulation of the adenoviral E1A gene by incorporation of a minimal promoter enhancer construct (PSE) from the human PSA gene, 2) demonstration of anti-PCa activity by CV706, both *in vitro* and *in vivo*, via an apoptotic process, 3) clear demonstration of synergy, both *in vitro* and *in vivo*, when CV706 and ionizing radiation are combined, 4) identification of mechanisms of synergy between CV706 and radiation, including radiation-induced enhancement of viral replication, augmentation of intratumoral apoptosis and necrosis and alteration in vascularization, 5) clinical translation of CV706 in men with locally-recurrent PCa following radiation therapy, 6) proof of concept in man of this approach, including safety and toxicity assessment, identification of viral replication and anti-tumor activity, 7) planned clinical trial of CV706 plus radiation in men with newly diagnosed clinically-localized PCa, 8) identification of HIF-1 expression in PCa and its regulation by the EGF/PI3K/PTEN/AKT/FRAP pathway, providing rationale for design of gene therapeutic strategies based on HIF-1 transcription, 9) exploration of adenoviral E4orf6 protein expression as a radiation sensitizer.

Body

Important findings of the research supported by this award are listed below. In several areas, reference is made to appendices that provide a complete review and discussion of the relevant data. This report reflects data collected in the laboratory of Dr. Jonathan Simons, the first P.I. of the grant, as well as data collected over the last 12 months in the laboratory of Dr. Theodore DeWeese, who assumed the balance of the award upon the departure of Dr. Simons from the Johns Hopkins University.

Task Number 1.

Sufficient quantities of CV706 (previously named CN706) were prepared to allow for proposed experiments. Using the 293 microtitre system, titers of 1 X 10^{13} particles per ml were produced. Using these stocks, the t1/2 for I.V. bolus injections in animals was determined. In animals with LNCaP and LA-PC4 xenografts, the t1/2 is 1 hour. These data were presented by Dr. Simons at the AACR meeting in 1999. In addition, elements of these results were also presented by Ramakrishna, et al, at the 1999 AACR meeting and are abstracted, in part, in **Appendix 1**. Other studies confirmed that both intratumoral injection as well as intravenous delivery of CV706 resulted in the reduction of PCa xenograft size without evident toxicity.

Other extensive pre-clinical evaluation was performed, including complete animal toxicologic analysis (non-DOD funded). Together, these data supported submission of an IND as well as a protocol for a Phase I trial of intraprostatic CV706 to the FDA and NIH/RAC. Drs. Simons and DeWeese made both written and oral presentations to these organizations and approval for the first clinical translation of a replication-competent adenovirus for PCa therapy was awarded.

Further laboratory experiments determined that certain transcription factors may be particularly well suited as targets for gene therapy vectors like CV706. The Simons laboratory found that HIF-1α was overexpressed in human PCa cell lines and rat cell lines as well (**Appendix 2**). It was proposed that HIF-1α (and others) could serve as a candidate transcription factor for oncolytic vectors. For creation of the oncolytic vectors, Dr. Simons developed a high-throughput screen for calibrating hypoxic gene induction in PCa cell lines. In this analysis, immunhistochemistry of standardly-prepared fixed tissue from a number of anatomic sites, including normal, pre-malignant and cancerous tissue was analyzed. The results revealed that HIF-1α, as well as other genes commonly associated with hypoxia, are upregulated in pre-neoplastic and tumor cells but not in normal tissue. It was proposed that by using affymetrix chips for transcriptional profiling, the baseline levels of non-hypoxia-inducible genes could be determined. In addition, production of tissue microarrays for large-scale immunohistochemical analysis of gene product production was proposed (**Appendix 3-6**).

Task Number 2.

As noted in **Task 1**, preparation of CV706 macrocultures and establishment of PCa xenografts were successfully performed. Evaluation of CV706-induced apoptosis was determined by several methods (including endlabeling and annexin 5). These experiments revealed significant viral mediated apoptosis in PCa xenografts following both intratumoral and intravenous administration of the vector [(**Appendix 7**, both panels reflect CV706-treated LNCaP xenografts, bright cells are apoptotic) and **Appendix 8**].

Importantly, it seems that necrosis is also one of the most important modes of cell death induced by CV706 in the PSA-producing PCa xenograft models used (LNCaP). A complete histologic analysis revealed that the amount of necrosis in tumors treated with CV706 was significantly higher than in control tumors (258.2 ± 80.8 vs. 5.4 ± 2.2, $p < 0.0001$) (**Appendix 8**), indicating that alteration in blood flow may be a very important mechanism of CV706 action.

Evidence from these experiments suggested that treatment of PSA-producing PCa xenografts with CV706 resulted in microinfarctions and decrement in neo-vascularization. Further exploration of these preliminary observations revealed that PCa xenograft treatment with CV706 resulted in a 50% reduction in CD31 positively staining cells as compared to xenografts treated with vehicle alone (14.8 ± 3.9 vs. 33.7 ± 8.2, $p= 0.004$) as well as a significantly reduced number of blood vessels (58.5 ± 3.1 vs. 87.5 ± 6.3) (**Appendix 8**). Together with our earlier work, these data provided the technical expertise for translation of the assays to clinical specimens derived from our Phase I study. Moreover, these assays have continued to be applied in the analysis of tumors collected in our continued pre-clinical analysis of gene therapeutic strategies.

Based on the work detailed above (supported, in part by DOD), as well as that not detailed here (supported by other mechanisms), clinical translation of CV706 was accomplished (funded by Clinical Research Agreement with Calydon, Inc. Sunnyvale, CA). We decided to make the first clinical translation into patients with locally-recurrent PCa following radiation therapy. At present, there is no standard therapy available for these patients and thus, provided an opportunity to develop adenoviral therapies for the disease. The details and results of this Phase I study are available in **Appendix 9**. In brief, CV706 was stereotactically-delivered into the prostate of 20 patients with biopsy-proven, locally recurrent PCa, under real-time ultrasound guidance. Patients received between 1×10^{11} and 1×10^{13} viral particles in cohorts of 3-5 patients, with the dose escalation increasing in half-log increments. Results from the study reveal that CV706 was well tolerated and did not result in either irreversible Grade 3 or any Grade 4 toxicity. We also were able to establish evidence of viral activity with an evident dose-related reduction in serum PSA and evidence of apoptosis on post-treatment biopsy material. We also were able to establish evidence of intraprostatic viral replication by both immunohistochemistry for hexon protein and by identification of intracellular virion by electron microscopy. Finally, we were able to follow viral shedding in the blood (by quantitative PCR of viral DNA) and in the urine, as well as timing of neutralizing antibody production. This work, along with that detailed in **Task 3**, provided the

necessary clinical and laboratory data to allow for intravenous administration of a second generation replication-restricted, PSA-selective oncolytic vector in a Phase I/II study as well as the combination of CV706 + radiation in the definitive management of patients with newly diagnosed, clinically-localized PCa.

Task Number 3.

Dr. Simons' laboratory, in collaboration with Calydon, Inc., assisted in the generation of a PSE-E1A/PSE-E1B regulated oncolytic adenoviral vector. Further development of this virus by Calydon, Inc. resulted in the generation of a replication-restricted oncolytic Ad5 virus with expression of E1A under the control of the probasin promoter (a strong, prostate-specific promoter) and expression of E1B under control of a minimal PSA enhancer-promoter construct. The resultant virus exhibits approximately 100 fold greater specificity for prostate cells when compared to CV706. This virus is now in an industry-sponsored Phase I trial at Johns Hopkins for men with hormone refractory, metastatic PCa.

Further experiments were designed to evaluate and select methods of increasing viral antineoplastic activity, ideally in a fashion that could be clinically translated, as directed by the overall goals of **Task 3** and the award. Preliminary data from our laboratory revealed there to be a supradditive interaction between radiation and CV706 in the treatment of PCa xenografts in nude mice (**Appendix 1**). As radiation is a commonly used, standard therapy for PCa, it seemed logical to explore its use in combination with an oncolytic adenoviral therapy, where the predominant mode of cell death differs from that produced by radiation, where no overlapping toxicity is known to exist and where possible synergy may be produced.

As such, experiments were designed to explore *in vitro* and *in vivo* interactions between radiation and CV706 in the treatment of human PCa cells. When radiation was combined with CV706, our *in vitro* studies revealed that this combination resulted in a reduction in cell viability to < 8% by 10 days after treatment whereas the viability of cells treated with virus alone or radiation alone was reduced to alone 60% at the same time point. There was no statistically significant difference in cell viability in cells treated with virus alone or radiation alone. Isobolograms were generated from the modes to determine the presence of synergy, additivity or antagonism between radiation and CV706. This analysis revealed that the combined data points fell to the left of the envelope of additivity, indicating synergistic activity and cytotoxicity (**Appendix 8**). Given these encouraging results, *in vivo* experiments were designed which similarly revealed that the combination of CV706 and radiation resulted in nearly a 7-fold increase in tumor control relative to that which would be expected if the therapies were merely additive (**Appendix 8**). In an attempt to determine the mechanism(s) of this evident synergy, one-step growth curve experiments were performed. LNCaP cells were treated with virus alone or virus plus radiation and the number of infectious particles was determined on 293 cells by standard plaque assay. These experiments revealed that the combination of radiation and CV706 resulted in the production of about 15-fold more virus, confirming that radiation augments viral replication (**Appendix 8**). Finally,

histopathologic review of treated xenografts consistently revealed that those tumors treated with both radiation and CV706 exhibited statistically-significantly greater necrosis ($p < 0.0001$), apoptosis, and alteration in vascularization as measured by CD31 + cells ($p < 0.0001$) and number of blood vessels counted ($p < 0.01$) (**Appendix 8**).

Given the evident synergy between radiation and CV706 in our pre-clinical models as well as the favorable Phase I results with CV706, we have recently designed a Phase I trial of CV706 and standard, conformal radiation therapy for men with newly diagnosed, clinically-localized PCa. This study has been FDA and NIH RAC reviewed and is in final approval stages at Johns Hopkins, with an anticipated start date of March, 2002.

Recently, data were published which reveal that an adenoviral protein encoded by E4orf6 can disrupt V(D)J recombination by interacting with DNA-PK.(1) This suggested to us the possibility that the E4orf6 protein would disrupt DNA double strand break repair, as is known to occur in mice with disrupted DNA-PK alleles (2) or in cells treated with wortmannin, a drug known to inhibit DNA-PK activity.(3) DNA double strand break repair is critical in the cellular response to ionizing radiation. That is, cells with defective DNA double strand break repair, including cells from the DNA-PK knock-out mice and those treated with wortmannin, are known to be very radiation sensitive. As such, we sought to determine if expression of E4orf6 in a target PCa cell (DU 145) would increase the radiation sensitivity of these cells and would be the first step before design and construction of a vector delivery system. To study this, we transiently transfected DU 145 PCa cells with a plasmid containing both GFP and E4orf6 constructs such that selection of highly expressing cells could be performed by flow cytometry. On this enriched population, we then performed clonogenic survival assays following radiation given at doses between 2 and 10 Gy. Interestingly, we were not able to document any significant radiation sensitization, despite obvious E4orf6 expression identified by SDS-PAGE/immunoblotting and immunohistochemical staining of E4orf6 on cytospins of the GFP-expressing cells used in the clonogenic assays. In order to eliminate the possibility that E4orf6 sensitization might be cell-type specific, we performed the same set of analyses in the RKO human colorectal cell line. In a similar fashion, these experiments failed to reveal any evidence of radiation sensitization by E4orf6 (**Appendix 10**). While these data clearly demonstrate that forced expression of E4orf6 is not a viable gene therapy radiation sensitization strategy, they do add significantly to the literature by suggesting that DNA-PK mediated DNA double strand break repair (requiring inhibition of DNA-PK kinase activity) and the ability to perform V(D)J recombination, also modulated by DNA-PK, are separable events, and that E4 orf6 only modulates V(D)J recombination. These data do, however, provide us with the expertise and experience to conduct further experiments designed to learn if other viral proteins known to modulate DNA-PK activity have radiation sensitizing properties and could be successfully translated to the clinic.

Key Research Accomplishments

- Development of a replication-restricted, PSA-selective oncolytic adenoviral vector (CV706), with prostate selectivity achieved through regulation of the adenoviral E1A gene by incorporation of a minimal promoter enhancer construct (PSE) from the human PSA gene
- Determination of anti-PCa activity by CV706, both *in vitro* and *in vivo*, via both apoptosis and necrosis
- Clear demonstration of synergy, both *in vitro* and *in vivo*, with combination of CV706 and ionizing radiation
- Identification of mechanisms of synergy between CV706 and radiation, including radiation-induced enhancement of viral replication, augmentation of intratumoral apoptosis and necrosis and alteration in vascularization
- Clinical translation of CV706 in men with locally-recurrent PCa following radiation therapy
- Proof-of-concept in man of PSA-selective, replication-restricted, oncolytic adenoviral therapy, including safety and toxicity assessment, identification of viral replication and anti-tumor activity
- Planned clinical trial of CV706 plus radiation in men with newly diagnosed clinically-localized PCa
- Identification of HIF-1 expression in PCa and its regulation by the EGF/PI3K/PTEN/AKT/FRAP pathway, providing rationale for design of gene therapeutic strategies based on HIF-1 transcription
- Exploration of adenoviral E4orf6 protein expression as a radiation sensitizer

Reportable Outcomes

- Manuscripts and Abstracts

  Please see Appendices 1-7.

- patents and licenses applied for and/or issued

  None

- degrees obtained that are supported by this award

  None

- development of cell lines, tissues or serum repositories

  None

- informatics such as databases and animal models, etc.

  None

- funding applied for based on work supported by this award

  None

- employment or research opportunities applied for and/or received on experiences/training supported by this award

  Dr. Hua Zhong, former post-doctoral fellow in the laboratory of Dr. Jonathan Simons. Research performed by Dr. Zhong was funded, in part, by this award. He was successfully recruited as an Assistant Professor in the Department of Medical Oncology at Emory University.

Conclusions

This research has provided important basic and translational data, ideas and concepts to the field of oncolytic gene therapy in general and to the field of prostate cancer gene therapy specifically. Given that tens of thousands of men die from prostate cancer each year and many more suffer from local recurrence of their disease, new and unique therapeutic approaches are in order. As is described in the body of this report, we have made significant strides to this end. Namely, a novel, PSA-selective, replication restricted oncolytic adenovirus, CV706, was constructed, which we have documented kills cells by both apoptotic and necrotic pathways and readily kills human prostate cancer xenografts following both intratumoral and intravenous delivery. In addition, we have shown that CV706 also acts *in vivo* by altering tumor vascularization. Given these data (and animal toxicologic studies not performed under this award), we successful translated this concept and this vector system to the clinic in a Phase I study of men with locally recurrent prostate cancer following radiation.

More recently, our studies have revealed that a significant synergy exists between radiation and CV706 in both *in vitro* and *in vivo* prostate cancer model systems. The complete mechanism of this synergy has not been elucidated, but our studies do indicate that radiation significantly enhances viral replication. These data, combined with our first Phase I clinical data, and the fact that some 40-50% of men receive some form of radiation therapy for their prostate cancer, now support our Phase I study of radiation plus CV706 in the treatment of men with newly diagnosed, clinically-localized prostate cancer. This trial is slated to begin at Johns Hopkins in March, 2002. In addition, given the evident synergy between radiation and adenoviral infection, we have performed other experiments to determine the mechanism of this synergy. To this end, we have completed a thorough evaluation of the adenoviral protein E4orf6, a protein known to abrogate some of the functions of DNA-PK, including V(D)J recombination and certain components of DNA double strand break repair. Our data reveal that forced intracellular expression of E4orf6 in human prostate cancer and colorectal cancer cells does not increase cellular radiation sensitivity. However, these data have provided us the expertise and reagents necessary to explore other viral proteins known to alter DNA-PK function in an attempt to identify clinically-translatable concepts for viral mediated alteration of radiation response.

Other important findings from this work have included the discovery that the HIF-1α gene, important in the field of hypoxia, is overexpressed in prostate cancer (and other cancers as well). This and other transcription factors that are differentially expressed in prostate cancer as compared to normal prostate could be used for development of Ad5 vectors for prostate cancer. Others have considered using hypoxia-inducible constructs with suicide gene therapy, showing *in vitro* and *in vivo* activity. Together, the data generated have enhanced our ability to successfully translate adenoviral gene therapy concepts to the clinic in Phase I studies and have provide new avenues of research which hold the promise for future development, particularly as adjuncts with more traditional therapies like radiation and cytotoxic drugs.

References

(1) Boyer, J., Rohleder, K., Ketner, G. Adenovirus E4 34k and E4 11k inhibit double strand break repair and are physically associated with the cellular DNA-dependent protein kinase. *Virology* **263**: 307-312, 1999.

(2) Blunt, T., Finnie, N.J., Taccioli, G.E., et al. Defective DNA-dependent protein kinase activity is linked to V(D)J recombination and DNA repair defects associated with the murine scid mutation. *Cell* **80**: 813-823, 1999.

(3) Chernikova, S.B., Wells, R.L., Elkind, M.M. Wortmannin sensitizes mammalian cells to radiation by inhibiting the DNA-dependent protein kinase-mediated rejoining of double-strand breaks. *Radiation Res.* **151**: 159-166, 1999.

Appendices

Appendix 1 - Proceedings of the American Association for Cancer Research Vol 40, Abstract #4156, March 1999

Appendix 2 - Proceedings of the American Association for Cancer Research Vol 40, Abstract #2181, March 1999

Appendix 3 - Cancer Research Vol 60, 1541-1545, March 15, 2000

Appendix 4 - Biochemical and Biophysical Research Communications Vol 284, 352-356, 2001

Appendix 5 - Cancer Research Vol 59, 5830-5835, November 15, 1999

Appendix 6 - Cancer Research Vol 58, 5280-5284, December 1, 1998

Appendix 7 - Figures

Appendix 8 - Cancer Research Vol 61, 5453-5460, July 15, 2001

Appendix 9 - Cancer Research Vol 61, 7464-7472, October 15, 2001

Appendix 10 - Int J Radiation Onc Biol Phys, Submitted 1/2002

Proceedings of the American Association for Cancer Research, Vol. 40, March 1999

#4156 Synergism of ionizing radiation and gene therapy with the replication competent CN706 adenovirus in the LAPC-4 prostate cancer cell line.
Ramakrishna, N.R., Rioseco-Camacho, N., Sawyers, C.L., Yu, D.C., Henderson, D., Simons, J.W., and DeWeese, T.L. *The Johns Hopkins University Oncology Center, Baltimore, MD 21287; University of California Los Angeles School of Medicine, Los Angeles, CA 90095 and Calydon Corporation, Sunnyvale, CA 94025.*

A replication competent adenovirus CN706 preferentially replicates in PSA-positive prostate cancer cells. This vector is being tested in a phase I clinical trial utilizing stereotactic intraprostatic injection. We tested whether the efficacy might be augmented by combining cytoreductive gene therapy using CN706 with ionizing radiation in the PSA-positive LAPC-4 prostate cancer cell line. XRT was administered to LAPC-4 cells in doses of 1–4 Gy prior to or following viral infection with 0.1–10 moi of CN706. The combined effects of XRT and virus on cell growth were measured with a growth inhibition assay. Infection of the androgen receptor wild-type LAPC-4 cells with CN706 results in dose dependent growth inhibition and cell death. The use of virus alone or XRT alone resulted in decreased cell ATP to approximately 35% of that seen in untreated controls at 10 days post-infection. The combination of XRT and virus resulted in a decrease in cell ATP to approximately 8% of the untreated controls. The effect of the combination of radiation and viral infection on growth inhibition was approximately 35% greater than expected if the actions of both agents were purely additive. These data suggest that a combination of radiation and oncolytic virus may result in synergistic tumoricidal effects. Isobologram analyses and further experiments are underway to determine the underlying mechanisms for this interaction.

Proceedings of the American Association for Cancer Research, Vol. 40, March 1999

#2181 Expression of hypoxia-inducible factor 1α in human prostate cancer. Zhong, H., Semenza, G.L., Agani, F., Laughner, E., Isaacs, W.B., and Simons, J.W. *Johns Hopkins University School of Medicine, Baltimore, MD 21287.*

Solid tumors often have abnormal blood supply and hypoxic regions. Hypoxia-inducible factor 1 (HIF-1) is a critical transcription factor that regulates genes involved in adaptation to hypoxia. Recent studies suggest the involvement of HIF-1 in tumor progression. In the present study, HIF-1α expression was evaluated in human prostatic cancer (PCA) cell lines and PCA tissues in the levels of mRNA and protein. Hypoxia (1% O_2) induced expression of HIF-1α protein and HIF-1 DNA-binding activity was found in 5 human PCA cell lines tested. The transcription of HIF-1 regulated genes (LDH-A and Eno-1) were also shown in upregulated levels under hypoxia. Using ribonuclease protection assay, the mean of HIF-1α mRNA level exhibited a moderate increase in 14 PCA samples (24.120±15.248) compared to in 10 normal prostate tissues (17.788±10.221). Five of the eight tumor/normal pairs presented increase in the amount of HIF-1α mRNA compared to the respective normal tissues (23.818±8.237/ 18.999±8.836). However, HIF-1α protein was identified in the cultured normoxic and hypoxic PC-3 cells, all 5 xenografts tested as well as surgical samples of human PCA (6/7) by immunohistochemistry but not in normal human prostate tissues (0/5). Within tumors, HIF-1α positive cells displayed striking localization to the tumor margins, the periphery of necrotic regions, and surrounding areas of neovascularization. In most cases, the magnitude of HIF-1α expression was consistent with the Ki67 index. This pilot data provides the first *in vivo* evidence of HIF-1α expression in human cancer cells. The results suggest that HIF-1α may play a critical role in tumor formation, proliferation, neovascularization, and metastatic progression.

[CANCER RESEARCH 60, 1541–1545, March 15, 2000]

Advances in Brief

Modulation of Hypoxia-inducible Factor 1α Expression by the Epidermal Growth Factor/Phosphatidylinositol 3-Kinase/PTEN/AKT/FRAP Pathway in Human Prostate Cancer Cells: Implications for Tumor Angiogenesis and Therapeutics[1]

Hua Zhong, Kelly Chiles, David Feldser, Erik Laughner, Colleen Hanrahan, Maria-Magdalena Georgescu, Jonathan W. Simons,[2] and Gregg L. Semenza

The Johns Hopkins Oncology Center, Brady Urological Institute [H. Z., C. H., J. W. S.] and Departments of Pediatrics and Medicine and Institute of Genetic Medicine [K. C., D. F., E. L., G. L. S.], The Johns Hopkins University School of Medicine, Baltimore, Maryland 21287, and Laboratory of Molecular Oncology, The Rockefeller University, New York, New York 10021 [M-M. G.]

Abstract

Dysregulated signal transduction from receptor tyrosine kinases to phosphatidylinositol 3-kinase (PI3K), AKT (protein kinase B), and its effector FKBP-rapamycin-associated protein (FRAP) occurs via autocrine stimulation or inactivation of the tumor suppressor PTEN in many cancers. Here we demonstrate that in human prostate cancer cells, basal-, growth factor-, and mitogen-induced expression of hypoxia-inducible factor 1 (HIF-1) α, the regulated subunit of the transcription factor HIF-1, is blocked by LY294002 and rapamycin, inhibitors of PI3K and FRAP, respectively. HIF-1-dependent gene transcription is blocked by dominant-negative AKT or PI3K and by wild-type PTEN, whereas transcription is stimulated by constitutively active AKT or dominant-negative PTEN. LY294002 and rapamycin also inhibit growth factor- and mitogen-induced secretion of vascular endothelial growth factor, the product of a known HIF-1 target gene, thus linking the PI3K/PTEN/AKT/FRAP pathway, HIF-1, and tumor angiogenesis. These data indicate that pharmacological agents that target PI3K, AKT, or FRAP in tumor cells inhibit HIF-1α expression and that such inhibition may contribute to therapeutic efficacy.

Introduction

Tumor progression involves the selection of cells with somatic mutations that activate oncogenes and inactivate tumor suppressor genes. These mutations have the effect of driving cells through the cell cycle in an uncontrolled manner and preventing apoptosis. Two adaptations that are universal characteristics of solid tumors, indicating that they are necessary for tumor progression, are increased glycolytic metabolism and angiogenesis (reviewed in Ref. 1). These adaptations are also driven by genetic alterations in tumor cells, but their molecular basis has remained obscure. Loss of function mutations in tumor suppressor genes or activating mutations in oncogenes have been shown to dysregulate signal transduction pathways leading from growth factors (such as EGF[3]) and their cognate receptor tyrosine kinases to PI3K, which catalyzes the conversion of phosphatidylinositol 4-phosphate, and phosphatidylinositol 4,5-biphosphate to phosphatidylinositol 3,4-biphosphate and phosphatidylinositol 3,4,5-triphosphate, respectively (reviewed in Ref. 2). These products are allosteric activators of phosphatidylinositol-dependent kinase 1, which phosphorylates and activates AKT (protein kinase B). Targets of AKT include BAD, an inhibitor of apoptosis, and FRAP, an activator of $p70^{s6k}$, which is required for ribosomal biogenesis and cell cycle progression (reviewed in Ref. 2). These findings have delineated mechanisms by which the PI3K/AKT pathway promotes cell proliferation and inhibits cell death. This pathway is negatively regulated by PTEN, which dephosphorylates phosphatidylinositol 3,4-biphosphate and phosphatidylinositol 3,4,5-triphosphate (reviewed in Ref. 2). In PCA, PTEN loss of function correlates with increased angiogenesis and appears to be critical for progression to hormone-refractory metastatic disease (3–6). However, the basis for these correlations has not been determined. The role of HIF-1 as an essential transcriptional activator of genes encoding glucose transporters, glycolytic enzymes, and VEGF is well established (reviewed in Ref. 7). In this study, we demonstrate that modulation of the EGF/PI3K/AKT/FRAP pathway alters the expression of HIF-1α protein, HIF-1-dependent transcriptional activity, and VEGF protein in human PCA cells. These results provide a mechanism contributing to the overexpression of HIF-1α in PCA and other solid cancers (8) and have important implications regarding cancer progression and therapy.

Materials and Methods

Tissue Culture. The human PCA cell lines DU145, PC-3, PPC-1, and TSU were maintained in RPMI 1640 supplemented with 10% heat-inactivated FBS (complete media). Cells were exposed to hypoxia as described previously (9–11).

Immunoblot Assays. Cells ($0.5–1.0 \times 10^6$) were seeded onto 150-mm tissue culture dishes (Falcon) and incubated for 36–48 h in complete media (except for AKT assays, in which cells were plated directly in media with 0.1% FBS). The cells were incubated in media with 0–0.1% FBS for 24 h and then given fresh media with 0–0.1% FBS alone or with 10% FBS, EGF (Life Technologies, Inc.), PMA, or 4α-PMA, either alone or with LY294002, PD098059, rapamycin, or wortmannin (Alexis Corp.), for 6–8 h. For analysis of HIF-1α expression, nuclear extracts were prepared, and aliquots were analyzed using monoclonal antibody H1α67 (Novus Biologicals, Inc.) as described previously (8). Blots were stripped and incubated with anti-topoisomerase 1 antibodies (TopoGEN). Aliquots of whole cell lysates were subjected to immunoblot assay using anti-AKT and phospho-AKT antibodies (New England Biolabs). All immunoblots were developed using enhanced chemiluminescence reagents (Amersham).

Transient Transfection Assays. DU145 cells were seeded onto 24-well culture plates at a density of 4×10^4 cells/well and incubated for 24 h in complete media. The cells were transfected with 12.5 ng of control plasmid pTK-RL (Promega) containing the herpes simplex virus thymidine kinase promoter and *Renilla reniformis* (sea pansy) luciferase coding sequences; 100 ng of reporter plasmid p2.1 containing a 68-bp hypoxia response element from the *ENO1* gene, an SV40 promoter, and *Photinus pyralis* (firefly) luciferase

Received 12/2/99; accepted 2/3/00.

The costs of publication of this article were defrayed in part by the payment of page charges. This article must therefore be hereby marked *advertisement* in accordance with 18 U.S.C. Section 1734 solely to indicate this fact.

[1] Supported by NIH Prostate Cancer SPORE Grant CA-58236; NIH Grant RO1-HL55338 and Children's Brain Tumor Foundation (to G. L. S.); AEGON Gift for Accelerated Breast and Prostate Cancer Research, CaP CURE Foundation, and Department of Defense Grant DAMD 17-98-1-8475 (to J. W. S.).

[2] To whom requests for reprints should be addressed, at Brady Urological Institute, Marburg 409, Johns Hopkins Hospital, 600 North Wolfe Street, Baltimore, MD 21287-2411.

[3] The abbreviations used are: EGF, epidermal growth factor; PI3K, phosphatidylinositol 3-kinase; FRAP, FKBP-rapamycin-associated protein; PCA, prostate cancer; HIF-1, hypoxia-inducible factor 1; VEGF, vascular endothelial growth factor; FBS, fetal bovine serum; IGF, insulin-like growth factor; PMA, phorbol 12-myristate 13-acetate.

coding sequences (12); and 500 ng of pCEP4 (Invitrogen) or expression vector encoding AKT-MYR, AKT (K179M), wild-type PTEN, PTEN (C124S), or p85Δ (13–16). KD-AKT, C124S PTEN, and p85Δ have each been shown to have dominant negative effects in cells expressing the respective wild-type protein. Cells were exposed to plasmid DNA for 8 h in 1 μl of Fugene-6 (Boehringer Mannheim). Cells were then incubated in DMEM with 0.1% FBS for 16 h, followed by exposure to 10% FBS, 100 nM PMA, and 1% O_2 or no treatment for 24 h. Cells were lysed in 100 μl of buffer, and Dual-Luciferase (Promega) reporter assays were performed on 20-μl aliquots.

VEGF ELISA Assays. TSU cells were seeded onto 6-well culture plates at a density of 4×10^4 cells per well, incubated for 24 h in complete media, and then given serum-free media for 16 h, followed by fresh serum-free media, either alone or with 10% FBS, EGF, or PMA alone or with LY294002 or rapamycin, for 24 h. Conditioned media were removed for storage at −80°C, and cells were counted. VEGF protein concentration in the media was determined by ELISA using a commercial kit (R&D Systems).

Results

We demonstrated previously that human PCA lines, most notably PC-3 cells, express HIF-1α protein and HIF-1 DNA-binding activity under nonhypoxic conditions, and expression is further increased in response to hypoxia (11). Potential clinical implications of these findings were underscored by the immunohistochemical demonstration that HIF-1α is overexpressed (relative to adjacent normal tissue) in common human solid tumors, including PCA (8). HIF-1α expression was also induced in transformed cells exposed to EGF, fibroblast growth factor 2, IGF-1, or IGF-2 (10). Because of the known role of EGF signaling via the PI3K pathway (reviewed in Ref. 2), we investigated whether up-regulation of this pathway contributed to increased HIF-1α expression in PCA cells. As an initial means of modulating the activity of this pathway, we examined the effect of serum starvation and stimulation. TSU, PC-3, DU145, and PPC-1 cells were cultured at low density in serum-free medium for 24 h and then exposed to 0% or 10% FBS for 6 h. All four cell lines demonstrated some degree of HIF-1α expression under serum-free conditions that increased in response to serum stimulation (Fig. 1*A*). To examine responses to specific mitogens, cells were exposed to 100 nM PMA or 20 ng/ml EGF. PMA strongly induced HIF-1α expression in DU145, TSU, and PPC-1 cells (Fig. 1*B*). Exposure of TSU cells to 20 ng/ml EGF also markedly induced HIF-1α expression, whereas the effect of EGF on DU145 and PPC-1 cells was more modest. In DU145 and TSU cells, similar levels of HIF-1α expression were induced by exposure to PMA or hypoxia, whereas the biologically inactive 4α-PMA had no effect (Fig. 1*C*).

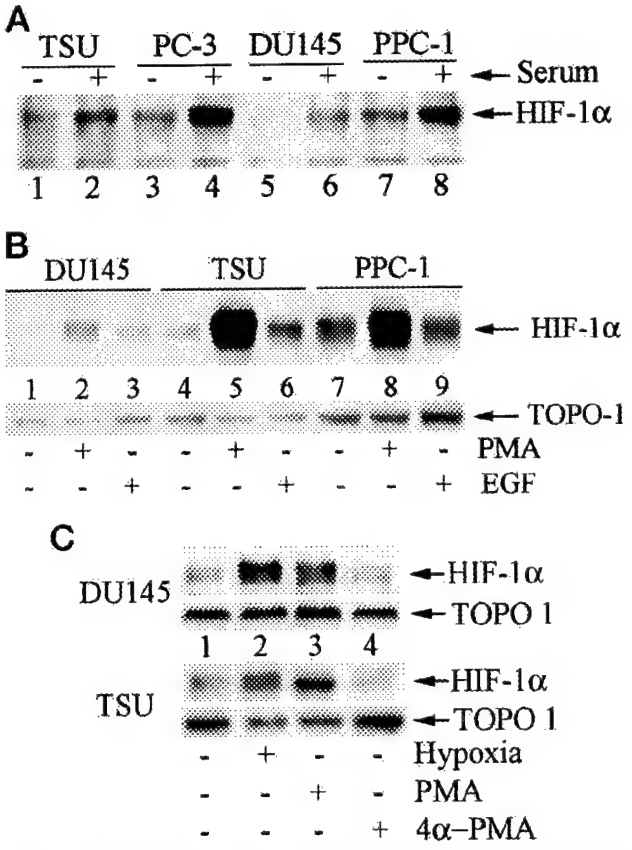

Fig. 1. Induction of HIF-1α expression in PCA cells exposed to serum, PMA, EGF, or hypoxia. *A*, effect of serum starvation and stimulation. Cells were cultured in serum-free media for 24 h and then incubated in media containing 0% or 10% FBS for 6 h before immunoblot assay using an anti-HIF-1α monoclonal antibody. *B*, effect of PMA and EGF stimulation. Cells cultured in media containing 0.1% FBS for 24 h were untreated (*Lanes 1, 4,* and *7*) or exposed to 100 nM PMA (*Lanes 2, 5,* and *8*) or 20 ng/ml EGF (*Lanes 3, 6,* and *9*) for 8 h before immunoblot assay for HIF-1α (*top panel*). The blot was then stripped and assayed for topoisomerase I (*bottom panel*) as a control for sample loading and transfer. *C*, effect of hypoxia and PMA. DU145 (*top panels*) and TSU (*bottom panels*) cells cultured in media containing 0.1% FBS for 20 h were untreated (*Lane 1*) or exposed to 1% O_2 (*Lane 2*), 100 nM PMA (*Lane 3*), or 100 nM 4α-PMA (*Lane 4*) for 8 h before HIF-1α and topoisomerase I immunoblot assays.

To determine whether PI3K pathway activity was required for HIF-1α expression, PCA cells were exposed to LY294002 or wortmannin, inhibitors of PI3K, or to rapamycin, an inhibitor of FRAP (17), a signaling molecule downstream of PI3K (Fig. 2*A*). PC-3 cells were cultured in 0.1% FBS in the presence of varying concentrations of LY294002 under hypoxic (1% O_2) or nonhypoxic (20% O_2) conditions. HIF-1α expression under nonhypoxic conditions was partially inhibited by 1 μM LY294002 and completed inhibited by 10 μM LY294002 (Fig. 2*B, top panel*). In contrast, hypoxia-induced HIF-1α expression was only partially inhibited by 10 μM LY294002 and was more completely inhibited by 50 μM LY294002. Wortmannin was a more potent inhibitor in nonhypoxic cells because partial inhibition and complete inhibition of HIF-1α expression were observed in the presence of 10 and 100 nM wortmannin, respectively, in nonhypoxic cells, whereas only modest inhibition was observed with 200 nM wortmannin in hypoxic cells (Fig. 2*B, middle panel*). Rapamycin was the most potent drug tested; it inhibited HIF-1α expression at concentrations of 10 and 50 nM in nonhypoxic and hypoxic cells, respectively (Fig. 2*B, bottom panel*). Induction of HIF-1α expression in PC-3 or TSU cells exposed to either 10% FBS, 100 nM PMA, or 20 ng/ml EGF was completely inhibited by 50 μM LY294002 (Fig. 2*C*). PMA-induced HIF-1α expression was completely inhibited in the presence of 10 μM LY294002 or 10 nM rapamycin (data not shown). Under the experimental conditions used, none of the inhibitors caused cell death during the study period as determined by analysis of cellular ATP concentration, morphology, or trypan blue exclusion (data not shown). Taken together, these results suggest that basal and mitogen-induced HIF-1α expression in PCA cells is highly dependent on PI3K activity, whereas other signaling pathways stimulate hypoxia-induced expression.

AKT lies between PI3K and FRAP in this signaling pathway (Fig. 2*A*). In TSU cells cultured in serum-free media, a modest degree of AKT phosphorylation was detected, which increased in response to EGF stimulation (Fig. 3, *top panel, Lanes 1* and *2*). These data are consistent with previous reports of EGF-stimulated AKT activity in PCA cells (18, 19). Both basal and EGF-induced AKT phosphorylation were blocked by LY294002 (*Lane 3*). In contrast, the mitogen-activated protein kinase/extracellular signal-regulated kinase (MEK) inhibitor PD098059 (Fig. 2*A*) had no inhibitory effect (Fig. 3, *top panel, Lane 4*), suggesting that mitogen-activated protein kinase activity is not required in these cells. In PC-3 cells, which show the highest level of HIF-1α expression under nonhypoxic conditions (Fig.

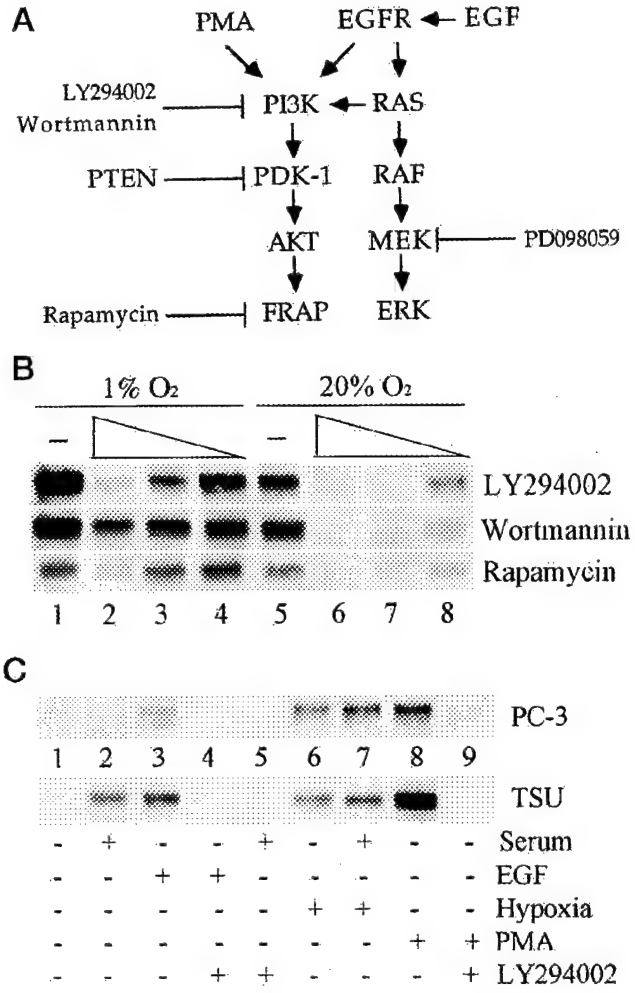

Fig. 2. Effect of pharmacologic inhibitors on HIF-1α exprssion. *A*, relevant signal transduction pathways activated by EGF and PMA. *B*, effect of PI3K and FRAP inhibitors on basal and hypoxia-induced HIF-1α expression. PC-3 cells were cultured in media containing 0.1% FBS for 20 h, followed by the addition of LY294002 (0, 50, 10, or 1 μM), wortmannin (0, 200, 100, or 10 nM), or rapamycin (0, 50, 10, or 1 nM) and incubation in 1% (*Lanes 1–4*) or 20% (*Lanes 5–8*) O_2 for 8 h before HIF-1α immunoblot assay. *C*, effect of PI3K inhibition on serum-, EGF-, and PMA-induced HIF-1α expression. PC-3 and TSU cells were incubated in media containing 0.1% FBS for 24 h and then exposed to 10% FBS, 20 ng/ml EGF, 100 nM PMA, or 1% O_2 in the presence or absence of 50 μM LY294002 for 6 h before HIF-1α immunoblot assay.

1*A*; Ref. 11), the extent of AKT phosphorylation was even greater than that in TSU cells but was nevertheless completely blocked by treatment with LY294002 (Fig. 3, *top panel, Lanes 5* and *6*), whereas treatment with rapamycin (which inhibits the pathway downstream of AKT) or PD098059 had no inhibitory effect (*Lanes 7* and *8*). Hypoxia had no effect on AKT phosphorylation in PC-3 cells (*Lanes 9–12*). Total AKT protein levels were not affected by EGF, LY294002, PD098059, or hypoxia (Fig. 3, *bottom panel*).

To determine whether PI3K pathway activity affects HIF-1-mediated gene transcription, DU145 cells were cotransfected with the reporter gene p2.1 (12) containing a 68-bp hypoxia response element from the promoter of the human *ENO1* gene (which encodes the glycolytic enzyme enolase) and expression vectors encoding wild-type or mutant components of the PI3K pathway. Reporter gene activity increased 2.4-fold in response to PMA stimulation (Fig. 4*A*) in the presence of empty expression vector. In contrast, reporter gene activity was below basal levels in PMA-stimulated cells transfected with vector encoding KD-AKT, a catalytically-inactive (kinase-dead) form of AKT containing a K179M missense mutation (14); wild-type PTEN; or p85Δ, a dominant-negative form of the PI3K p85 regulatory subunit (16). Reporter activity was induced 17-fold by hypoxia, and this response was partially inhibited by KD-AKT, wild-type PTEN, or PI3K-p85Δ (Fig. 4*B*). These results, which are consistent with the effects of the PI3K inhibitor LY294002 on HIF-1α expression reported above (Fig. 2), demonstrate that PI3K and PTEN-regulated AKT activity are required for HIF-1-mediated transcription in response to PMA.

To determine whether activation of the PI3K pathway was sufficient to activate HIF-1-mediated gene transcription, DU145 cells that express wild-type PTEN (5) were cotransfected with reporter p2.1 and expression vectors encoding AKT-MYR, a myristoylated and constitutively active form of AKT (13), or a catalytically inactive form of PTEN containing a C124S missense mutation. The transfected cells were incubated in 10% FBS (Fig. 4*C*), 0.1% FBS (Fig. 4*D*), or 0.1% FBS with 100 nM PMA (Fig. 4*E*). Under all three conditions, both constitutively active AKT and dominant-negative PTEN induced reporter gene expression, with the greatest response observed in PMA-stimulated cells.

To demonstrate that the PI3K-mediated induction of HIF-1 transcriptional activity results in biological activity, the secretion of VEGF protein by TSU cells was analyzed by ELISA. Cells were serum-starved for 6 h and then exposed to no treatment, 10% FBS, 50 nM PMA, or 20 ng/ml EGF for 24 h. Despite the short incubation time, FBS, PMA, and EGF each increased VEGF protein levels in the tissue culture supernatant, and PMA resulted in the greatest induction (Fig. 4*F*), as was also observed with respect to HIF-1α expression (Fig. 1). Treatment with low concentrations of either LY294002 (10 μM) or rapamycin (10 nM) markedly inhibited the induction of VEGF expression by FBS, PMA, or EGF (Fig. 4*F*), similar to the effect of these inhibitors on mitogen-induced HIF-1α expression (Fig. 2). Thus, both HIF-1α-dependent gene transcription (Fig. 4, *A–E*) and the expression of a HIF-1-regulated gene product (Fig. 4*F*) are modulated by the activity of the PI3K/AKT/FRAP pathway in PCA cells.

Discussion

In this study, we demonstrate that activation of the PI3K/PTEN/AKT/FRAP pathway by EGF, PMA, serum, or autocrine stimulation results in increased expression of HIF-1α protein, HIF-1 transcriptional activity, and VEGF protein expression in PCA cells. HIF-1α protein expression is regulated by ubiquitination and proteasomal degradation (reviewed in Ref. 7). Additional studies are required to determine whether this process is modulated by PI3K/AKT/FRAP activity and, if so, whether such modulation involves direct phosphorylation of HIF-1α.

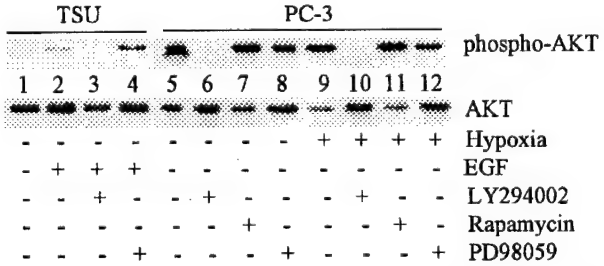

Fig. 3. Analysis of AKT phosphorylation. TSU and PC-3 cells cultured in serum-free media for 24 h were untreated or exposed to 20 ng/ml EGF, 50 μM LY294002, 20 nM rapamycin, or 100 μM PD098059 under nonhypoxic (20% O_2) or hypoxic (1% O_2) conditions as indicated for 8 h before immunoblot assay using antibodies against phosphorylated (*top panel*) or total (*bottom panel*) AKT protein.

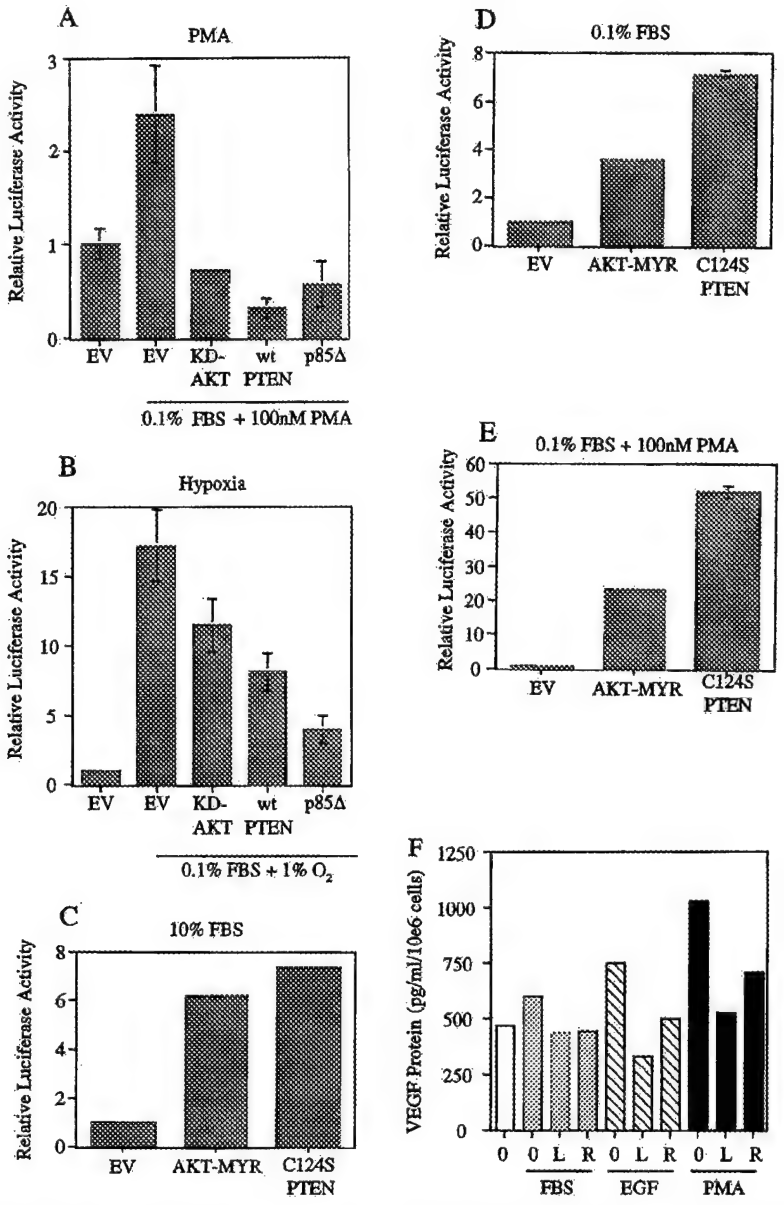

Fig. 4. Effect of altered PI3K, PTEN, or AKT activity on HIF-1-dependent gene expression. *A–E*, DU145 cells were cotransfected with a control plasmid containing the HSV TK promoter upstream of *Renilla* luciferase coding sequences, a reporter plasmid containing a hypoxia response element upstream of a SV40 promoter and firefly luciferase coding sequences, and expression vector containing no insert (*EV*) or cDNA encoding catalytically inactive (kinase-dead; *KD*) or constitutively active (myristoylated; *MYR*) AKT, wild-type (wt) or mutant (C124S) PTEN, or a deleted form of the p85 subunit of PI3K (*p85Δ*). Eight h after transfection, the cells were incubated in 10% (*C*) or 0.1% (*D*) FBS for 16 h and then harvested, or serum-deprived cells were exposed to PMA (*A* and *E*) or 1% O_2 (*B*) for an additional 24 h. For each sample, the ratio of firefly to *Renilla* luciferase was determined and normalized to the value obtained from untreated cells transfected with empty vector (*EV*) to generate the relative luciferase activity. Data represent the mean and SE for three independent transfections. Note that the scale of the *y* axis differs between graphs. *F*, VEGF protein secretion by TSU cells. After 16 h of serum starvation, cells were untreated (□) or exposed to 10% FBS (▨), 20 ng/ml EGF (▧), or 50 nM PMA (■) for 24 h, either alone (*O*) or in the presence of 10 μM LY294002 (*L*) or 10 nM rapamycin (*R*). VEGF protein concentrations in conditioned media were determined by ELISA and corrected for cell number. Each *bar* represents the mean of VEGF concentrations from duplicate plates of cells, which differed by ≤20% in all cases.

These results provide a molecular basis for the previously reported expression of HIF-1α under nonhypoxic conditions in PCA cells (11). It is likely that, *in vivo*, increased activity of the PI3K pathway contributes to the dramatic overexpression of HIF-1α in PCA and other human cancers (8). The tumor suppressor PTEN, which negatively regulates the PI3K pathway, is a target for mutation in PCA, breast cancer, gliomas, and other tumor types (3–6, 19–21). In PCA, inactivation of PTEN expression is associated with disease progression and angiogenesis (3, 4). It is well established that HIF-1 activates genes encoding glucose transporters, glycolytic enzymes, heme oxygenase-1, IGF-2, IGF-binding proteins, inducible nitric oxide synthase, transferrin, and VEGF, all of which have been implicated in tumor progression (reviewed in Ref. 7). In particular, the association between PTEN loss of function and angiogenesis may be explained by the induction of HIF-1α, leading to increased VEGF expression. Colon cancer cells transfected with a HIF-1α expression vector demonstrated increased VEGF mRNA expression as well as increased growth and angiogenesis of tumor xenografts (22).

In addition to PTEN, loss of function mutations in tumor suppressor

genes encoding VHL (23) and p53 (8, 22) result in increased expression of HIF-1α and VEGF. Gain of function mutations in oncogenes also induce HIF-1α expression, as demonstrated for v-*src* (24) and inferred for autocrine activation of EGF and IGF-I receptors, based on the results presented above and in previous studies (9, 10). Induction of transcription via the *VEGF* gene promoter by activated H-RAS also requires PI3K/AKT activity and an intact HIF-1 binding site (16). Thus, V-SRC, H-RAS, and receptor tyrosine kinases all lead to increased activity of both the PI3K/AKT pathway (2, 18, 19, 25) and HIF-1.

Several conclusions can be drawn from the available data. First, in human tumors, increased expression of HIF-1α is induced by genetic alterations as well as by physiological stimulation. Second, expression of HIF-1 may play a major role in promoting angiogenesis and metabolic adaptation in PCA and other common solid tumors. In addition to the data regarding the effects of increased HIF-1α expression cited above, loss of HIF-1 expression in tumor cells is associated with decreased xenograft growth and angiogenesis (24, 26). Third, whereas genetic alterations affecting signal transduction pathways are highly variable among human tumors, increased expression of HIF-1α may represent a common final pathway. Fourth, if HIF-1 mediated angiogenesis and metabolic adaptation play important roles in tumor progression, as suggested by previous studies (7, 8, 22–24, 26), then pharmacological inhibition of HIF-1 activity may represent a useful treatment strategy. Furthermore, the effect of PI3K/AKT/FRAP pathway inhibitors on HIF-1α expression may provide a basis for therapeutic efficacy.

Acknowledgments

We are grateful to Naheed Ahmed, Tung Chan, and Philip Tsichlis for AKT expression vectors and to Amato Giaccia for the p85Δ expression vector. We thank Kimberly Heaney for technical assistance.

References

1. Dang, C. V., and Semenza, G. L. Oncogenic alterations of metabolism. Trends Biochem. Sci., *24:* 68–72, 1999.
2. Cantley, L. C., and Neel, B. G. New insights into tumor suppression: PTEN suppresses tumor formation by restraining the phosphoinositide 3-kinase/AKT pathway. Proc. Natl. Acad. Sci. USA, *96:* 4240–4245, 1999.
3. Giri, D., and Ittmann, M. Inactivation of the PTEN tumor suppressor gene is associated with increased angiogenesis in clinically localized prostate carcinoma. Hum. Pathol., *30:* 419–424, 1999.
4. McMenamin, M. E., Soung, P., Perera, S., Kaplan, I., Loda, M., and Sellers, W. R. Loss of PTEN expression in paraffin-embedded primary prostate cancer correlates with high Gleason score and advanced stage. Cancer Res., *59:* 4291–4296, 1999.
5. Wu, X., Senechal, K., Neshat, M. S., Whang, Y. E., and Sawyers, C. L. The PTEN/MMAC1 tumor suppressor phosphatase functions as a negative regulator of the phosphoinositide 3-kinase pathway. Proc. Natl. Acad. Sci. USA, *95:* 15587–15591, 1998.
6. Suzuki, H., Freije, D., Nusskern, D. R., Okami, K., Cairns, P., Sidransky, D., Isaacs, W. B., and Bova, G. S. Interfocal heterogeneity of *PTEN/MMAC1* gene alterations in multiple metastatic prostate cancer tissues. Cancer Res., *58:* 204–209, 1998.
7. Semenza, G. L. Regulation of mammalian O_2 homeostasis by hypoxia-inducible factor 1. Annu. Rev. Cell Dev. Biol., *15:* 551–578, 1999.
8. Zhong, H., De Marzo, A. M., Laughner, E., Lim, M., Hilton, D. A., Zagzag, D., Buechler, P., Isaacs, W. B., Semenza, G. L., and Simons, J. W. Overexpression of hypoxia-inducible factor 1α in common human cancers and their metastases. Cancer Res., *59:* 5830–5835, 1999.
9. Agani, F., and Semenza, G. L. Mersalyl is a novel inducer of vascular endothelial growth factor gene expression and hypoxia-inducible factor 1 activity. Mol. Pharmacol., *54:* 749–754, 1998.
10. Feldser, D., Agani, F., Iyer, N. V., Pak, B., Ferreira, G., and Semenza, G. L. Reciprocal positive regulation of hypoxia-inducible factor 1α and insulin-like growth factor 2. Cancer Res., *59:* 3915–3918, 1999.
11. Zhong, H., Agani, F., Baccala, A. A., Laughner, E., Rioseco-Camacho, N., Isaacs, W. B., Simons, J. W., and Semenza, G. L. Increased expression of hypoxia-inducible factor-1α in rat and human prostate cancer. Cancer Res., *58:* 5280–5284, 1998.
12. Semenza, G. L., Jiang, B-H., Leung, S. W., Passantino, R., Concordet, J-P., Maire, P., and Giallongo, A. Hypoxia response elements in the aldolase A, enolase 1, and lactate dehydrogenase A gene promoters contain essential binding sites for hypoxia-inducible factor 1. J. Biol. Chem., *271:* 32529–32537, 1996.
13. Ahmed, N. N., Grimes, H. L., Bellacosa, A., Chan, T. O., and Tsichlis, P. N. Transduction of interleukin-2 antiapoptotic and proliferative signals via Akt protein kinase. Proc. Natl. Acad. Sci. USA, *94:* 3627–3632, 1997.
14. Franke, T. F., Yang, S-I., Chan, T. O., Datta, K., Kazlaukas, A., Morrison, D. K., Kaplan, D. R., and Tsichlis, P. N. The protein kinase encoded by the Akt proto-oncogene is a target of the PDGF-activated phosphatidylinositol 3-kinase. Cell, *81:* 727–736, 1995.
15. Georgescu, M-M., Kirsch, K. H., Akagi, T., Shishido, T., and Hanafusa, H. The tumor-suppressor activity of PTEN is regulated by its carboxyl-terminal domain. Proc. Natl. Acad. Sci. USA, *96:* 10182–10187, 1999.
16. Mazure, N. M., Chen, E. Y., Laderoute, K. R., and Giaccia, A. J. Induction of vascular endothelial growth factor by hypoxia is modulated by a phosphatidylinositol 3-kinase/Akt signaling pathway in Ha-ras transformed cells through a hypoxia inducible factor-1 transcriptional element. Blood, *90:* 3322–3331, 1997.
17. Brown, E. J., Albers, M. W., Shin, T. B., Ichikawa, K., Keith, C. T., Lane, W. S., and Schreiber, S. L. A mammalian protein targeted by G_1-arresting rapamycin-receptor complex. Nature (Lond.), *369:* 756–758, 1994.
18. Carson, J. P., Kulik, G., and Weber, M. J. Antiapoptotic signaling in LNCaP prostate cancer cells: a survival signaling pathway independent of phosphatidylinositol 3′-kinase and Akt/protein kinase B. Cancer Res., *59:* 1449–1453, 1999.
19. Lin, J., Adam, R. M., Santiestevan, E., and Freeman, M. R. The phosphatidylinositol 3′-kinase pathway is a dominant growth factor-activated cell survival pathway in LNCaP human prostate carcinoma cells. Cancer Res., *59:* 2891–2897, 1999.
20. Li, J., Yen, C., Liaw, D., Podsypanina, K., Bose, S., Wang, S. I., Puc, J., Miliaresis, C., Rodgers, L., McCombie, R., Bigner, S. H., Giovanella, B. C., Ittmann, M., Tycko, B., Hibshoosh, H., Wigler, M. H., and Parsons, R. *PTEN*, a putative protein tyrosine phosphatase gene mutated inhuman brain, breast, and prostate cancer. Science (Washington DC) *275:* 1943–1947, 1997.
21. Davies, M. A., Koul, D., Dhesi, H., Berman, R., McDonnell, T. J., McConkey, D., Yung, W. K., and Steck, P. A. Regulation of Akt/PKB activity, cellular growth, and apoptosis in prostate carcinoma cells by MMAC/PTEN. Cancer Res., *59:* 2551–2556, 1999.
22. Ravi, R., Mookerjee, B., Bhujwalla, Z. M., Sutter, C. H., Artemov, D., Zeng, Q., Dillehay, L. E., Madan, A., Semenza, G. L., and Bedi, A. Regulation of tumor angiogenesis by p53-induced degradation of hypoxia-inducible factor 1α. Genes Dev., *14:* 34–44, 2000.
23. Maxwell, P. H., Wiesener, M. S., Chang, G-W., Clifford, S. C., Vaux, E. C., Cockman, M. E., Wykoff, C. C., Pugh, C. W., Maher, E. R., and Ratcliffe, P. J. The tumor suppressor protein VHL targets hypoxia-inducible factors for oxygen-dependent proteolysis. Nature (Lond.), *399:* 271–275, 1999.
24. Jiang, B-H., Agani, F., Passaniti, A., and Semenza, G. L. V-SRC induces expression of hypoxia-inducible factor 1 (HIF-1) and transcription of genes encoding vascular endothelial growth factor and enolase 1: involvement of HIF-1 in tumor progression. Cancer Res., *57:* 5328–5335, 1997.
25. Datta, K., Bellacosa, A., Chan, T. O., and Tsichlis, P. N. Akt is a direct target of the phosphatidylinositol 3-kinase: activation by growth factors, v-src, and v-Ha-ras, in Sf9 and mammalian cells. J. Biol. Chem., *271:* 30835–30839, 1996.
26. Maxwell, P. H., Dachs, G. U., Gleadle, J. M., Nicholls, L. G., Harris, A. L., Stratford, I. J., Hankinson, O., Pugh, C. W., and Ratcliffe, P. J. Hypoxia-inducible factor-1 modulates gene expression in solid tumors and influences both angiogenesis and tumor growth. Proc. Natl. Acad. Sci. USA, *94:* 8104–8109, 1997.

Biochemical and Biophysical Research Communications **284**, 352–356 (2001)
doi:10.1006/bbrc.2001.4981, available online at http://www.idealibrary.com on IDEAL®

APPENDIX 4

Hypoxia-Inducible Factor 1α and 1β Proteins Share Common Signaling Pathways in Human Prostate Cancer Cells

Hua Zhong,*,[1] Colleen Hanrahan,† Henk van der Poel,† and Jonathan W. Simons*
**Winship Cancer Institute, Emory University School of Medicine, Atlanta, Georgia 30322; and †Oncology Center, Johns Hopkins University School of Medicine, Baltimore, Maryland 21205*

Received April 27, 2001

Hypoxia-inducible factor 1 (HIF-1) is a heterodimeric transcription factor consisting α and β subunits. It is critically involved in cancer cell hypoxia adaptation, glycolysis, and angiogenesis. HIF-1β is associated with HIF-1 functions as a dimerization partner of HIF-1α, and is on the other hand associated with carcinogenesis via dioxin signaling. Regulation of HIF-1β protein expression was investigated in human prostate cancer (PCA) cells. HIF-1β protein was expressed constitutively under nonhypoxic conditions in all human PCA cells tested, and was up-regulated by hypoxia, $CoCl_2$, EGF, serum, or PMA in moderate levels. Compared to that of HIF-1α, the constitutive, serum-, EGF-, and PMA-increased HIF-1β protein expression were also inhibited by selective PI3K or FRAP/TOR inhibitors but in higher doses. Hypoxia partially reversed the dose dependent inhibition of HIF-1β. These results suggest that HIF-1α and β share common signaling pathways for nuclear protein accumulation. © 2001 Academic Press

Key Words: **HIF-1β; HIF-1α; prostate; neoplasms; phosphatidylinositol-3 kinase; FRAP; angiogenesis; hypoxia; transcription factor; gene expression.**

Hypoxia-inducible factor 1 (HIF-1) is a heterodimeric basic helix-loop-helix-PER-ARNT-SIM (bHLH-PAS) transcription factor consisting HIF-1α and HIF-1β subunits. It is critically involved in cancer cell clonal selection, hypoxic adaptation, glycolysis, and angiogenesis (1). We have reported that HIF-1α is overexpressed in human prostate cancer as well as 12 other types of common human cancers (2–4). HIF-1β is known as the aryl hydrocarbon nuclear translocator (ARNT), as it was first shown to dimerize with the aryl hydrocarbon receptor (AHR) that is associated with dioxin signaling in the xenobiotic response (5, 6). HIF-1β is constitutively expressed in all cell culture models tested to date (7–11), and is localized in nucleus or nonnucleolar portion of the nucleus (7, 8). The up-regulation of HIF-1β protein was shown in the nuclear extracts of Hep3B as well as Hepa-1 cells in response to hypoxia (9, 11, 12). HIF-1β protein predominantly functions as a heterodimeric binding partner for other bHLH/PAS proteins to activate downstream genes expression. For example, HIF-1β forms a heterodimer with HIF-1α to activate transcription of target genes, whose gene products are critical in cancer progression (1). Forced overexpression of HIF-1α and HIF-1β results in reporter gene expression under nonhypoxia conditions and a superinduction in response to hypoxia (13). Moreover, HIF-1β-deficient mutant hepatoma cells, compared with their parental cells, showed dramatically reduced HIF-1 DNA-binding and transcriptional activity under hypoxic conditions (13, 14) as well as significantly reduced vascularity and a slow tumor xenograft growth rate (15, 16).

We have shown that HIF-1α protein expression and HIF-1-dependent transcriptional activity are modulated by EGF/PI3K/AKT/FRAP pathway in human prostate cancer (PCA) cells, delineating a new pathway for HIF-1 activation independent of oxygen tension (17). We found that HIF-1α and HIF-1β proteins are co-localized in human brain tumors with similar immunostaining patterns (4). Since HIF-1β is a major dimerization partner for HIF-1α, we therefore tested the hypothesis that HIF-1β expression is regulated by signaling pathways that modulate HIF-1α protein expression. We demonstrated, similar to HIF-1α, that expression of HIF-1β protein was increased by hypoxia and cobalt chloride ($CoCl_2$), and was altered by interfering with the PI3K pathway in human PCA cells regardless its high basal level. These results provide a possible mechanism contributing to the co-localization of HIF-1α and HIF-1β nuclear proteins in human can-

[1] To whom correspondence and reprint requests should be addressed at Winship Cancer Institute, 1365 Clifton Road, B4328, Atlanta, GA 30322. Fax: 404-778-5016. E-mail: hua_zhong@emory.org.

0006-291X/01 $35.00

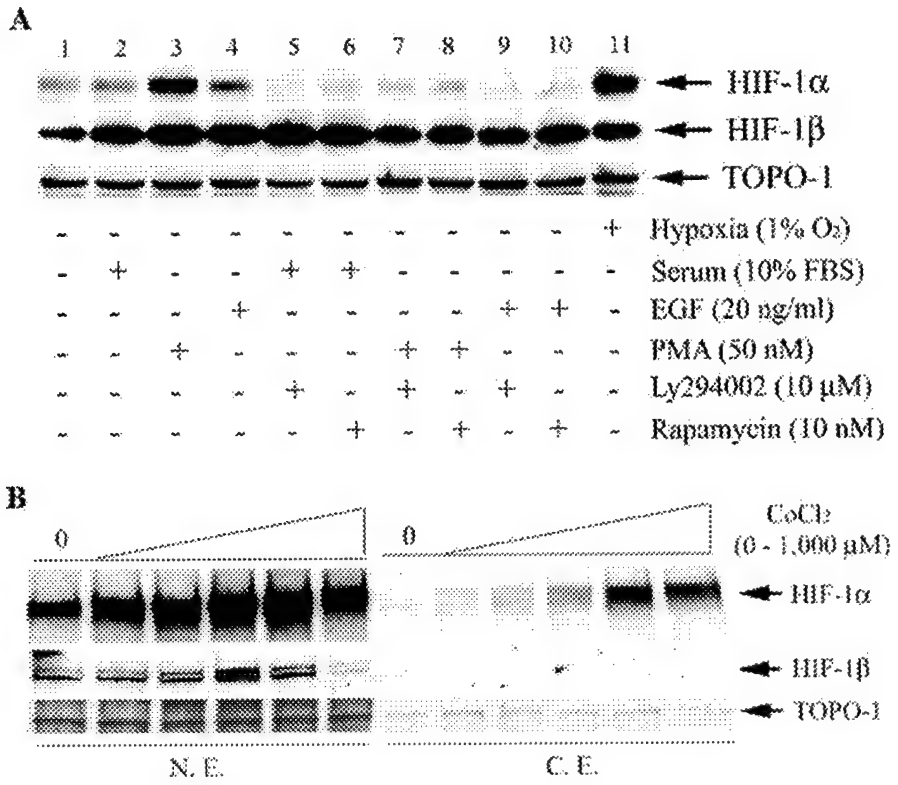

FIG. 1. Expression of HIF-1α and HIF-1β proteins was detected in nuclear extracts by immunoblot assay in PC-3 cells under different culture conditions. (A) Cells, after 24 h serum starvation, were incubated under nonhypoxic (lanes 1–10) or hypoxic (lane 11) conditions (20 and 1% O_2, respectively), and under serum (lanes 2, 5, and 6), EGF (lanes 4, 9, and 10), PMA (lanes 3, 7, and 8), Ly294002 (lanes 5, 7, and 9), and rapamycin (6, 8, and 10) administrations for 6 h before cell harvesting. (B) Cells were cultured with no serum media and different doses of $CoCl_2$ (0, 50, 100, 200, 500, or 1000 μM) for 10 h before cell harvesting. Proteins from nuclear (N.E.) and cytoplasmic (C.E.) fractions were used for Western blot.

cers (4) and show the possibility of developing novel therapeutics aimed at inhibiting HIF-1 functions.

MATERIALS AND METHODS

Cell lines and culture condition. The human PCA cell lines (PC-3, DU145, TSU, and LNCaP) were maintained with RPMI 1640 supplemented with 10% heat-inactivated fetal bovine serum (FBS) at 37°C in a humidified atmosphere and 5% CO_2 in air. Cell lines were tested routinely for mycoplasmal contamination. The cells were subjected to hypoxia in a sealed modular incubator chamber (Billups-Rothenberg, Del Mar, CA) flushed with 1% O_2, 5% CO_2, and 94% N_2 (1% O_2) or placed directly in a 5% CO_2 and 95% air incubator (20% O_2), and cultured at 37°C.

Reagents and antibodies. Phorbol 12-myristate 13-acetate (PMA), LY294002, wortmannin, and rapamycin were purchased from Alexis Biochemicals (San Diego, CA). Human recombinant epidermal growth factor (EGF) was purchased from Life Technologies (Rockville, MD). $CoCl_2$ was purchased from Sigma (St. Louis, MO). Purified mouse monoclonal anti-HIF-1α and β antibodies were obtained from Novus Biologicals (Littleton, CO). Polyclonal human antibody to human topoisomerase I (TOPO-I) was purchased from *Topo*GEN (Columbus, OH).

Preparation of nuclear extracts and immunoblot assays. Cells ($0.5–1.0 \times 10^6$) were seeded onto 150-mm tissue culture dishes and incubated for 36–48 h in complete media. The culture media was then aspirated and the cells were washed with Hanks' balanced salt solution. The cells were incubated in media with 0–0.1% FBS for 24 h, washed with Hanks' balanced salt solution again, and then given fresh media with 0–0.1% FBS alone or with 10% FBS, EGF, PMA, either alone or with LY294002, wortmannin, or rapamycin, for 6–8 h. To harvest, cells were washed twice with cold Dulbecco's phosphate-buffered saline (PBS), scraped into 5 ml cold PBS and pelleted by centrifugation at 500*g* for 5 min at 4°C. Nuclear extracts and immunoblot assays were prepared as previously described (12), except by using mouse monoclonal anti-HIF-1α (1:500) or β (1:1500) antibodies as primary antibodies instead.

RESULTS

Hypoxia, Serum, EGF, PMA, and $CoCl_2$ Increase the HIF-1β Level in Human PCA Cells

Compared to HIF-1α protein, HIF-1β protein was readily detectable by Western blot in all PCA cells tested (Figs. 1, 2, and 3), suggesting a higher basal HIF-1β protein level in these cells. HIF-1β protein was increased in moderate levels in response to hypoxia, serum, EGF, and PMA (50 or 100 nM) administrations in PC-3 cells (Figs. 1A and 2B), whereas HIF-1α protein was increased also in moderate levels in response to serum and EGF administrations but increased dramatically in response to hypoxia and PMA treatment

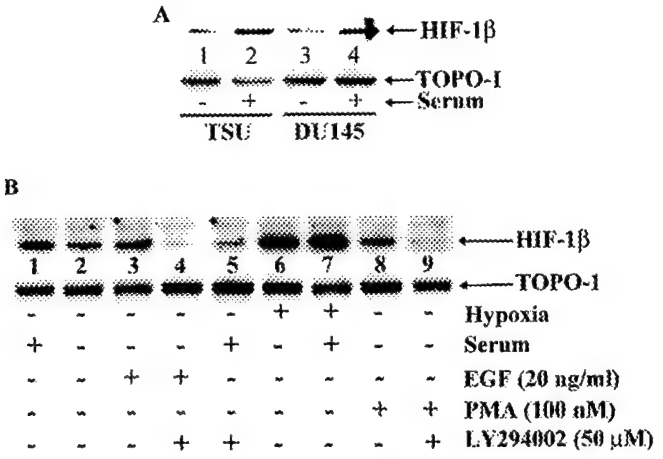

FIG. 2. Induction and inhibition of HIF-1β protein expression in human PCA cells. (A) Effect of serum starvation and stimulation. TSU and DU145 cells were cultured in serum-free media for 24 h and then incubated in media containing 0 or 10% FBS for 6 h before cell harvesting. (B) Effect of PI3K inhibition on serum-EGF, and PMA-induced HIF-1β/ARNT expression. PC-3 cells were incubated in media containing 0.1% FBS for 24 h and then exposed to 10% FBS, 20 ng/ml EGF, 100 nM PMA, or 1% O_2 in the presence or absence of 50 μM LY294002 for 6 h before cell harvesting.

(Fig. 1A). Up-regulation of HIF-1β protein by serum stimulation (10% FBS for 6 h) was also shown in TSU and DU145 cells after serum starvation (Fig. 2A). Interestingly, increased HIF-1β protein was shown in PC-3 cells treated with 50–500 μM/ml $CoCl_2$ with similar dose-dependent fashion to HIF-1α (Fig. 1B), but not with 1000 μM/ml $CoCl_2$ since cells started dying, detaching, and floating. However, unlike HIF-1α, HIF-1β protein was undetectable in cytoplasmic fraction (Fig. 1B).

HIF-1β Protein Was Decreased by Blockage of the PI3K/FRAP Pathway

To determine whether PI3K signal transduction pathway activity was required for HIF-1β expression, PC-3 cells were exposed to LY294002 or wortmannin, inhibitors of PI3K, or to rapamycin, an inhibitor of FRAP (18), a signaling molecule downstream of PI3K. Treatment PC-3 cells with 50 μM LY294002 significantly reduced the serum-, EGF-, and PMA-induced HIF-1β expression (Fig. 2B). PC-3 cells were cultured in 0.1% FBS in the presence of varying concentrations of wortmannin and rapamycin under hypoxic and/or nonhypoxic conditions. Both constitutive and hypoxia-induced HIF-1β expressions were inhibited by wortmannin in dose-dependent pattern. Hypoxia appears able to partially overcome the inhibition of HIF-1β expression by wortmannin, since HIF-1β expression under nonhypoxic conditions was partially inhibited by 10 nM wortmannin and completely inhibited by 100 nM wortmannin. In contrast, hypoxia-induced HIF-1β protein expression was only partially inhibited by 100 or 50 nM wortmannin and was not inhibited by 10 nM wortmannin. In addition, the constitutive HIF-1β expression was inhibited by rapamycin in dose-dependent pattern only under nonhypoxic conditions (Fig. 3B) and not under hypoxic conditions (data not show). Lower doses of these inhibitors that were demonstrated to decrease HIF-1α protein expression (Fig. 1A) (17), such as 10 μM Ly294002 (Fig. 1A), 1–10 nM Rapamycin (Figs. 1A and 3B), and 1 nM Wortmannin (data not show), had no effect or only minimal effect on down-regulation HIF-1β protein. As shown in Fig 1A, low doses of Ly294002 and rapamycin had no effect on serum-induced HIF-1β protein and had only minimal effect EGF- or PMA-induced HIF-1β protein.

DISCUSSION

Others and we have demonstrated that activation of the PI3K/PTEN/AKT/FRAP pathway by serum, EGF, or PMA results in increased HIF-1α protein, HIF-1 transcriptional activity, and VEGF protein expression in cancer cells (17, 19). In this study, we found that hypoxia, $CoCl_2$, EGF, PMA, or serum increased HIF-1β protein expression, and that pharmacological inhibition of the PI3K/AKT pathway decreased HIF-1β protein expression in human PCA cells. These results are similar to modulation of HIF-1α by the same pathways in human cancer cells, suggesting that HIF-1α and HIF-1β somehow share hypoxic and common nonmoxic pathways for nuclear protein accumulations. These results also suggest that PI3K/AKT pathway activity is critical for stabilization of not only HIF-1α but also HIF-1β proteins. Hence, those genetic alterations af-

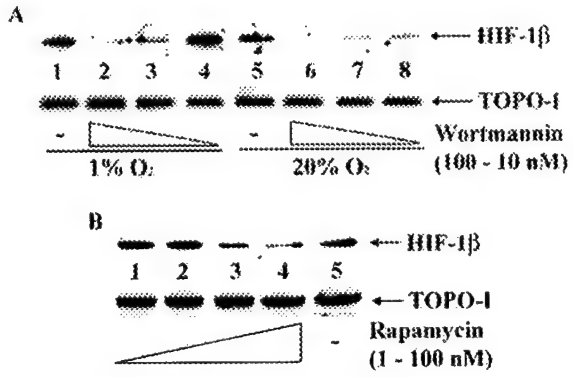

FIG. 3. Effect of pharmacological inhibitors on HIF-1β protein expression. (A) Effect of PI3K inhibitor on constitutive and hypoxia-induced HIF-1β/ARNT expression. PC-3 cells were cultured in media containing 0.1% FBS for 20 h, followed by the addition of wortmannin (0, 100, 50, 10 nM) and incubation in 1% (lanes 1–4) or 20% (lanes 5–8) O_2 for 8 h before cell harvesting. (B) Effect of FRAP inhibitor on constitutive HIF-1β/ARNT expression. PC-3 cells were cultured in media containing 0.1% FBS for 20 h, followed by the addition of rapamycin (1, 10, 50, 100, 0 nM) and incubation in 20% O_2 (lanes 1–5) for 8 h before cell harvesting.

fecting HIF-1α expression, such as gain of function mutations in oncogens (e.g., v-src) (16) and loss of function mutations in tumor suppressor genes (e.g., PTEN) (17, 19), may therefore also affect HIF-1β expression. In both PTEN wild-type (DU145) and mutated (PC-3) cells (20), HIF-1β protein expression was induced by serum treatment. This suggests that PTEN mutations do not able to completely cover up the effect of serum for induction of HIF-1β protein expression. Thus, a full understanding of HIF-1β protein regulation includes more than understanding PTEN mutational status alone.

In this study, hypoxia and serum have potentially additive effects on increased HIF-1β protein levels in PCA cells (Fig. 2B). In addition, hypoxia can partially overcome the inhibition of HIF-1β protein expression by PI3K inhibitor wortmannin and completely overcome the inhibition of HIF-1β protein expression by a low dose of wortmannin (10 nM). Above phenomena were also observed in HIF-1α (17). These data indicate that mechanisms involved in constitutively expressed, hypoxia or serum-increased HIF-1β or HIF-1α protein expression are different. Again, HIF-1α and HIF-1β may share hypoxic or normoxic pathways to some extent.

Unlike HIF-1α, HIF-1β is constitutively expressed, easily detectable, and has relative consistent basal levels among different cells in our results and others (10, 11). Moreover, the hypoxia and $CoCl_2$ enhanced HIF-1β protein expressions were moderate in comparison with the dramatically induced HIF-1α protein expression. Furthermore, low doses of PI3K/FRAP inhibitors decrease HIF-1α but not HIF-1β protein levels. These results may be associated with the high HIF-1β basal level resulted from unidentified factors. Interestingly, AHR protein, another dimeric partner of HIF-1β, was shown to be up-regulated by serum and mitogenic growth factors (FGF and PDGF) in murine 3T3 fibroblasts (21), demonstrating a possible involvement of PI3K activity. Like the HIF-1α, HIF-1β, and AHR, the expression of many other transcription factors is increased by serum, growth factors or especially hypoxia. These transcription factors include c-myc, AP1, SP1, NF-κB, HSF-1, and STAT. At this point, these transcription factors appear to share a common mechanism to response these stimuli.

HIF-1β is a bHLH/PAS protein and functions as a heterodimeric binding partner for other bHLH/PAS proteins, including AHR (6), and the α-class hypoxia-inducible factors (HIF-1α, HIF-2α, and HIF-3α) (1). The roles of HIF-1β in these functions are well established. For example, in response to 2,3,7,8-tetrachlorodibenzo-*p*-dioxin (TCDD) or other environment contaminant exposure, the AHR/HIF-1β complex binds to dioxin responsive enhancers (DREs) to activate genes involved in the metabolism of xenobiotics which is considered as one of the possible mechanisms leading to early carcinogenesis (5); in response to hypoxia, each α-class HIF/HIF-1β complex binds to hypoxia responsive elements (HRE) to activate the transcription of genes that regulate adaptation to low oxygen tension (1). Furthermore, simultaneous activation of these two pathways by TCDD and hypoxia demonstrate the competitive use of the common dimeric partner HIF-1β (22–24). Thus, the nuclear accumulation of HIF-1β appears to be essential in the activation mediated by TCDD, hypoxia or other stimuli involved in early carcinogenesis or progression of PCA.

To our knowledge, there have been no systematic studies published about regulation of HIF-1β protein in human cancer cells since this important transcription factor was identified nearly decade ago (5, 25). Consistent with previous findings (7, 9–11), we have shown that constitutive, $CoCl_2$ or hypoxia-induced HIF-1β protein is expressed in human PCA cells. These results are similar to that of HIF-1α under same experimental conditions reported previously (7, 9–12), whereas hypoxia and $CoCl_2$ appear to induce more HIF-1α protein expression than HIF-1β. HIF-1α protein expression is regulated by ubiquitination and proteasomal degradation (1). It will be interesting to know if HIF-1β is also regulated by same mechanisms as HIF-1α and to what extent, or if up-regulation of HIF-1β protein is just a simple consequence of increased HIF-1α protein since increased HIF-1α protein needs more binding partner. The coordinate expression of AHR and HIF-1β was observed in human embryonic epithelium and rat tissues at protein or mRNA level respectively (26, 27). Recently, we have demonstrated that expression of HIF-1α in brain tumors is associated with angiogenesis, invasion, and progression. In addition, similar immunostaining patterns for both HIF-1α and HIF-1β were observed in brain tumors (4). Interestingly, similar immunostaining patterns and distributions of HIF-1α and HIF-1β were also found in both human high-grade prostatic intraepithelial neoplasia (PIN) and prostate cancer lesions (Hua Zhong, unpublished data). Taken together, the coordinate expression and shared signaling pathways of HIF-1α and HIF-1β nuclear proteins provide strong bases for HIF-1 function in tumor biology, and for targeting HIF-1 in cancer prevention and treatment.

ACKNOWLEDGMENTS

H.Z. is AVON scholar supported by AVON Products Foundation. We thank Byron H. Lee for assistance in preparation of the manuscript. Grant sponsors: NIH Prostate Cancer SPORE Grant CA-58236 (J.W.S. and H.Z.), CaP CURE Foundation (J.W.S. and H.Z.), Department of Defense Grant DAMD 17-98-1-8475 (J.W.S.), and Avon Breast Cancer Crusade Fund (J.W.S. and H.Z.).

REFERENCES

1. Semenza, G. L. (2000) *Crit. Rev. Biochem. Mol. Biol.* **35**, 71–103.
2. Zhong, H., Agani, F., Baccala, A. A., Laughner, E., Rioseco-

Camacho, N., Isaacs, W. B., Simons, J. W., and Semenza, G. L. (1998) *Cancer Res.* **58,** 5280–5284.

3. Zhong, H., De Marzo, A. M., Laughner, E., Lim, M., Hilton, D. A., Zagzag, D., Buechler, P., Isaacs, W. B., Semenza, G. L., and Simons, J. W. (1999) *Cancer Res.* **59,** 5830–5835.
4. Zagzag, D., Zhong, H., Scalzitti, J. M., Laughner, E., Simons, J. W., and Semenza, G. L. (2000) *Cancer* **88,** 2606–2618.
5. Reyes, H., Reisz-Porszasz, S., and Hankinson, O. (1992) *Science* **256,** 1193–1195.
6. Hankinson, O. (1995) *Annu. Rev. Pharmacol. Toxicol.* **35,** 307–340.
7. Pollenz, R. S., Sattler, C. A., and Poland, A. (1994) *Mol. Pharmacol.* **45,** 428–438.
8. Hord, N. G., and Perdew, G. H. (1994) *Mol. Pharmacol.* **46,** 618–626.
9. Wang, G. L., Jiang, B. H., Rue, E. A., and Semenza, G. L. (1995) *Proc. Natl. Acad. Sci. USA* **92,** 5510–5514.
10. Holmes, J. L., and Pollenz, R. S. (1997) *Mol. Pharmacol.* **52,** 202–211.
11. Pollenz, R. S., Davarinos, N. A., and Shearer, T. P. (1999) *Mol. Pharmacol.* **56,** 1127–1137.
12. Jiang, B. H., Semenza, G. L., Bauer, C., and Marti, H. H. (1996) *Am. J. Physiol.* **271,** C1172–1180.
13. Forsythe, J. A., Jiang, B. H., Iyer, N. V., Agani, F., Leung, S. W., Koos, R. D., and Semenza, G. L. (1996) *Mol. Cell. Biol.* **16,** 4604–4613.
14. Wood, S. M., Gleadle, J. M., Pugh, C. W., Hankinson, O., and Ratcliffe, P. J. (1996) *J. Biol. Chem.* **271,** 15117–15123.
15. Maxwell, P. H., Dachs, G. U., Gleadle, J. M., Nicholls, L. G., Harris, A. L., Stratford, I. J., Hankinson, O., Pugh, C. W., and Ratcliffe, P. J. (1997) *Proc. Natl. Acad. Sci. USA* **94,** 8104–8109.
16. Jiang, B. H., Agani, F., Passaniti, A., and Semenza, G. L. (1997) *Cancer Res.* **57,** 5328–5335.
17. Zhong, H., Chiles, K., Feldser, D., Laughner, E., Hanrahan, C., Georgescu, M. M., Simons, J. W., and Semenza, G. L. (2000) *Cancer Res.* **60,** 1541–1545.
18. Brown, E. J., Albers, M. W., Shin, T. B., Ichikawa, K., Keith, C. T., Lane, W. S., and Schreiber, S. L. (1994) *Nature* **369,** 756–758.
19. Zundel, W., Schindler, C., Haas-Kogan, D., Koong, A., Kaper, F., Chen, E., Gottschalk, A. R., Ryan, H. E., Johnson, R. S., Jefferson, A. B., Stokoe, D., and Giaccia, A. J. (2000) *Genes Dev.* **14,** 391–396.
20. Whang, Y. E., Wu, X., Suzuki, H., Reiter, R. E., Tran, C., Vessella, R. L., Said, J. W., Isaacs, W. B., and Sawyers, C. L. (1998) *Proc. Natl. Acad. Sci. USA* **95,** 5246–5250.
21. Vaziri, C., Schneider, A., Sherr, D. H., and Faller, D. V. (1996) *J. Biol. Chem.* **271,** 25921–25927.
22. Chan, W. K., Yao, G., Gu, Y. Z., and Bradfield, C. A. (1999) *J. Biol. Chem.* **274,** 12115–12123.
23. Kim, J. E., and Sheen, Y. Y. (2000) *Biochem. Pharmacol.* **59,** 1549–1556.
24. Gradin, K., McGuire, J., Wenger, R. H., Kvietikova, I., Whitelaw, M. L., Toftgard, R., Tora, L., Gassmann, M., and Poellinger, L. (1996) *Mol. Cell. Biol.* **16,** 5221–5231.
25. Hoffman, E. C., Reyes, H., Chu, F. F., Sander, F., Conley, L. H., Brooks, B. A., and Hankinson, O. (1991) *Science* **252,** 954–958.
26. Abbott, B. D., Probst, M. R., and Perdew, G. H. (1994) *Teratology* **50,** 361–366.
27. Carver, L. A., Hogenesch, J. B., and Bradfield, C. A. (1994) *Nucleic Acids Res.* **22,** 3038–3044.

[CANCER RESEARCH 59, 5830–5835, November 15, 1999]

Overexpression of Hypoxia-inducible Factor 1α in Common Human Cancers and Their Metastases[1]

Hua Zhong, Angelo M. De Marzo, Erik Laughner, Michael Lim, David A. Hilton, David Zagzag, Peter Buechler, William B. Isaacs, Gregg L. Semenza,[2] and Jonathan W. Simons

The Johns Hopkins Oncology Center, Brady Urological Institute [H. Z., M. L., W. B. I., J. W. S.], Department of Pathology [A. M. D.], Departments of Pediatrics and Medicine, and Institute of Genetic Medicine [E. L., G. L. S.], The Johns Hopkins University School of Medicine, Baltimore, Maryland 21287; Department of Histopathology, Derriford Hospital, Plymouth PL6 8DH, United Kingdom [D. A. H.]; Department of Pathology, Division of Neuropathology, New York University Medical Center, New York, New York 10016 [D. Z.]; and Division of General Surgery, University of California-Los Angeles School of Medicine, Los Angeles, California 90095-6904 [P. B.]

ABSTRACT

Neovascularization and increased glycolysis, two universal characteristics of solid tumors, represent adaptations to a hypoxic microenvironment that are correlated with tumor invasion, metastasis, and lethality. Hypoxia-inducible factor 1 (HIF-1) activates transcription of genes encoding glucose transporters, glycolytic enzymes, and vascular endothelial growth factor. HIF-1 transcriptional activity is determined by regulated expression of the HIF-1α subunit. In this study, HIF-1α expression was analyzed by immunohistochemistry in 179 tumor specimens. HIF-1α was overexpressed in 13 of 19 tumor types compared with the respective normal tissues, including colon, breast, gastric, lung, skin, ovarian, pancreatic, prostate, and renal carcinomas. HIF-1α expression was correlated with aberrant p53 accumulation and cell proliferation. Preneoplastic lesions in breast, colon, and prostate overexpressed HIF-1α, whereas benign tumors in breast and uterus did not. HIF-1α overexpression was detected in only 29% of primary breast cancers but in 69% of breast cancer metastases. In brain tumors, HIF-1α immunohistochemistry demarcated areas of angiogenesis. These results provide the first clinical data indicating that HIF-1α may play an important role in human cancer progression.

INTRODUCTION

Altered glucose metabolism and cellular adaptation to hypoxia are fundamental to the basic biology and treatment of cancer. Four lines of evidence support this thesis: (*a*) clonal expansion of cancer cells depends on enhanced glucose transport and glycolysis (the Warburg effect; Refs. 1, 2); (*b*) tumors cannot grow beyond several mm^3 without angiogenesis because of the limited diffusion of O_2, glucose, and other nutrients (3, 4). In many cancers, the degree of vascularization is inversely correlated with patient survival (5); (*c*) the probability of invasion, metastasis, and death are positively correlated with the degree of intratumoral hypoxia (6, 7), which is caused by an architecturally defective microcirculation such that even cells adjacent to neovessels may be hypoxic (8). Cancer cell proliferation may also outpace the rate of angiogenesis (3); and (*d*) tumor hypoxia is associated with resistance to chemotherapy, immunotherapy, and radiotherapy (9). Despite the critical importance of these observations, their molecular basis is not well understood. Transcription factors that regulate expression of angiogenic growth factors (such as VEGF[3]) or glycolytic enzymes involved in the Warburg effect are compelling targets for interrogation. HIF-1 performs both of these functions.

HIF-1 is a bHLH-PAS transcription factor that plays an essential role in O_2 homeostasis (10–13). HIF-1 is a heterodimer composed of HIF-1α and HIF-1β subunits (10). Whereas HIF-1β (also known as the aryl hydrocarbon receptor nuclear translocator) is a common subunit of multiple bHLH-PAS proteins, HIF-1α is the unique, O_2-regulated subunit that determines HIF-1 activity (14, 15). HIF-1 transactivates genes whose protein products function either to increase O_2 availability or to allow metabolic adaptation to O_2 deprivation. Included among these are genes encoding erythropoietin, transferrin, endothelin-1, inducible nitric oxide synthase, heme oxygenase 1, VEGF, IGF-2, IGF-binding proteins -2 and -3, and 13 different glucose transporters and glycolytic enzymes (15, 16). Remarkably, most of these proteins are implicated in tumor progression (17). Analysis of isogenic tumor cell lines injected into nude mice revealed a dramatic correlation of HIF-1 expression levels with tumor growth and angiogenesis (18, 19).

Recently, we found that HIF-1α mRNA was overexpressed in six rat PCA cell lines compared with the normal prostate, and metastatic potential was correlated with HIF-1α mRNA levels in those cell lines (20). A human PCA cell line derived from a bone metastasis was found to overexpress HIF-1α protein under nonhypoxic culture conditions (20). Because HIF-1α expression was dysregulated in PCA cell lines, we tested the hypothesis that HIF-1α is generally overexpressed in solid tumors. In this study, we screened HIF-1α protein expression by immunohistochemistry in normal tissues and human cancers, including lung, prostate, breast, and colon carcinoma, which are the leading causes of U.S. cancer mortality.

MATERIALS AND METHODS

Production of Anti-HIF-1α MAb H1α67. A human HIF-1α cDNA fragment encoding amino acids 432–528 was cloned into pGEX2T. The GST/HIF-1α fusion protein was purified from bacteria (14) and used to immunize BALB/c mice. Spleen cells from immunized mice were fused with P3X63-Ag8-653 myeloma cells. Hybridoma supernatants were screened by ELISA against GST and GST/HIF-1α. Supernatant from clone 67 was affinity-purified using protein G-Sepharose (Pharmacia). The adsorbed protein was eluted with 0.1 M glycine-HCl (pH 2.7) and neutralized with 1 M Tris-HCl (pH 9.0). Nuclear extracts, prepared from human Hep3B and mouse ES cells (11), were subjected to immunoblot analysis as described previously (14) except that the primary MAb was H1α67 (1:500), and the secondary MAb was horseradish peroxidase-conjugated sheep antimouse immunoglobulin (1:2000).

Transient Transfection Assays. Human embryonic kidney 293 cells, growing exponentially on 10-cm dishes, were transfected by calcium phosphate coprecipitation with 10 μg of pCEP4 (Invitrogen), pCEP4/HIF-1α (21, 22), or PL477 (23), a HIF-2α expression vector that was generously provided by Dr. Christopher Bradfield (University of Wisconsin, Madison, WI). For reporter gene assays, the cells were cotransfected with pSVβgal and 2xWT33-luciferase, which contains two copies of a 33-bp hypoxia-response element from the human erythropoietin gene cloned upstream of a basal SV40 promoter (22).

Received 6/18/99; accepted 10/6/99.

The costs of publication of this article were defrayed in part by the payment of page charges. This article must therefore be hereby marked *advertisement* in accordance with 18 U.S.C. Section 1734 solely to indicate this fact.

[1] This work was supported by NIH Grant R01-HL55338 (to G. L. S.), NIH Prostate Cancer SPORE Grant CA-58236, CaP CURE Foundation, and Department of Defense Prostate Cancer Grant DAMD 17-98-1-8475 (to J. W. S.). Under a licensing agreement between the Johns Hopkins University and Novus Biologicals, Inc., G. L. S. is entitled to a share of royalties received by the University from sales of the technology described in this publication. The terms of this arrangement are being managed by the University in accordance with its conflict of interest policies.

[2] To whom requests for reprints should be addressed, at The Johns Hopkins Hospital, CMSC 1004, 600 North Wolfe Street, Baltimore, MD 21287. Phone: (410) 955-1619; Fax: (410) 955-0484; E-mail: gsemenza@jhmi.edu.

[3] The abbreviations used are: VEGF, vascular endothelial growth factor; HIF-1, hypoxia-inducible factor 1; IGF, insulin-like growth factor; MAb, monoclonal antibody; bHLH, basic helix-loop-helix; PCA, prostate cancer; GST, glutathione *S*-transferase; ES, embryonic stem; LI, labeling index.

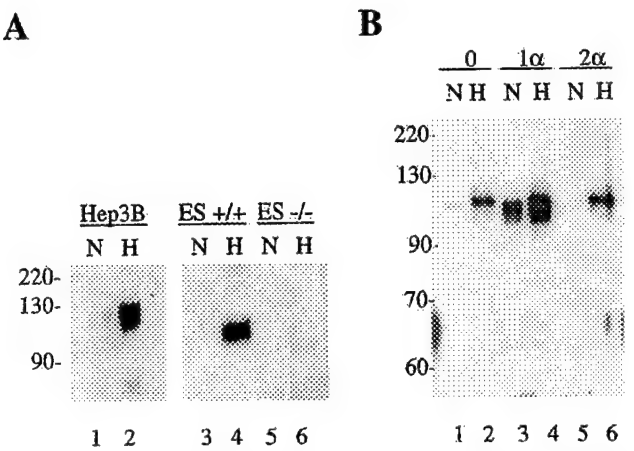

Fig. 1. Immunoblot detection of HIF-1α by MAb H1α67. *A*, detection of HIF-1α induced by hypoxia in wild-type Hep3B and ES cells but not in HIF-1α-null ES cells. Human Hep3B cells and mouse ES cells that were either wild-type (+/+) or homozygous for a targeted mutation (11) that eliminated expression of HIF-1α (−/−) were exposed to nonhypoxic (*N*; 20% O_2) or hypoxic (*H*; 1% O_2) culture conditions for 6 h before nuclear extract preparation and immunoblot assay using MAb H1α67. *At left*, migration of molecular weight markers (*kDa*). Migration of human and mouse HIF-1α differed as previously described (34). *B*, detection of overexpressed HIF-1α but not overexpressed HIF-2α. Human 293 cells were transfected with an empty vector (*0*; *Lanes 1* and *2*) or expression vectors encoding human HIF-1α (*1α*; *Lanes 3* and *4*) or human HIF-2α (*2α*; *Lanes 5* and *6*). Transfected cells were incubated for 24 h under nonhypoxic (*N*) or hypoxic (*H*) conditions. Nuclear extracts were prepared and 30-μg aliquots were subjected to immunoblot assay using MAb H1α67 at 1:500 dilution.

Table 1 *HIF-1α protein expression in normal human tissues*

Tissues	N^a	−	+	++	+++	++++	Positive cells
Adrenal	8	5		3			Cortical cells
Fetal liver	1		1				Hepatocytes
Kidney	9	6	1	2			Distal tubular epithelium
Pancreas	11	7		4			Acinar cells
Spleen	10	9		1			Proliferating B cells
Testis	7		7				Seminiferous tubules
Tonsil	3	1		1	1		Proliferating B cells
Brain	10	10					
Breast	18	18					
Heart	7	7					
Large intestine	24	24					
Liver	15	15					
Lung	10	10					
Ovary	10	10					
Pituitary	2	2					
Placenta	2	2					
Prostate	12	12					
Small intestine	1	1					
Stomach	1	1					
Thyroid	10	10					
Uterus	3	3					
Total	174	153	9	11	1	0	

[a] *N*, number of cases analyzed; −, no staining; +, nuclear staining in less than 1% of cells; ++, in 1–10% of cells; +++, in 10–50%; ++++, greater than 50%.

Immunohistochemistry. Formalin-fixed, paraffin-embedded tissue specimens were obtained and handled by standard surgical oncology procedures. Serial 4-μm sections were prepared, and one was stained with H&E. Flanking sections were stained for HIF-1α using Catalyzed Signal Amplification System (DAKO) which is based on streptavidin-biotin-horseradish peroxidase complex formation. In brief, after deparaffinization and rehydration, slides were treated with target retrieval solution (DAKO) at 97°C for 45 min, and the manufacturer's instructions were followed. MAb H1α67 (1 mg/ml) was used at a dilution of 1:1000. Nuclei were lightly counterstained with hematoxylin. Negative controls were performed using nonimmune serum or PBS instead of the MAb. A preadsorption test was also performed using GST/HIF-1α protein. Twenty-four-well plates were coated with GST/HIF-1α protein (2.9 mg/ml), air-dried, and incubated with H1α67 (1:1,000 dilution), followed by immunohistochemistry. Automated immunohistochemistry was performed using a BioTek-Tech Mate 100 Automated Stainer (Ventana-BioTek Solutions, Inc., Tucson, AZ) with the following MAbs: (*a*) anti-Ki67 (MAb MIB-1, Immunotech, 1:100); (*b*) antihuman p53 protein (MAb DO-7, DAKO, 1:250); (*c*) antihuman bcl-2 (MAb 124, DAKO, 1:25); (*d*) anticytokeratin (AE1/AE3, Boerhinger Mannheim, 1:2000); and (*e*) anti-prostate-specific antigen (MAb 5126, Immunotech, dilution 1:50).

Three investigators (H. Z., A. M. D., and J. W. S) independently evaluated the immunohistochemistry. All of the PCA bone metastases were verified by cytokeratin and prostate-specific antigen staining. The immunohistochemical results for HIF-1α protein were classified as follows: −, no staining; +, nuclear staining in less than 1% of cells; ++, nuclear staining in 1–10% of cells and/or with weak cytoplasmic staining; +++, nuclear staining in 10–50% of cells and/or with distinct cytoplasmic staining; ++++, nuclear staining in more than 50% of cells and/or with strong cytoplasmic staining. When independent scoring of a case differed, the case was rechecked, and the final score was determined by recounting HIF-1α positive cells using a multiheaded microscope with all of the three reviewers simultaneously view-

Table 2 *HIF-1α protein expression in human tumors and their metastases*

Tumor types	N^a	−	+	++	+++	++++
Malignant primary tumors						
Prostate adenocarcinoma	11	2	5	1	3	
Colon adenocarcinoma	22		1	4	6	11
Breast adenocarcinoma	52	37	5	4	1	5
Lung adenocarcinoma	2					2
Lung small cell carcinoma	1					1
Renal clear cell carcinoma	1			1		
Pancreas carcinoma	5	1	2	2		
Ovarian carcinoma	2			1	1	
Gastric carcinoma	2		1			1
Brain tumors	9	4	2			3
Mesothelioma	1				1	
Melanoma	4		3	1		
Malignant fibrous histiocytoma	1		1			
Hepatocellular carcinoma	8	8				
Thyroid carcinoma	2	2				
Lymphoma	3	3				
Rhabdomyosarcoma	1	1				
Epithelioid sarcoma	1	1				
Carcinoid	3	3				
Malignant tumors in total	131	62	20	14	12	23
Metastatic tumors						
Lymph node metastases from:						
Prostate adenocarcinoma	1	1				
Breast adenocarcinoma	13	4	5	0	2	2
Colon adenocarcinoma	10	1	1	1	5	2
Bone metastases from:						
Prostate adenocarcinoma	10	6	2	1	1	
Vena caval invasion from:						
Renal clear cell carcinoma	1					1
Undifferentiated carcinoma	1					1
Metastatic tumors in total	36	12	8	2	8	6
Benign tumors						
Breast fibroadenoma	10	10				
Uterine leiomyoma	2	2				
Benign tumors in total	12	12				

[a] *N*, number of cases analyzed; −, no staining; +, nuclear staining in less than 1% of cells; ++, in 1–10% of cells; +++, in 10–50%; ++++, greater than 50%.

Table 3 *Relationship between expression of HIF-1α and p53, bcl-2, and Ki67 in human cancers*[a]

Number of cases in each category are shown.

	p53		bcl-2		Ki67 LI (%)			
	−	+	−	+	<5	5–15	15–50	>50
HIF-1α (−)[a]	38	11	24	21	38	10	2	6
HIF-1α (+/++)	3	9	8	2	9	8	7	3
HIF-1α (+++/++++)	7	7	12	2	0	2	8	33
	$P < 0.01$[b]		$P = 0.05$[b]		$P < 0.001$[c]			

[a] −, no staining; +, nuclear staining in less than 1% of cells; ++, in 1–10% of cells; +++, in 10–50%; ++++, greater than 50%.
[b] Kruskal-Wallis test.
[c] Nonparametric Jonckhere-Terpstra test.

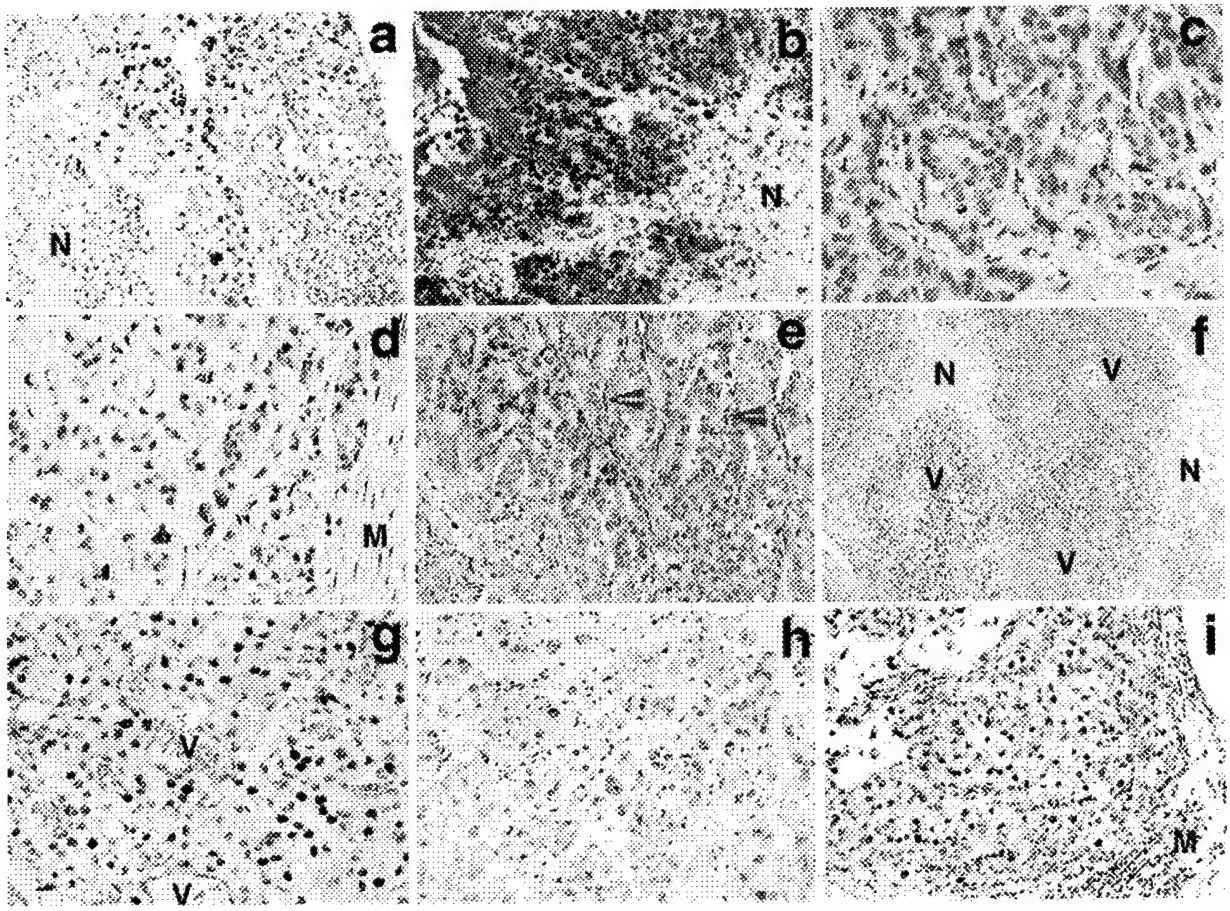

Fig. 2. Immunohistochemical analysis of HIF-1α expression in common human cancers. Tumor sections were from: *a*, lung adenocarcinoma; *b*, lung small cell carcinoma; *c*, breast adenocarcinoma; *d* and *e*, colon adenocarcinoma; *f*, glioblastoma multiforme; *g*, brain hemangioblastoma; *h*, pancreas carcinoma; and *i*, renal clear cell carcinoma. *N*, necrosis; *M*, tumor margin; *V*, blood vessel; *red arrows*, stromal cells. ×100 (f); ×200 (*a*, *b*, *h*, and *i*); ×400 (*c*, *d*, *e*, and *g*).

ing the slide. For Ki67 analysis, nuclei from approximately 1000 tumor cells from 10 randomly selected fields were counted, and the LI was determined as the percentage of positive nuclei. Bcl-2 reactivity was scored positive if >10% of tumor cells showed distinct cytoplasmic staining. Aberrant p53 accumulation was scored positive if nuclear staining was present in >10% of tumor cells.

Nonparametric statistical analyses were conducted by Dr. Steven Piantadosi, Johns Hopkins Oncology Center Biostatistics Center, using Microsoft Excel (Microsoft Corporation, Redmond, WA) and STAT-XACT, Version 4 for Windows (Cytel Software, Berkeley CA, 1998). As a singly ordered table, the Kruskal-Wallis test was used to evaluate the correlation between HIF-1α and aberrant p53 or bcl-2 expression. As a doubly ordered table, the correlation between HIF-1α protein expression and Ki67 LI was analyzed by Jonkchere-Terpstra test (24).

RESULTS

Characteristics of Anti-HIF-1α MAb H1α67. A GST fusion protein containing amino acids 432–528 of human HIF-1α was used as immunogen for MAb production. Five hybridoma clones were identified that reacted with GST/HIF-1α but not with GST. Clone 67 was chosen for further characterization. MAb H1α67 was identified as IgG2b/κ subtype and purified from hybridoma supernatants by protein-G affinity chromatography. Immunoblot assays demonstrated that MAb H1α67 recognized a hypoxia-induced protein of approximately M_r 120,000 that was identical in size to HIF-1α, in Hep3B cells and wild-type ES cells, but not in HIF-1α-null (11) ES cells (Fig. 1*A*). MAb H1α67 showed reactivity against human, monkey, sheep, mouse, bovine, rat, and ferret HIF-1α (data not shown).

MAb H1α67 also recognized human HIF-1α purified 11,250-fold by anion-exchange and DNA-affinity chromatography (25) at concentrations too low to allow protein quantitation (data not shown). As a final test of its specificity, cells were transfected with expression vectors encoding no protein, HIF-1α, or HIF-2α (Fig. 1*B*). MAb H1α67 detected overexpressed HIF-1α *(Lanes 3–4)*, whereas cells overexpressing HIF-2α *(Lanes 5–6)* gave the same pattern as cells transfected with the empty vector *(Lanes 1–2)*. HIF-2α expression in the transfected cells was confirmed by cotransfection of a reporter gene containing a hypoxia response element, which was activated 9- to 13-fold over background in cells transfected with HIF-1α expression vector and 33- to 106-fold over background in cells transfected with the HIF-2α expression vector (data not shown). These highly stringent tests provide convincing evidence that MAb H1α67 specifically recognizes HIF-1α.

Screening of HIF-1α Protein Expression in Normal and Malignant Human Tissues. HIF-1α expression was extensively screened in normal tissues and human cancers resected during routine surgical oncology procedures. Twenty-one normal human tissues (174 specimens), 19 primary malignant cancers (131 specimens), and 36 metastases from 6 tumor types were interrogated (Tables 1 and 2). Most normal human tissues (14 types) showed no HIF-1α immunoreactivity (153 of 174 clinical specimens, 88% negative). In some autopsy

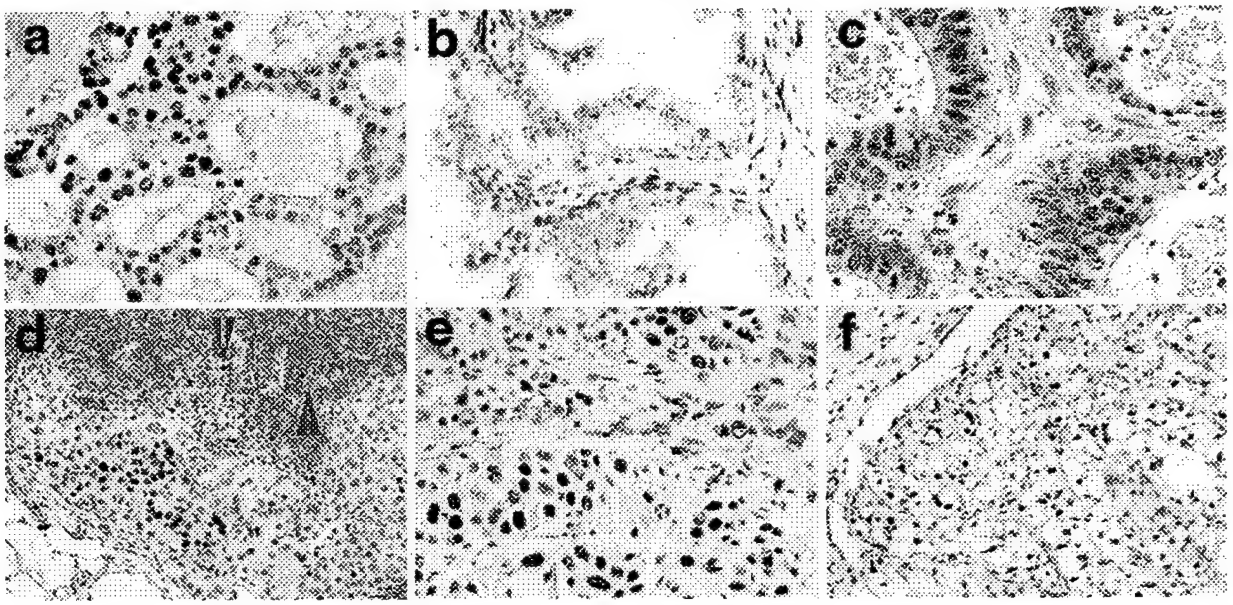

Fig. 3. Immunohistochemical analysis of HIF-1α expression in preneoplastic lesions and cancer metastases. Analysis of sections from: *a*, breast ductal carcinoma *in situ*; *b*, prostatic intraepithelial neoplasia; *c*, lymph node metastasis from colon adenocarcinoma; *d*, lymph node metastasis from breast adenocarcinoma; *e*, bone metastasis from prostate adenocarcinoma; and *f*, vena caval invasion by renal clear cell carcinoma. *Red arrows*, HIF-1α-positive lymphocytes. ×200 (*d* and *f*); ×400 (*a*, *b*, *c*, and *e*).

specimens, weak staining was detected in adrenal cortical cells (3 of 8), renal distal tubular epithelium (3 of 9), pancreatic acinar cells (4 of 11), fetal hepatocytes (1 of 1), proliferating B cells from tonsil (2 of 3) and spleen (1 of 9), and seminiferous tubules of testis (7 of 7; Table 1).

Overexpression of HIF-1α protein was found in 69 (53%) of 131 primary malignant tumors representing 13 of 19 tumor types screened (Table 2). Cases of human prostate, breast, lung, colon, pancreas, brain, gastric, ovarian, and renal cell carcinomas, mesothelioma, and melanoma were positive. Immunohistochemistry was performed on adjacent sections of vena caval invasion from a renal cell carcinoma using MAb H1α67 that was preadsorbed with GST/HIF-1α protein. Whereas nonadsorbed MAb resulted in strong (++++) staining, preadsorbed MAb resulted in no (−) staining (data not shown).

Two-thirds of all of the regional lymph node and bone metastases were also positive for HIF-1α overexpression. HIF-1α was overexpressed in only 29% of primary breast cancers, whereas 69% of breast metastases were positive. All four of the preneoplastic and premalignant lesions found incidentally within biopsy specimens were positive for HIF-1α immunoreactivity, including two cases of breast comedotype ductal carcinoma *in situ*, one case of prostatic intraepithelial neoplasia, and one case of colonic adenoma (Fig. 3, *a* and *b*). In contrast, all 12 of the benign tumors (breast fibroadenoma and uterine leiomyoma) were negative (Table 2).

HIF-1α immunostaining was heterogeneous with signal concentrated primarily within the nucleus (Figs. 2 and 3). Cytoplasmic staining was also detected in colon (Fig. 2*e*), breast, pancreas, and prostate adenocarcinomas. The results were reproducible, and cytoplasmic staining was not observed in flanking normal tissue. Within tumors, clusters of HIF-1α positive cells were most dense at the invading edge of tumor margins, the periphery of necrotic regions, and surrounding areas of neovascularization (Fig. 2, *b* and *f*). Some lymphocytes in lymph nodes containing metastatic cancer cells were positive for HIF-1α immunostaining (Fig. 3*d*), but expression was not detected in nonmalignant stromal cells under the assay conditions used for this study.

To investigate whether HIF-1α expression levels correlated with the degree of tumor angiogenesis and/or disease progression, we evaluated nine brain tumors of different grades and degrees of neovascularization. HIF-1α expression was strongest in glioblastomas multiforme and hemangioblastomas (Fig. 2, *f* and *g*), which are respectively the most malignant and most highly vascularized primary tumors arising in the central nervous system. In glioblastomas, the staining was especially intense in pseudopalisading tumor cells surrounding areas of necrosis.

Comparison of HIF-1α Expression with the Expression of p53, bcl-2, and Ki67. On the basis of tissue availability, most tumor samples used for HIF-1α staining were also stained with anti-Ki67 MAb; some tumor samples, the majority of which were colon and breast cancers, were also stained with anti-p53 and/or anti-bcl-2 MAbs. These markers were scored in a blinded manner relative to the HIF-1α staining. Expression of HIF-1α protein was positively correlated with aberrant p53 accumulation ($P < 0.01$), but the correlation with bcl-2 expression was of marginal statistical significance ($P = 0.05$; Table 3). Nonparametric statistical analyses demonstrated a highly significant correlation of HIF-1α protein expression with Ki67 LI as a marker of cellular proliferation ($P < 0.001$; Table 3). HIF-1α expression also correlated with Ki67 LI in some normal cell types. Fetal hepatocytes, proliferating B cells in tonsil and spleen, and seminiferous tubules of testis demonstrated weak HIF-1α expression, and these cell types manifested high Ki67 LI relative to other normal tissue types.

DISCUSSION

HIF-1α protein was overexpressed in multiple types of human cancer and in regional and distant metastases. This study has identified increased HIF-1α expression (relative to adjacent normal tissue) in 13 tumor types including lung, prostate, breast, and colon carcinoma, which are the leading causes of U.S. cancer mortality. HIF-1α protein was also overexpressed in preneoplastic and premalignant lesions such as colonic adenoma, breast ductal carcinoma *in situ*, and prostate intraepithelial neoplasia. These data suggest that overexpression of HIF-1α can occur very early in carcinogenesis, before histological evidence of angiogenesis or invasion. Additional studies are

under way to assess whether HIF-1α may represent a novel biomarker for precancerous lesions that warrant clinical surveillance or therapeutic intervention. It is provocative that every benign noninvasive tumor analyzed was negative for HIF-1α overexpression.

HIF-1α activates the transcription of genes encoding transferrin, VEGF, endothelin-1, and inducible nitric oxide synthase, which are implicated in vasodilation, neovascularization, and tumor metastasis (15, 17). Particularly strong HIF-1α expression was observed in glioblastoma multiforme and hemangioblastoma. High VEGF mRNA expression has been reported in these highly malignant and vascularized brain tumors (26). HIF-1α-positive cells were prominent at tumor margins and surrounding areas of neovascularization. In colonic adenocarcinoma, cancer cells at the leading edge of infiltrating carcinoma manifested the most intense HIF-1α immunostaining. Comparison of tumor and flanking normal tissue allows the patient to serve as his own control and supports the hypothesis that HIF-1α overexpression is associated with angiogenesis, invasion, and metastasis. Experimentally, xenografts of mutant mouse hepatoma cells lacking HIF-1 expression manifested significantly reduced growth rates and vascularization compared with parental and revertant cells that expressed HIF-1 (18, 19). Conversely, human colon carcinoma cells transfected with a HIF-1α expression vector manifested significantly increased growth rates in nude mice as compared with parental cells.[4]

The patterns of immunohistochemical staining in different human cancers suggest that HIF-1α overexpression may result from both physiological (hypoxia) and nonphysiological mechanisms. It is clear from previous studies that many human tumors have regions of significant hypoxia (6–8). This pattern was most obvious in glioblastoma multiforme in which HIF-1α was detected in viable tumor cells that were closest to areas of necrosis and farthest from a blood vessel, as previously demonstrated for the expression of VEGF mRNA in these tumors (26, 27). In contrast, expression of HIF-1α in hemangioblastoma could not be attributed to hypoxia because tumor cells immediately adjacent to patent blood vessels stained intensely, which indicated that factors other than hypoxia may contribute to HIF-1α expression in human cancers.

A growing number of observations indicate that genetic alterations also affect HIF-1α expression in cancer cells:

(*a*) we have correlated HIF-1α expression with cell proliferation, both in cultured PCA cells (20) and *in vivo* (Table 3). Treatment of cultured cells with insulin, IGF-1, or IGF-2 induced expression of HIF-1α protein, which was in turn required for expression of IGF-2 mRNA (16), suggesting the involvement of HIF-1α in an autocrine growth factor loop. Remarkably, all of the 22 primary colon cancers analyzed overexpressed HIF-1α, and the most highly up-regulated gene in colon cancer encodes IGF-2 (28);

(*b*) cells transfected with the *v-Src* oncogene overexpressed HIF-1α, HIF-1 DNA-binding and transcriptional activity, and downstream genes including VEGF (18);

(*c*) HIF-1α overexpression was associated with aberrant p53 accumulation in human tumors (Table 3). The anti-p53 MAb used in this study recognizes an epitope in the NH_2 terminus of the wild-type and mutant forms of human p53 protein. Point mutations in the *TP53* gene occur frequently in human cancers, leading to increased expression of a nonfunctional p53 protein with a prolonged half-life that is detectable by immunohistochemistry. Thus, the presence of strong nuclear staining in the majority of cancer cells is frequently observed (29). Expression of HIF-1α protein, HIF-1 DNA-binding activity, and VEGF mRNA are increased in p53−/− knockout colon carcinoma cells as compared with the parental p53+/+ cells[4]; and

(*d*) in renal clear cell carcinoma cell lines, the loss of von Hippel-Lindau tumor suppressor function results in constitutive high-level expression of HIF-1α (30). The primary (Fig. 2*i*) and metastatic (Fig. 3*f*) renal clear cell carcinomas analyzed here represent the first demonstration of this overexpression *in vivo*. Thus, in addition to hypoxia, both oncogene activation and tumor suppressor gene inactivation are associated with increased HIF-1α expression.

Some tumors did not stain positive for HIF-1α in this study. These tumors may overexpress HIF-1α but at levels that were below the limits of detection by immunohistochemistry using current methodology. Alternatively, other bHLH-PAS transcription factors that may have similar biological properties to HIF-1α, such as HIF-2α (also known as EPAS1, HLF, HRF, and MOP2) or HIF-3α (23, 31–33), may also mediate hypoxic adaptation. Nevertheless, HIF-1α was overexpressed in the majority of preneoplastic, malignant, and metastatic cancers analyzed. Given the overexpression of HIF-1α in common human cancers relative to normal tissues and its vital importance in mediating hypoxic adaptation, additional investigations of HIF-1α as a biomarker of metastatic potential and as a novel target for therapeutics are warranted.

ACKNOWLEDGMENTS

The authors acknowledge Dr. Mary Ann Accavitti and the Hybridoma Core Facility (University of Alabama at Birmingham, Birmingham, AL) for MAb production; the important contributions of Drs. Josef Prchal, Christopher Bradfield, Donald S. Coffey, Frank Kujhada, William G. Nelson, and Steven Piantadosi; and the technical assistance of Jurga Sauvengot, Natalia Rioseco-Camacho, Bahar Mikhak, Colleen Hanrahan, and Kimberly Heaney.

REFERENCES

1. Warburg, O. H. The Metabolism of Tumours (translated from the German edition by F. Dickens), pp.11–25. London: Constable & Co. Ltd., 1930.
2. Racker, E. A New Look at Mechanisms in Bioenergetics, pp.153–175. New York: Academic Press, 1976.
3. Dang, C. V., and Semenza, G. L. Oncogenic alterations of metabolism. Trends Biochem. Sci., *24:* 68–72, 1999.
4. Hanahan, D., and Folkman, J. Patterns and emerging mechanisms of the angiogenic switch during tumorigenesis. Cell, *86:* 353–364, 1996.
5. Zetter, B. R. Angiogenesis and tumor metastasis. Annu. Rev. Med., *49:* 407–424, 1998.
6. Brizel, D. M., Scully, S. P., Harrelson, J. M., Layfield, L. J., Bean, J. M., Prosnitz, L. R., and Dewhirst, M. W. Tumor oxygenation predicts for the likelihood of distant metastases in human soft tissue sarcoma. Cancer Res., *56:* 941–943, 1996.
7. Hockel, M., Schlenger, K., Aral, B., Mitze, M., Schaffer, U., and Vaupel, P. Association between tumor hypoxia and malignant progression in advanced cancer of the uterine cervix. Cancer Res., *56:* 4509–4515, 1996.
8. Helmlinger, G., Yuan, F., Dellian, M., and Jain, R. K. Interstitial pH and pO_2 gradients in solid tumors *in vivo*: high-resolution measurements reveal a lack of correlation. Nat. Med., *3:* 177–182, 1997.
9. Brown, J. M., and Giaccia, A. J. The unique physiology of solid tumors: opportunities (and problems) for cancer therapy. Cancer Res., *58:* 1408–1416, 1998.
10. Wang, G. L., Jiang, B. H., Rue, E. A., and Semenza, G. L. Hypoxia-inducible factor 1 is a basic-helix-loop-helix-PAS heterodimer regulated by cellular O_2 tension. Proc. Natl. Acad. Sci. USA, *92:* 5510–5514, 1995.
11. Iyer, N. V., Kotch, L. E., Agani, F., Leung, S. W., Laughner, E., Wenger, R. H., Gassmann, M., Gearhart, J. D., Lawler, A. M., Yu, A. Y., and Semenza, G. L. Cellular and developmental control of O_2 homeostasis by hypoxia-inducible factor 1α. Genes Dev., *12:* 149–162, 1998.
12. Ryan, H. E., Lo, J., and Johnson, R. S. HIF-1α is required for solid tumor formation and embryonic vascularization. EMBO J., *17:* 3005–3015, 1998.
13. Carmeliet, P., Dor, Y., Herbert, J. M., Fukumura, D., Brusselmans, K., Dewerchin, M., Neeman, M., Bono, F., Abramovitch, R., Maxwell, P., Koch, C. J., Ratcliffe, P., Moons, L., Jain, R. K., Collen, D., and Keshet, E. Role of HIF-1α in hypoxia-mediated apoptosis, cell proliferation and tumour angiogenesis. Nature (Lond.), *394:* 485–490, 1998.
14. Jiang, B. H., Semenza, G. L., Bauer, C., and Marti, H. H. Hypoxia-inducible factor 1 levels vary exponentially over a physiologically relevant range of O_2 tension. Am. J. Physiol., *271:* C1172–C1180, 1996.
15. Semenza, G. L. Regulation of mammalian O_2 homeostasis by hypoxia-inducible factor 1. Annu. Rev. Cell Dev. Biol., *15:* 551–578, 1999.
16. Feldser, D., Agani, F., Iyer, N. V., Pak, B., Ferreira, G., and Semenza, G. L. Reciprocal positive regulation of hypoxia-inducible factor 1α and insulin-like growth factor 2. Cancer Res., *59:* 3915–3918, 1999.

[4] R. Ravi, A. Bedi, and G. L. Semenza, unpublished data.

17. Kerbel, R. S. New targets, drugs, and approaches for the treatment of cancer: an overview. Cancer Metastasis Rev., *17:* 145–147, 1998.
18. Jiang, B. H., Agani, F., Passaniti, A., and Semenza, G. L. V-SRC induces expression of hypoxia-inducible factor 1 (HIF-1) and transcription of genes encoding vascular endothelial growth factor and enolase 1: involvement of HIF-1 in tumor progression. Cancer Res., *57:* 5328–5335, 1997.
19. Maxwell, P. H., Dachs, G. U., Gleadle, J. M., Nicholls, L. G., Harris, A. L., Stratford, I. J., Hankinson, O., Pugh, C. W., and Ratcliffe, P. J. Hypoxia-inducible factor-1 modulates gene expression in solid tumors and influences both angiogenesis and tumor growth. Proc. Natl. Acad. Sci. USA, *94:* 8104–8109, 1997.
20. Zhong, H., Agani, F., Baccala, A. A., Laughner, E., Rioseco-Camacho, N., Isaacs, W. B., Simons, J. W., and Semenza, G. L. Increased expression of hypoxia inducible factor-1α in rat and human prostate cancer. Cancer Res., *58:* 5280–5284, 1998.
21. Forsythe, J. A., Jiang, B. H., Iyer, N. V., Agani, F., Leung, S. W., Koos, R. D., and Semenza, G. L. Activation of vascular endothelial growth factor gene transcription by hypoxia-inducible factor 1. Mol. Cell. Biol., *16:* 4604–4613, 1996.
22. Jiang, B. H., Rue, E., Wang, G. L., Roe, R., and Semenza, G. L. Dimerization, DNA binding, and transactivation properties of hypoxia-inducible factor 1. J. Biol. Chem., *271:* 17771–17778, 1996.
23. Hogenesch, J. B., Chan, W. K., Jackiw, V. H., Brown, R. C., Gu, Y. Z., Pray-Grant, M., Perdew, G. H., and Bradfield, C. A. Characterization of a subset of the basic-helix-loop-helix-PAS superfamily that interacts with components of the dioxin signaling pathway. J. Biol. Chem., *272:* 8581–8593, 1997.
24. Lehmann, E. L., and D'Abrera, H. J. M. Nonparametrics: Statistical Methods Based on Ranks, Rev. Ed. 1, pp. 58–76. Upper Saddle River, NJ: Prentice Hall, 1998.
25. Wang, G. L., and Semenza, G. L. Purification and characterization of hypoxia-inducible factor 1. J. Biol. Chem., *270:* 1230–1237, 1995.
26. Chan, A. S., Leung, S. Y., Wong, M. P., Yuen, S. T., Cheung, N., Fan, Y. W., and Chung, L. P. Expression of vascular endothelial growth factor and its receptors in the anaplastic progression of astrocytoma, oligodendroglioma, and ependymoma. Am. J. Surg. Pathol., *22:* 816–826, 1998.
27. Shweiki, D., Itin, A., Soffer, D., and Keshet, E. Vascular endothelial growth factor induced by hypoxia may mediate hypoxia-initiated angiogenesis. Nature (Lond.), *359:* 843–845, 1992.
28. Zhang, L., Zhou, W., Velculescu, V. E., Kern, S. E., Hruban, R. H., Hamilton, S. R., Vogelstein, B., and Kinzler, K. W. Gene expression profiles in normal and cancer cells. Science (Washington DC), *276:* 1268–1272, 1997.
29. Baas, I. O., Mulder, J. W., Offerhaus, G. J., Vogelstein, B., and Hamilton, S. R. An evaluation of six antibodies for immunohistochemistry of mutant p53 gene product in archival colorectal neoplasms. J. Pathol., *172:* 5–12, 1994.
30. Maxwell, P. H., Wiesener, M. S., Chang, G. W., Clifford, S. C., Vaux, E. C., Cockman, M. E., Wykoff, C. C., Pugh, C. W., Maher, E. R., and Ratcliffe, P. J. The tumour suppressor protein VHL targets hypoxia-inducible factors for oxygen-dependent proteolysis. Nature (Lond.), *399:* 271–275, 1999.
31. Flamme, I., Frohlich, T., von Reutern, M., Kappel, A., Damert, A., and Risau, W. HRF, a putative basic helix-loop-helix-PAS-domain transcription factor is closely related to hypoxia-inducible factor-1α and developmentally expressed in blood vessels. Mech. Dev., *63:* 51–60, 1997.
32. Gu, Y. Z., Moran, S. M., Hogenesch, J. B., Wartman, L., and Bradfield, C. A. Molecular characterization and chromosomal localization of a third α-class hypoxia inducible factor subunit, HIF3α. Gene Expr., *7:* 205–213, 1998.
33. Tian, H., McKnight, S. L., and Russell, D. W. Endothelial PAS domain protein 1 (EPAS1), a transcription factor selectively expressed in endothelial cells. Genes Dev., *11:* 72–82, 1997.
34. Yu, A. Y., Frid, M. G., Shimoda, L. A., Wiener, C. M., Stenmark, K., and Semenza, G. L. Temporal, spatial, and oxygen-regulated expression of hypoxia-inducible factor-1 in the lung. Am. J. Physiol., *275:* L818–L826, 1998.

[CANCER RESEARCH 58, 5280–5284, December 1, 1998]

Increased Expression of Hypoxia Inducible Factor-1α in Rat and Human Prostate Cancer[1]

Hua Zhong, Faton Agani, Angelo A. Baccala, Erik Laughner, Natalia Rioseco-Camacho, William B. Isaacs, Jonathan W. Simons,[2] and Gregg L. Semenza

James Buchanan Brady Urological Institute Research Laboratories [H. Z., A. A. B., N. R.-C., W. B. I., J. W. S.], the Center for Medical Genetics [G. L. S.], Department of Pediatrics and Medicine [F. A., E. L., G. L. S.], and Oncology Center [H. Z., J. W. S.], Johns Hopkins Hospital, Baltimore, Maryland 21287-2411

Abstract

Hypoxia-inducible factor 1 (HIF-1) is a transcription factor that regulates genes involved in adaptation to hypoxia. Expression of HIF-1α was evaluated in rat and human prostate cancer cell lines. Increased expression of HIF-1α mRNA in rat prostate cancer cell lines and hypoxia-induced expression of HIF-1α protein in human prostate cancer cell lines are associated with increased cell growth rates and metastatic potential. HIF-1α mRNA was undetectable in the normal rat ventral prostate by Northern blot hybridization. HIF-1α protein expression and HIF-1 DNA binding activity were detected in normoxic PC-3 cells. Human prostate cancer cells plated at low density manifested higher functional HIF-1α expression than cells plated at high density independent of O_2 tension. HIF-1α may become dysregulated in prostate cancer and thus drive the transcription of hypoxia-adaptive genes involved in tumor progression. This is also the first evidence that human cancer cells can express functional HIF-1α protein under normoxic conditions.

Introduction

Tissue hypoxia is critical in tumor formation, where it has been associated with malignant progression and resistance to radiotherapy and chemotherapy. For example, patients with cervical carcinomas measured *in vivo* to have pO_2 <10 mm Hg have poorer disease-free survival (1). The intratumoral pO_2 has been determined in different cancer xenograft models to vary between 14 mm Hg (2% O_2) and 0 mm Hg (2, 3). These pO_2 levels activate expression of HIF-1[3] both in *in vitro* and *in vivo* (4–6). HIF-1α protein levels, which determine HIF-1 DNA binding activity and transcription of HIF-1-regulated genes, increase exponentially as intracellular pO_2 is reduced (4, 7).

HIF-1 is a heterodimeric basic helix-loop-helix transcription factor that regulates many genes adaptive for hypoxic survival via binding to hypoxia response elements often located within the promoters of those genes (4, 8, 9). HIF-1-regulated genes include glucose transporters 1 and 3 and glycolytic enzymes such as LDH-A, ENO-1, pyruvate kinase, phosphofructokinase L, phosphoglycerate kinase 1, aldolase A, and GAPDH. These gene products are essential for the high glycolytic rates of cancer cells (Warburg effect; Ref. 10). Expression of these HIF-1-regulated glycolytic enzyme genes is thus essential in the bioenergetics of malignant transformation. Although the Warburg effect was described in solid tumor seven decades ago, little molecular information has been reported on altered gene expression in hypoxic cells of common solid tumors such as PCA. Recent studies suggest that HIF-1 is also involved in tumor angiogenesis and progression. HIF-1 activity-deficient hepatoma (Hepa-1) cells are suppressed in angiogenesis and growth characteristics (11, 12). Tumor vascularization may be stimulated by HIF-1α in part as a result of up-regulation VEGF (9, 11, 13, 14).

The pivotal role of HIF-1 in oxygen homeostasis suggests that its expression may be critical in the lethal phenotype of PCA. Several published results implicate HIF-1 in metastatic PCA, which causes the death of about 40,000 United States men yearly. First, in the only available spontaneously arising animal model of PCA, intratumoral pO_2 levels are low enough to induce HIF-1 (15). In addition, pO_2 values of the anaplastic and highly metastatic Dunning rat prostate tumors are even lower than those of well-differentiated and minimally metastatic tumors (15). Second, the *endothelin-1* gene, which has previously been demonstrated to be involved in the pathophysiology of osteoblastic human PCA bone metastases (16), has been shown to be transcriptionally regulated by HIF-1 (17). Third, elevated GAPDH expression, which is regulated by HIF-1 (9), is associated with increased cell motility, invasion, and metastatic potential of rat prostatic adenocarcinoma (18). Fourth, another HIF-1-regulated glycolytic enzyme gene, *LDH-A*, has been used extensively as a serum marker of bone metastatic PCA disease activity (19). Yet, to our knowledge, analysis of HIF-1α expression in PCA has not been reported. Therefore, we tested the hypothesis that increased HIF-1α expression was associated with PCA progression and metastasis.

Materials and Methods

Cells, Culture Condition, and Animals. Dunning rat PCA cell lines (AT2.1, AT6.1, AT6.3, G, Mat-Lu, and Mat-LyLu) were generously provided by Dr. J. T. Isaacs (Johns Hopkins Oncology Center, Baltimore, MD) and were cultured as described previously (20). The human PCA cell lines (PC-3, DU-145, TSU, LNCaP, and PPC-1) were maintained with RPMI 1640 supplemented with 10% heat-inactivated FCS. The cells were subjected to hypoxia (1% O_2 for 24 h), and Hep3B cells were described previously (4). The low-density (50% confluence with sparse cell-cell contact) and the high-density cells (90% confluence with plate-wide cell-cell contact) were monitored by phase contrast microscopy by two independent observers. Rat ventral prostates were isolated from Copenhagen (Harlan) rats at 8 weeks of age under methoxyflurane anesthesia. The prostate samples were immediately stored in liquid nitrogen. The animal study protocols were conducted according to approved institutional guidelines for animal use.

Total RNA Isolation and Northern Blot Analysis. Total RNA was isolated with RNeasy mini kit (Qiagen). Northern blot was performed as described previously (5). Human HIF-1α cDNA probe (593-bp *Hin*dIII/*Msp*I fragment) and β-actin cDNA probe (1.8-kb; Clontech) were used. Autoradiographic signals were quantitated by Eagle eye computerized densitometry (Stratagene). The densitometric values of HIF-1α were normalized to the values of β-actin to control for variation in sample loading and transfer.

Immunoblot Analysis and EMSA. Crude nuclear extract and immunoblot analysis were performed as described previously (4). Proteins were detected

Received 9/16/98; accepted 10/16/98.

The costs of publication of this article were defrayed in part by the payment of page charges. This article must therefore be hereby marked *advertisement* in accordance with 18 U.S.C. Section 1734 solely to indicate this fact.

[1] This work was supported by Prostate Cancer SPORE Grant CA-58236 from the NIH, a grant from the CaPCure Foundation, and Prostate Cancer Grant DAMD 17-98-1-8475 from the Department of Defense.

[2] To whom requests for reprints should be addressed, at James Buchanan Brady Urological Institute, Marburg 409, Johns Hopkins Hospital, 600 North Wolfe Street, Baltimore, MD 21287-2411.

[3] The abbreviations used are: HIF-1, hypoxia-inducible factor 1; PCA, prostate cancer; LDH-A, lactate dehydrogenase A; ENO-1, enolase 1; GAPDH, glyceraldehyde-3-phosphate dehydrogenase; PCA, prostate cancer; VEGF, vascular endothelial growth factor; EMSA, electrophoretic mobility shift assay.

Table 1 *Biological characteristics of Dunning rat and human prostate cancer cell lines*[a]

Cell lines	Doubling time (days)	Androgen sensitivity	Metastatic ability	PSA[b]	Host survival (days)
AT2.1	2.5 ± 0.2	No	Low	NA[b]	63 ± 3
AT6.1	4.0 ± 0.3	No	High	NA	
AT6.3	4.0 ± 0.3	No	High	NA	
G	4.0 ± 0.2	Yes	Low	NA	120 ± 10
MatLu	2.7 ± 0.3	No	High	NA	35 ± 1
MatLyLu	1.5 ± 0.1	No	High	NA	26 ± 1
PC-3	1.1	No		−	
DU-145	1.2	No		−	
TSU	1.5	No		−	
LNCaP	2.8	Yes		+	
PPC-1	1.3	No		−	

[a] References 20–25.
[b] PSA, prostate-specific antigen; NA, not applicable.

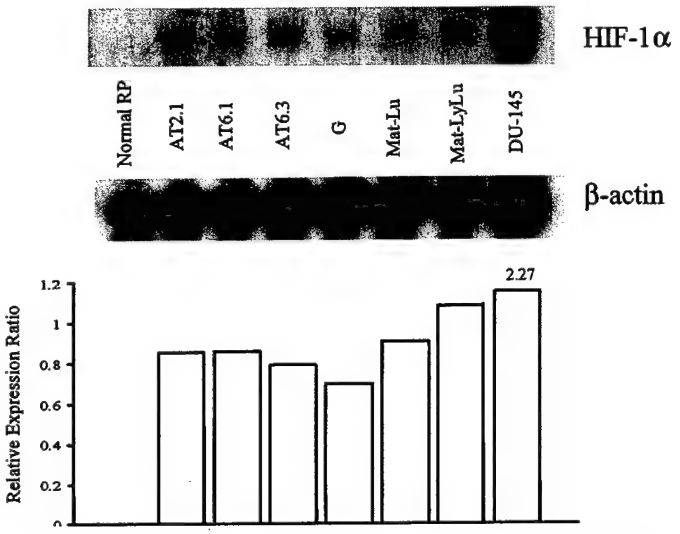

Fig. 1. HIF-1α mRNA expression in rat prostate cancer cell lines. All cells were incubated under standard culture conditions (20% O_2 and 5% CO_2; 37°C). Total RNA (15 μg) was isolated from normal rat prostate (*Normal RP*), Dunning rat prostate cancer cell lines (AT2.1, AT6.1, AT6.3, G, Mat-Lu, and Mat-LyLu), and human prostate cancer cell line (DU-145). RNA samples were blotted onto a nylon membrane and hybridized a ^{32}P-labeled HIF-1α cDNA probe as described in "Materials and Methods." The blots were rehybridized under the same conditions with a ^{32}P-labeled β-actin probe. Radioactive signals were detected by autoradiography and quantified by densitometry. The relative expression ratio represents the mean of two independent experiments.

with anti-HIF-1α (4) and reprobed with anti-topoisomerase I (Topogen). EMSA was performed using crude nuclear extract and oligonucleotide probe W18 as described previously (5).

Immunocytochemistry. PC-3 cells (0.5 × 10^6/ml) grown overnight on Lab-Tek chambered coverglass slides (Nunc.) were cultured for 24 h at 20 or 1% O_2, washed in cold PBS, fixed in ice-cold acetone for 5 min, washed in PBS again, and stored at 4°C for use within 1 week for staining. Immunostaining was performed using the rabbit ABC immunostain system (Santa Cruz Biotechnology), following the recommended protocol. Cells were incubated overnight with 1:100 dilution of rabbit HIF-1α polyclonal antibody (4) in a humid chamber at 4°C. After the expected stain intensity developed, cells were counterstained with Mayer's hematoxylin.

Results

HIF-1α mRNA Expression Is Elevated in Rat and Human Prostate Cancer Cells. HIF-1 consists of HIF-1α and HIF-1β subunits, and HIF-1α is the O_2-regulated subunit (4, 5, 7). We first analyzed whether HIF-1α mRNA is expressed in cultured rat and human PCA cell lines as compared with normal prostate tissue. Dunning rat PCA cell lines are derived from a spontaneously arising parental R-3327 tumor (20). These sublines exhibit a wide range of tumor phenotypes with regard to androgen sensitivity, growth rate, histological and biochemical differentiation, and metastatic ability (Table 1). Expression of HIF-1α mRNA was found in every tested rat and human PCA cell line under standard culture condition (20% O_2 and 5% CO_2; 37°C), whereas no detectable HIF-1α mRNA was detected in the normal adult rat ventral prostate in two independent experiments (Fig. 1).

The basal levels of HIF-1α mRNA expression varied between the different cell lines. The Mat-Lu and Mat-LyLu cells have higher metastatic ability, faster growth rates, and higher basal HIF-1α mRNA levels than those sublines with low metastatic potential (AT2.1 and G) or those which have high metastatic potential but have slower growth rates (AT6.1 and AT6.3). The relative HIF-1α mRNA expression ratio of Mat-LyLu cells, which have the highest metastatic ability (>90%) and the highest growth rate (1.5 ± 0.1 days) among these cells, was 50% greater than that of G cells. G cells have the lowest metastatic potential (<5%) and slow growth rate (4.0 ± 0.2 days; Ref. 26).

Expression of HIF-1α Protein in Human Prostate Cancer Cells. HIF-1α protein expression and HIF-1 DNA binding activity were analyzed in cultured human PCA cell lines. Every cell line tested was

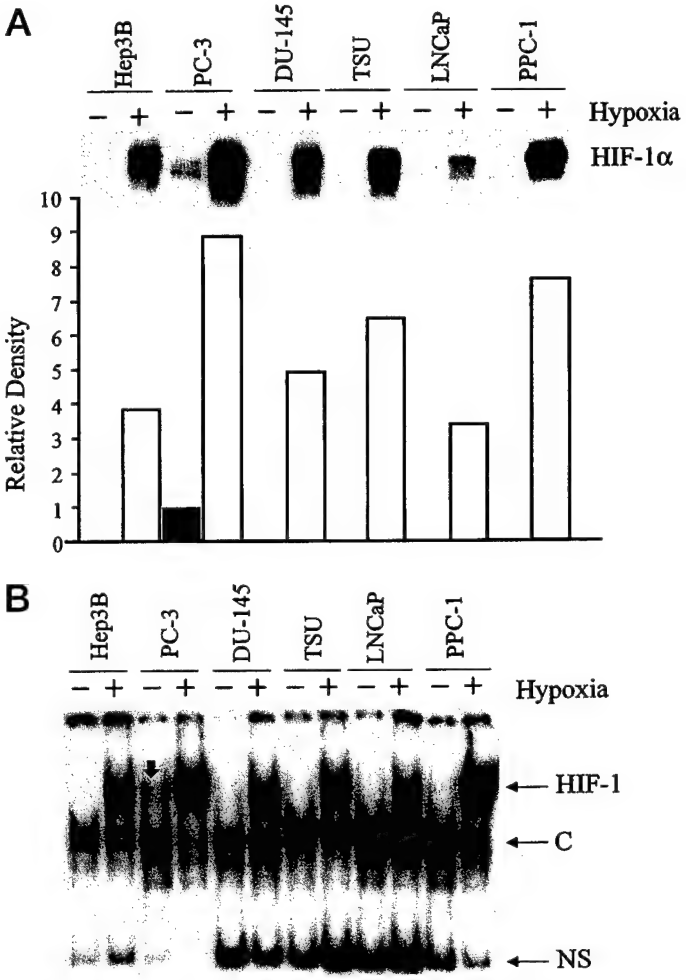

Fig. 2. Analysis of HIF-1α protein expression and HIF-1 DNA binding activity in human prostate cancer cell lines. Cells in high density were incubated under normoxic (−) or hypoxic (+) conditions (20% and 1% O_2, respectively) at 37°C for 24 h before cell harvesting. In *A*, HIF-1α was detected in nuclear extracts by immunoblot assay. Relative density represents the mean of two independent experiments. In *B*, HIF-1 was detected in nuclear extracts by EMSA using an oligonucleotide probe. *C*, constitutive DNA binding activity. *NS*, nonspecific DNA binding activity. *Thick arrow*, HIF-1 DNA binding activity was detected in normoxic PC-3 cells.

Fig. 3. HIF-1α immunostaining in PC-3 cells. Cells were exposed to 20% (*A* and *B*) or 1% (*C*) O_2 for 24 h. *A*, negative controls with no primary antibody. Nuclear localization of HIF-1α staining shows intense staining in nucleoli. *Arrow*, nucleoli staining.

shown to induce HIF-1α protein expression and HIF-1 DNA binding activity in response to 24 h of continuous hypoxia (1% O_2), with Hep3B serving as a positive control (Fig. 2). The levels of hypoxia-induced HIF-1α protein at 24 h varied between the different human PCA cell lines. Hypoxia-induced HIF-1α protein levels were highest in PC-3 cells and lowest in LNCaP cells. Thus far, detectable HIF-1α protein in normoxic cells is only reported present in oncogene-transformed fibroblasts (12). Surprisingly, HIF-1α protein and HIF-1 DNA binding activity were detected in PC-3 cells under normoxic conditions (20% O_2; Figs. 2 and 4). Furthermore, HIF-1α protein was also detected in both hypoxic and normoxic PC-3 cells by immunocytochemistry, with staining being prominent in the nucleus. The nucleoli appear to have the most intensive staining (Fig. 3).

In conducting these experiments, we noted that another factor affected the degree of induced HIF-1α expression in PCA cells: cell plating density *in vitro*. HIF-1α protein levels and HIF-1 DNA binding activity were assayed in cultured cells at different plating densities. In both PC-3 and LNCaP cells, which express respectively the most and least induced protein, increased HIF-1α protein and HIF-1 DNA binding activity were present in cells plated at low density compared with cells plated at high density under both hypoxic and normoxic conditions (Fig. 4).

Discussion

In this study, we characterized the expression of HIF-1α and HIF-1 DNA binding activity in a panel of rat and human PCA cell lines that vary greatly in their phenotypes. Constitutive HIF-1α mRNA was expressed in every studied Dunning rat PCA subline at variable levels, which is consistent with their heterogeneity with respect to many biological properties including cell growth rates and metastatic potential. The lethal phenotype of PCA is associated with androgen independence. The only two available androgen-dependent cell lines (Dunning rat PCA cell line G and human PCA cell line LNCaP) had the lowest HIF-1α gene expression in mRNA (G cells) or protein (LNCaP cells) levels, suggesting that HIF-1α expression may increase in progression to androgen-refractory PCA. Our present results have shown that HIF-1α mRNA was expressed at higher levels in those rat PCA cells characterized by fast growth and high metastatic potential. In contrast, HIF-1α mRNA expression was not detectable in total RNA by Northern blot in normal adult rat ventral prostate. Furthermore, in human prostatectomy specimens, we have found lower HIF-1α mRNA levels in normal prostate tissue compared with adjacent cancer tissue.[4] Taken together, these data strongly suggest that elevated HIF-1α mRNA expression in PCA cells may be important in their neoplastic phenotype and may be up-regulated in the process of cell transformation and tumorigenesis.

More than seven decades ago, Warburg demonstrated that there was an increased rate of glycolysis in tumor cells, resulting in the exces-

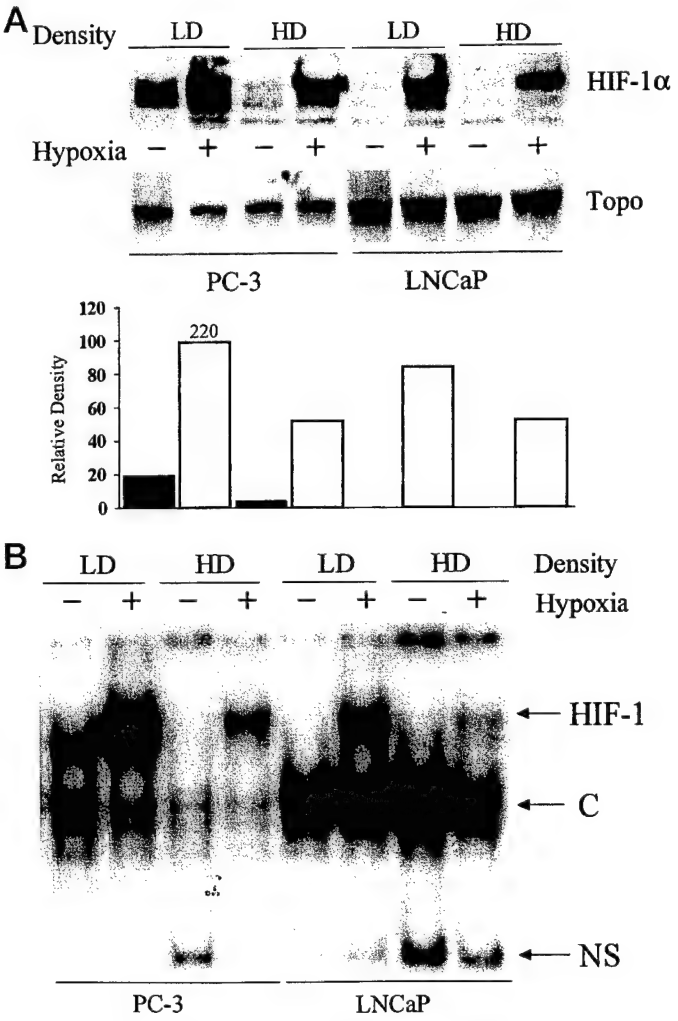

Fig. 4. HIF-1α protein expression and HIF-1 DNA binding activity in human prostate cancer cells. Cells were incubated under normoxic (−) or hypoxic (+) conditions (20% and 1% O_2, respectively) at low density (*LD*) or high density (*HD*) culture conditions at 37°C for 24 h before cell harvesting. In *A*, HIF-1α (*top panel*) was detected in nuclear extracts by immunoblot assay. Topoisomerase I (*bottom panel*) was detected after the same membrane was stripped. In *B*, HIF-1 was detected in nuclear extracts by EMSA using an oligonucleotide probe. *C*, constitutive DNA binding activity. *NS*, nonspecific DNA binding activity.

[4] Unpublished data.

sive production of lactic acid from glucose under normoxic conditions (10). The molecular genetics of the Warburg effect has remained poorly elucidated. Previous studies have demonstrated the ability of HIF-1 to up-regulate genes encoding virtually all of the glycolytic enzymes (7–9). GAPDH, ENO-1, and LDH-A mRNA expression are also up-regulated by hypoxia in all five human PCA cell lines.[5] These results, taken together, suggest that HIF-1α may play a critical role in mediating the Warburg effect in PCA.

Normally, HIF-1α protein expression is very tightly regulated by cellular O_2 tension and is undetectable by Western blots in normoxic cells (4–6). Indeed, hypoxia induced stable and functional HIF-1α protein across the panel of biologically diverse human PCA cell lines. However, we discovered constitutive expression of HIF-1α protein in human PCA PC-3 cells at normoxic conditions (20% O_2). To our knowledge, this is the first evidence that stable HIF-1α protein expression and function can be decoupled from O_2 tension in human cancer cells, and yet can be further induced by hypoxia. Apparently, an O_2-independent mechanism is affecting HIF-1α protein in PC-3 cells. Alterations in the *HIF-1α* gene sequence and potential signal transduction pathways in PC-3 cells are under investigation. Of note, PC-3 cells are cloned from a PCA bone metastases, and compared with the other human PCA cell lines studied, are characterized by the highest rates of Matrigel-independent xenograft formation, vascularization, and metastasis.[6]

Other genetic factors can influence *HIF-1α* gene expression. For example, the v-Src oncogene product has been demonstrated to increase the expression of HIF-1α mRNA and protein, HIF-1 DNA binding activity, and the expression of HIF-1-regulated genes (*VEGF* and *ENO1*) under both hypoxic and normoxic conditions (12). These observations suggest that genetic alterations in tumor cells may lead to increased HIF-1 activity, which may in turn allow tumors to adapt to tissue hypoxia, such that they can maintain cellular proliferation, prevent apoptosis, and undergo angiogenesis and metastasis. Heterogeneity of genetic alterations between our PCA cell lines may account for the observed differences between tumors in expression of HIF-1α mRNA and protein.

In addition to genes encoding glucose transporter, glycolytic enzymes, and VEGF (7–9, 13), HIF-1 target genes include those encoding inducible nitric oxide synthetase, heme oxygenase-1, and endothelin-1 (17, 27, 28). These genes encode very important factors for angiogenesis, vasodilation, tumor progression, and osteoblastic activation in PCA bone metastasis (16, 29, 30). Prostatic acid phosphatase has been used as a biomarker for osseous PCA metastasis, late stage, and tumor progression or regression in response to therapy in PCA. Coincidentally, acid phosphatase is induced in hypoxic tumor cells (31), but it is not known whether prostatic acid phosphatase gene expression is regulated by HIF-1. Prostate-specific antigen protein expression, which reflects prostate cell differentiation, is not apparently up-regulated by hypoxia in LNCaP cells (data not shown). Our demonstration of HIF-1α protein and HIF-1 DNA binding activity in human hypoxic PCA cells provides a fundamental requirement for potential gene therapy approaches targeting hypoxic PCA cells using expression vectors containing HIF-1 binding sites (32).

We discovered greater HIF-1α protein expression in cells plated at low density relative to high density. The positive regulation of HIF-1α expression as a function of low cell plating density is not clear. Studies are under way to dissect the mechanisms involved. However, differences in signaling pathways involved in cell cycle kinetics and/or cell-cell contact inhibition may contribute to the differential in HIF-1α protein induced by hypoxia. In the present study, the cells with higher growth rates consistently manifested higher HIF-1α expression than the cells with lower growth rates. Interestingly, in embryonic stem cells, complete HIF-1α deficiency was associated with significantly decreased rates of cell proliferation (9).

These preliminary results have characterized *HIF-1α* gene expression in rat and human prostate cancer cells. Unexpectedly, HIF-1α protein expression is detected in normoxic PC-3 cells, suggesting that HIF-1α may be a direct or indirect target of genomic alterations occurring during tumor progression. The functional consequences of increased HIF-1α expression in PCA now require elucidation based on these studies. Characterization of the HIF-1α-regulated genes involved in cell cycle, apoptotic pathways, angiogenesis, motility, bioenergetics, signal transduction, cytokine expression, and metastases all may provide insights into the molecular mechanisms that allow PCA cells to adapt to hypoxia. Finally, the development of therapeutics directed against HIF-1α in metastatic PCA may provide novel approaches to the management of this presently intractable malignancy.

Acknowledgments

We acknowledge the helpful comments of Dr. Donald S. Coffey and the assistance of Kimberly Cordwell in preparation of the manuscript. This work is dedicated to the memory, papers, and teachings of Efraim Racker.

References

1. Höckel, M., Schlenger, K., Aral, B., Mitze, M., Schäffer, U., and Vaupel P. Association between tumor hypoxia and malignant progression in advanced cancer of the uterine cervix. Cancer Res., *56:* 4509–4515, 1996.
2. Helmlinger, G., Yuan, F., Dellian, M., and Jain, R. K. Interstitial pH and p_{O2} gradients in solid tumors *in vivo*: high-resolution measurements reveal a lack of correlation. Nat. Med., *3:* 177–182, 1997.
3. Mason, R. P., Antich, P. P., Babcock, E. E., Constantinescu, A., Peschke, P., and Hahn, E. W. Non-invasive determination of tumor oxygen tension and local variation with growth. Int. J. Radiat. Oncol. Biol. Phys., *29:* 95–103, 1994.
4. Jiang, B. H., Semenza, G. L., Bauer, C., and Marti, H. H. Hypoxia-inducible factor 1 levels vary exponentially over a physiologically relevant range of O_2 tension. Am. J. Physiol., *271:* C1172–C1180, 1996.
5. Wang, G. L., Jiang, B. H., Rue, E. A., and Semenza, G. L. Hypoxia-inducible factor 1 is a basic-helix-loop-helix-PAS heterodimer regulated by cellular O_2 tension. Proc. Natl. Acad. Sci. USA, *92:* 5510–5514, 1995.
6. Wiener, C. M., Booth, G., and Semenza, G. L. *In vivo* expression of mRNAs encoding hypoxia-inducible factor 1. Biochem. Biophys. Res. Commun., *225:* 485–488, 1996.
7. Semenza, G. L., Jiang, B. H., Leung, S. W., Passantino, R., Concordet, J. P., Maire, P., and Giallongo, A. Hypoxia response elements in the aldolase A, enolase 1, and lactate dehydrogenase A gene promoters contain essential binding sites for hypoxia-inducible factor 1. J. Biol. Chem., *271:* 32529–32537, 1996.
8. Semenza, G. L., Roth, P. H., Fang, H. M., and Wang, G. L. Transcriptional regulation of genes encoding glycolytic enzymes by hypoxia-inducible factor 1. J. Biol. Chem., *269:* 23757–23763, 1994.
9. Iyer, N., Kotch, L., Agani, F., Leung, S. W., Laughner, E., Wenger, R. H., Gassmann, M., Gearhart, J. D., Lawler, A. M., Yu, A. Y., and Semenza, G. L. Cellular and developmental control of O_2 homeostatasis by hypoxia-inducible factor 1α. Genes Dev., *12:* 149–162, 1998.
10. Warburg, O. H. The metabolism of tumours. Translated from the German edition by F. Dickens. London: Constable & Co., Ltd., 1930, pp. 11–25.
11. Maxwell, P. H., Dachs, G. U., Gleadle, J. M., Nicholls, L. G., Harris, A. L., Stratford, I. J., Hankinson, O., Pugh, C. W., and Ratcliffe, P. J. Hypoxia-inducible factor-1 modulates gene expression in solid tumors and influences both angiogenesis and tumor growth. Proc. Natl. Acad. Sci. USA, *94:* 8104–8109, 1997.
12. Jiang, B. H., Agani, F., Passaniti, A., and Semenza, G. L. v-SRC induces expression of hypoxia-inducible factor (HIF-1) and transcription of genes encoding vascular endothelial growth factor and enolase 1: involvement of HIF-1 in tumor progression. Cancer Res., *57:* 5328–5335, 1997.
13. Carmeliet, P., Dor, Y., Herbert, J. M., Fukumura, D., Brusselmans, K., Dewerchin, M., Neeman, M., Bono, F., Abramovitch, R., Maxwell, P., Koch, C. J., Ratcliffe, P., Moons, L., Jain, R. K., Collen, D., and Keshet, E. Role of HIF-1α in hypoxia-mediated apoptosis, cell proliferation and tumor angiogenesis. Nature (Lond.), *394:* 485–490, 1998.
14. Forsythe, J. A., Jiang, B. H., Iyer, N. V., Agani, F., Leung, S. W., Koos, R. D., and Semenza, G. L. Activation of vascular endothelial growth factor gene transcription by hypoxia-inducible factor 1. Mol. Cell. Biol., *16:* 4604–4613, 1996.
15. Yeh, K. A., Biade, S., Lanciano, R. M., Brown, R. Q., Fenning, M. C., Babb, J. S., Hanks, G. E., and Chapman, J. D. Polarographic needle electrode measurements of oxygen in rat prostate carcinomas: accuracy and reproducibility. Int. J. Radiat. Oncol. Biol. Phys., *33:* 111–118, 1995.

[5] H. Zhong, E. Laughner, W. B. Issacs, G. L. Semenza, and J. W. Simons, manuscript in preparation.

[6] J. W. Simons and S. P. Hedican, unpublished observations.

16. Nelson, J. B., Hedican, S. P., George, D. J., Reddi, A. H., Piantadosi, S., Eisenberger, M. A., and Simons, J. W. Identification of endothelin-1 in the pathophysiology of metastatic adenocarcinoma of the prostate. Nat. Med., *1:* 944–948, 1995.
17. Hu, J., Discher, D. J., Bishopric, N. H., and Webster, K. A. Hypoxia regulates expression of the endothelin-1 gene through a proximal hypoxia-inducible factor-1 binding site on the antisense strand. Biochem. Biophys. Res. Commun., *245:* 894–899, 1998.
18. Epner, D., Partin, A. W., Schalken, J. A., Isaacs, J. T., and Coffey, D. S. Association of glyceraldehyde-3-phosphate dehydrogenase expression with cell motility and metastatic potential of rat prostatic adenocarcinoma. Cancer Res., *53:* 1995–1997, 1993.
19. Denis, L. J., and Prout, G. R., Jr. Lactic dehydrogenase in prostatic cancer. Invest. Urol., *1:* 101–111, 1963.
20. Isaacs, J. T., Isaacs, W. B., Feitz, W. F. J., and Scheres, J. Establishment and characterization of seven Dunning rat prostate cancer cell lines and their use in developing methods for predicting metastatic abilities of prostate cancers. Prostate, *9:* 261–281, 1986.
21. Kaighn, M. E., Narayan, S., Ohnuki, Y., Lechner, J. F., and Jones, L. W. Establishment and characterization of a human prostatic carcinoma cell line (PC-3). Invest. Urol., *17:* 16–23, 1979.
22. Horoszewicz, J. S., Leong, S., Chu, T. M., Wajsman, Z. L., Friedman, M., Papsidero, L., Kim, J., Chai, L. S., Kakati, S., Arya, S. K., and Sandberg, A. A. The LNCaP cell line–a new model for studies on human prostatic carcinoma. *In:* G. P. Murphy (ed.), Models for Prostate Cancer, pp. 115–132. New York: Alan R. Liss, Inc., 1980.
23. Stone, K. R., Mickey, D. D., Wunderli, H., Mickey, G. H., and Paulson, D. F. Isolation of a human prostate carcinoma cell line (DU-145). Int. J. Cancer, *21:* 274–281, 1978.
24. Brothman, A. R., Lesho, L. J., Somers, K. D., Wright, G. L., and Merchant, D. J. Phenotypic and cytogenetic characterization of a cell line derived from primary prostatic carcinoma. Int. J. Cancer, *44:* 898–903, 1989.
25. Iizumi, T., Yazaki, T., Kanoh, S., Kondo, I., and Koiso, K. Establishment of a new prostatic carcinoma cell line (TSU–PR1). J. Urol., *137:* 1304–1306, 1987.
26. Carter, H. B., Partin, A. W., and Coffey, D. S. Prediction of metastatic potential in an animal model of prostate cancer: flow cytometric quantification of cell surface charge. J. Urol., *142:* 1388–1341, 1989.
27. Palmer, L. A., Semenza, G. L., Stoler, M. H., and Johns, R. A. Hypoxia induces type II NOS gene expression in pulmonary artery endothelial cells via HIF-1. Am. J. Physiol., *274* (2 Pt 1)*:* L212–L219, 1998.
28. Lee, P. J., Jiang, B. H., Chin, B. Y., Lyer, N. V., Alam, J., Semenza, G. L., and Choi, A. M. K. Hypoxia-inducible factor-1 mediates transcriptional activation of the heme oxygenase-1 gene in response to hypoxia. J. Biol. Chem., *272:* 5275–5381, 1997.
29. Ambs, S., Merriam, W. G., Bennett, W. P., Felley-Bosco, E., Ogunfusika, M. O., Oser, S. M., Klein, S., Shields, P. G., Billiar, T. R., and Harris, C. C. Frequent nitric oxide synthase-2 expression in human colon adenomas: implication for tumor angiogenesis and colon cancer progression. Cancer Res., *58:* 334–341, 1998.
30. Deramaudt, B. M., Braunstein, S., Remy, P., and Abraham, N. G. Gene transfer of human heme oxygenase into coronary endothelial cells potentially promotes angiogenesis. J. Cell. Biochem., *68:* 121–127, 1998.
31. Freitas, I., Bono, B., Bertone, V., Griffini, P., Baronzio, G. F., Bonandrini, L., and Gerzeli, G. Characterization of the metabolism of perinecrotic cells in solid tumor by enzyme histochemistry. Anticancer Res., *16:* 1491–1502, 1996.
32. Dachs, G. U., Patterson, A. V., Firth, J. D., Ratcliffe, P. J., Townsend, K. M. S., Stratford, I. J., and Harris, A. L. Targeting gene expression to hypoxic tumor cells. Nat. Med., *3:* 515–520, 1997.

APPENDIX 7

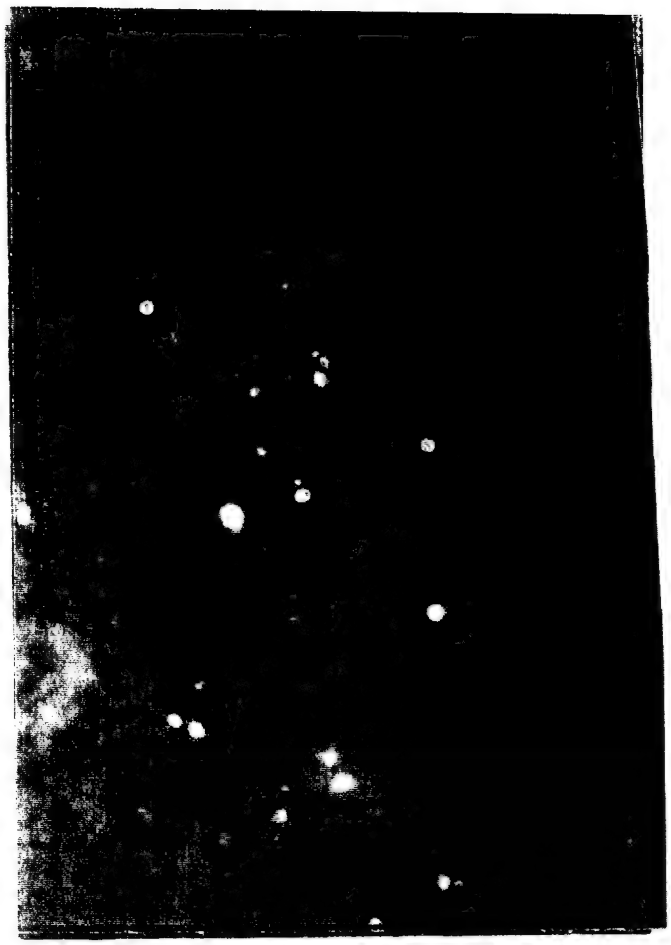

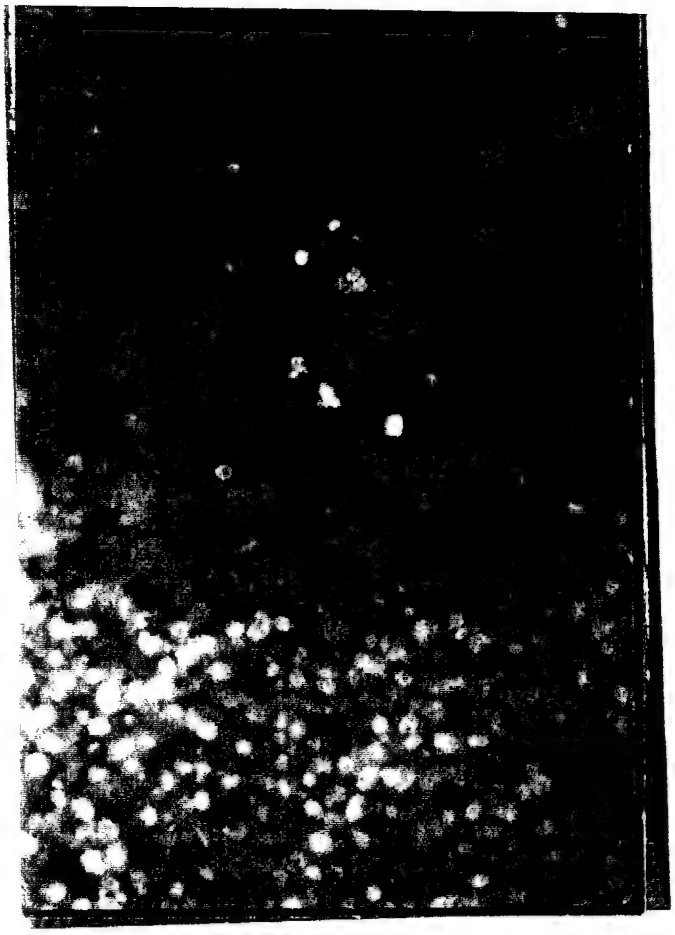

[CANCER RESEARCH 61, 5453–5460, July 15, 2001]

APPENDIX 8

CV706, a Prostate Cancer-specific Adenovirus Variant, in Combination with Radiotherapy Produces Synergistic Antitumor Efficacy without Increasing Toxicity[1]

Yu Chen, Theodore DeWeese, Jeanette Dilley, Yiwei Zhang, Yuanhao Li, Nagarajan Ramesh, Jake Lee, Rukmini Pennathur-Das, John Radzyminski, Joseph Wypych, Dominic Brignetti, Sara Scott, Jennifer Stephens, David B. Karpf, Daniel R. Henderson, and De-Chao Yu[2]

Calydon Incorporated, Sunnyvale, California 94089 [Y. C., J. D., Y. Z., Y. L., N. R., J. L., R. P-D., J. R., J. W., D. B., D. B. K., D. R. H., D-C. Y.], and Division of Radiation Oncology and the Department of Urology, The Johns Hopkins Hospital, The Johns Hopkins University School of Medicine, Baltimore, Maryland 21287 [T. D., S. S., J. S.]

ABSTRACT

Radiation is an effective means of treating localized prostate cancer. However, up to 40% of men with certain risk factors will develop biochemical failure 5 years after radiotherapy. CV706, a prostate cell-specific adenovirus variant, is currently in clinical trials for the treatment of recurrent organ-confined prostate cancer. We demonstrated previously that a single administration of CV706 at 5×10^8 particles/mm^3 of tumor eliminated established tumors within 6 weeks in nude mouse xenografts (Rodriguez *et al.*, *Cancer Res. 57:* 2559–2563, 1997). We now demonstrate that CV706-mediated cytotoxicity is synergistic with radiation. *In vitro*, addition of radiation to CV706 resulted in a synergistic increase of cytotoxicity toward the human prostate cancer cell line LNCaP and a significant increase of virus burst size, with no reduction in specificity of CV706-based cytopathogenicity for prostate cancer cells. *In vivo*, prostate-specific antigen (+) LNCaP xenografts of human prostate cancer were treated with CV706 (1×10^7 particles/mm^3 of tumor), 10 Gy of single fraction local tumor radiation, or both. Tumor volumes of the group treated with CV706 or radiation was 97% or 120% of baseline 6 weeks after treatment. However, when the same dose of CV706 was followed 24 h later with the same dose of radiation, the tumor volume dropped to 4% of baseline at this time point and produced antitumor activity that was 6.7-fold greater than a predicted additive effect of CV706 and radiation. Histological analyses of tumors revealed that, compared with CV706 or radiation alone, combination treatment with two agents increased necrosis by 180% and 690%, apoptosis by 330% and 880%, and decreased blood vessel number by 1290% and 600%, respectively. Importantly, no increase in toxicity was observed after combined treatment when compared with CV706 or radiation alone. These data demonstrate that CV706 enhances the *in vivo* radioresponse of prostate tumors and support the clinical development of CV706 as a neoadjuvant agent with radiation for localized prostate cancer.

INTRODUCTION

It has been known for many years that between 20 to 30% of localized prostate cancer patients continue to have positive biopsy specimens after radiotherapy (1). In the case of EBRT,[3] evidence supporting incomplete tumor ablation has come from several posttreatment biopsy studies (2) that find histopathology consistent with cancer even when digital rectal examination demonstrates a favorable tumor response. With the advent of PSA testing to evaluate patients after radiotherapy, it has been observed that approximately 80% of patients show progressive decreases in PSA in the first 12~18 months after radiotherapy, but by 7 years after therapy, as many as half of the patients will have a PSA that is progressively increasing, depending on pretreatment prognostic factors of the cancers (3–5). Even for men with T_1/T_2 disease, up to 40% experience biochemical failure 5 years after standard EBRT (6). Therefore, strategies to improve the outcome of local therapy with irradiation through radiosensitization are needed (7, 8).

Recent clinical and animal studies (9, 10) have described improved results when androgen ablation is combined with radiation. The clinical gains from such combination therapy have been encouraging in some groups of patients (9) but have unfortunately been associated with significant long-term side effects (11). We have developed previously (12–14) two selectively replication-competent adenovirus variants, CV706 and CV787, both of which replicate preferentially in and destroy prostate cells that produce PSA. A Phase I/II clinical trial of men with locally recurrent prostate cancer after radiotherapy has shown that half of the patients treated with a single intraprostatic administration of CV706 at 1×10^{13} particles demonstrated at least a 50% decrease in PSA, clearly demonstrating antitumor activity without serious side effects (15). Recently (16), synergistic antitumor efficacy was observed in human prostate cancer xenografts when the prostate cancer-specific adenovirus variant CV787 was combined with taxanes (paclitaxel and docetaxel). Because adenovirus E1A is known to be a potent inducer of chemosensitivity and radiosensitivity through p53-dependent and independent mechanisms (17), we have investigated the possible radiosensitizing effects of CV706 on prostate tumor cells. The present report provides evidence that CV706 has a synergistic antitumor effect both on irradiated human prostate cancer cells and tumor xenografts.

MATERIALS AND METHODS

Cell Culture and Virus. The human LNCaP (prostate carcinoma), OVCAR-3 (ovary carcinoma), and HBL-100 (breast epithelia) cell lines were obtained from the American Type Culture Collection (Rockville, MD). The human embryonic kidney cell line, 293, which expresses the adenoviral *E1A* and *E1B* gene products, was purchased from Microbix Biosystem, Inc. (Toronto, Ontario, Canada). Cells were maintained at 37°C with 5% CO_2 in RPMI 1640 supplemented with 10% fetal bovine serum (Hyclone, Utah), 100 units/ml penicillin, and 100 μg/ml of streptomycin (Life Technologies, Inc., Gaithersburg, MD).

CV706 is a prostate-specific replication competent adenovirus variant that was engineered at Calydon. One prostate-specific TRE, the human PSA promoter and prostate-specific enhancer, was inserted upstream of the E1A-encoding region in the viral genome (12). Similarly, CV787 is also a prostate-specific replication competent adenovirus variant, which contains two prostate-specific TREs, the probasin promoter and prostate-specific enhancer, inserted upstream of the E1A- and E1B-encoding regions in the viral genome, respectively (14). Both CV706 and CV787 are currently in clinical trials, the former for organ-confined prostate cancer and the latter for metastatic hormone refractory prostate cancer.

Cell Viability and Radiation. MTT assays were performed to measure cell viability as described previously (14). Briefly, HBL-100, OVCAR-3, and

Received 3/6/01; accepted 5/7/01.

The costs of publication of this article were defrayed in part by the payment of page charges. This article must therefore be hereby marked *advertisement* in accordance with 18 U.S.C. Section 1734 solely to indicate this fact.

[1] Supported in part by NIH/NCI CA58236 (to T. D., S. S., and J. S.).

[2] To whom requests for reprints should be addressed, at Calydon, Inc., 1324 Chesapeake Terrace, Sunnyvale, CA 94089. Phone: (408) 752-9877; Fax: (408) 734-2670; E-mail: dyu@calydon.com.

[3] The abbreviations used are: EBRT, external beam radiotherapy; CV, Calydon virus; FTV, fractional tumor volume; MTT, 3-(4,5-dimethylthiazol-2–4)-2,5-diphenyl-2H-tetrazolium bromide; MOI, multiplicity of infection; PSA, prostate-specific antigen; TRE, transcription response element; i.t., intratumoral; TUNEL, terminal deoxynucleotidyl transferase-mediated nick end labeling; PFU, plaque-forming unit.

LNCaP cells (2×10^4 cells/well; 96-well plate) were either infected with CV706 or CV787 at various MOIs (from 0.0001 to 1) and/or treated with radiation at the indicated dosages. Cells were incubated in growth medium for 24 h to allow for viral replication. After 24 h, cells were exposed to a single dose of γ-radiation (0~40 Gy; Mark 1 Research Irradiator Model #1608A; Cesium 137 source). Cell viability was measured at the times indicated by removing the media and replacing it with 50 μl of 1 mg/ml solution of MTT (Sigma Chemical Co., St. Louis, MO) and incubating for 3 h at 37°C (14).

Statistical Analysis. The dose-response interactions between CV706 and radiation at the point of IC_{50} were evaluated by the isobologram method of Steel and Peckham (18) as modified by Aoe *et al.* (19). The IC_{50} is defined as the concentration of drug that produces 50% cell growth inhibition; *i.e.*, a 50% reduction in absorbance. Isobolograms (three isoeffect curves; mode 1 and mode 2) were computed as described previously (16). FTV relative to untreated controls was determined based on the method described previously (16, 20).

One-step Growth Curve and Virus Yield. One-step growth curves of data obtained from CV706 grown in LNCaP cells in the presence and absence of radiation were charted and used to determine burst size. Monolayers of LNCaP cells were infected with CV706 at MOIs of 0.01, 0.1, and 1. After 24-h incubation at 37°C with 5% CO_2, cells were exposed to a single dose of γ-radiation at 10 Gy. At the indicated times thereafter, duplicate cell samples were harvested and lysed by three cycles of freeze thawing. Virus yield was determined by plaque assay as described (13).

***In Vivo* Antitumor Efficacy.** Six-to-eight-week-old athymic BALB/c *nu/nu* mice were obtained from Simonson Laboratories (Gilroy, CA) and acclimatized to laboratory conditions 1 week before tumor implantation. Xenografts were established either by injecting 1×10^6 LNCaP cells s.c. near the small of the back suspended in 100 μl of RPMI 1640 and 100 μl of Matrigel (back tumor) or by injecting cells into the right gastrocnemius muscle (i.m.; leg tumor). When tumors reached between 300 mm^3 and 500 mm^3, mice were randomized into groups of four. The first group received CV706 at day 0 via i.t. administration. CV706 was diluted in PBS containing 10% glycerol and injected into the tumor as 0.4 μl of diluted virus (1×10^7 particles/mm^3 of tumor) using a 28-gauge needle. The second group was given radiation only. For radiation, mice were immobilized in lucite chambers, and their whole body was shielded with lead except for the tumor-bearing sites on their back or tumor-bearing hind leg. This tumor-bearing site was irradiated with a Mark 1 Research Irradiator (Model #1608A; J. H. Shepherd Associates) at various doses (0, 5, 10, and 20 Gy) 1 day after CV706 injection or mock injection. The third group was given CV706 i.t. at day 0 and irradiated at the same doses at day 1. As a control, a fourth group was treated with virus dilution buffer (*i.e.*, control) i.t. at day 0. Tumors were measured weekly in two dimensions by external caliper, and the volume of back tumors was estimated by the formula {[*length* (mm) × *width* $(mm)^2$]/2; Ref. 14}. The volume of i.m. leg tumors was determined using the following formula: *volume* $(cm^3) = d'^3 - (0.6)^2 d'$, where d' is the average diameter of the tumor-bearing leg (cm), and the product $(0.6)^2 d'$ is the correction factor for normal leg volume (21). Animals were killed humanely when their tumor burden became excessive. The difference in relative tumor volumes between treatment groups was compared for statistical significance using the type 2 (two-sample equal variance), two-tailed *t* test. Blood samples were collected at various time points by retro-orbital bleed for determining PSA (14). Federal and institutional guidelines for animal care were followed.

Histochemistry Analysis. Four groups of mice ($n = 6$) were treated with vehicle, CV706 (1×10^7 particles/mm^3 of tumor), radiation (10 Gy), or a combination of CV706 and radiation. Half the animals were sacrificed on day 7, and the other half were sacrificed on day 14. The tumor samples were embedded in paraffin blocks, and 4-μm sections were cut and stained with H&E. Histology methods for detecting adenovirus antigens were as described (14). The necrotic cells were scored on coded slides by light microscopy at 400× magnification. The extent of necrosis was based on scoring 500 cells/section as either necrotic or nonnecrotic. The average necrosis score was calculated based on counting 10 fields distributed evenly across the area of the tumor section. The light-microscopic features used to identify necrosis included cell size, indistinct cell border, eosinophilic cytoplasm, loss or condensation of the nucleus, and associated inflammation (22). To assess the effect of CV706, radiation, or combination treatment on tumor vascularization, the number of blood vessels was counted at a magnification of 400×, and the average number of blood vessels was calculated from 10 fields distributed evenly across the area of whole tumor section (23). Apoptotic cells were detected using TUNEL assay (Roche Molecular Biochemicals, Indianapolis, IN) as suggested by the manufacturer. The morphological features used to identify apoptosis in the tumor sections have been described previously (22), associated with positive TUNEL staining. The apoptotic cells were scored on coded slides at 400× magnification, and the average score of apoptotic cells was calculated from 10 fields of nonnecrotic areas selected randomly across each tumor section. Anti-CD31 antibody was purchased from BD PharMingen (San Diego, CA), and the immunohistochemical staining procedure for detecting of CD31 antigen was performed as described by the manufacturer's protocol (24–26).

RESULTS

CV706 in Combination with Radiation Produces Synergistic Cytotoxicity in Prostate Carcinoma LNCaP Cells. To study the potential interaction between the prostate-specific adenovirus variant CV706 and radiation *in vitro*, the effectiveness of combined treatment of several combinations of CV706 and radiation at various doses was evaluated in the PSA-producing prostate carcinoma LNCaP cell line. LNCaP cells were either mock-infected or infected with CV706. One day later, the cells received a single dose of γ-radiation (0, 5 Gy, 10 Gy, and 20 Gy), and the cell viability was then determined at various time points by the MTT assay. Several viral MOIs and radiation doses were tested to determine the dose-response curves in LNCaP cells, such that the selected dose shows greater combined efficacy with radiation plus virus but minimal cell killing when treated with the same dose of virus or radiation alone. As shown in Fig. 1*A*, infecting LNCaP cells with CV706 at an MOI of 0.01 resulted in 80% cell survival 5 days after infection, whereas radiation at a dose of 10 Gy resulted in 78% survival 5 days after treatment. However, when CV706 and radiation were combined at these doses, cell survival dropped to 20% 5 days after treatment (Fig. 1*A*). Cell viability dropped further to 8% 9 days after combination treatment, whereas cells treated with virus alone at an MOI of 0.01 or radiation 10 Gy alone retained 70% or 60% cell viability, respectively. To determine whether the timing of administration for the tested agents affected the combined cytotoxic effect, LNCaP cells were treated with radiation 24 h before or after infection with CV706. Results showed that there

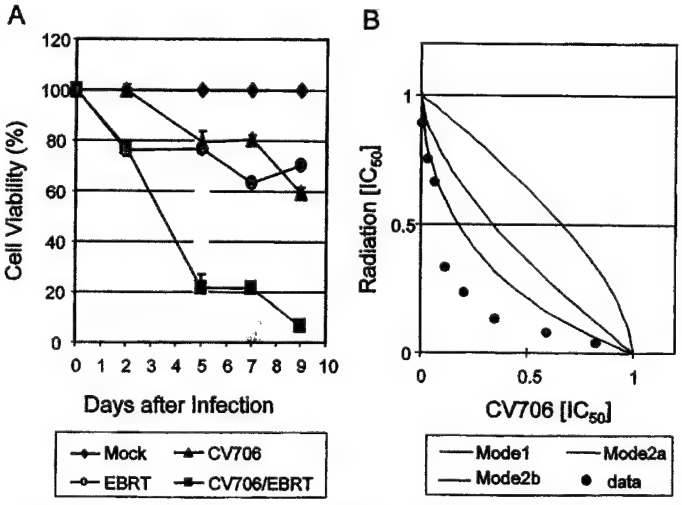

Fig. 1. Viability of prostate cancer LNCaP cells treated with vehicle, CV706, radiation, or CV706 plus radiation. *A*, LNCaP cells were treated with CV706 (MOI, 0.01) 24 h before exposure to radiation (10 Gy). *B*, isobologram analysis of the observed data from the combination of CV706 and radiation. The concentration that produced IC_{50} is expressed as 1.0 in the ordinate and the abscissa of the isobologram. *Y* axis, CV706 (IC_{50}); *X* axis, radiation (IC_{50}).

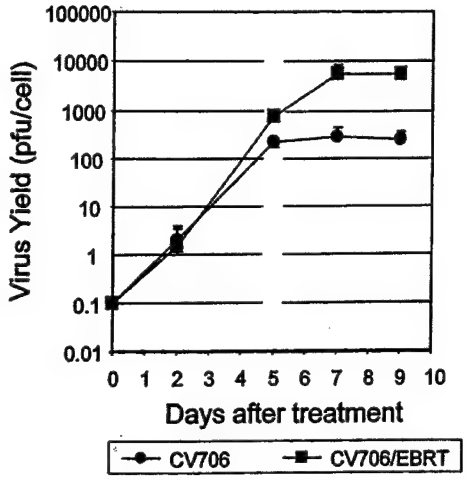

Fig. 2. One-step growth curve of CV706 (MOI, 0.1) in human prostate cancer LNCaP cells with (■) or without (●) radiation (10 Gy).

were no significant differences in cytotoxic activity between cells treated with radiation before infection or after infection with CV706 (data not shown).

Isobolograms were generated from the modes to determine the presence of synergy, additivity, or antagonism between CV706 and radiation. Dose-response curve analysis indicated that the IC_{50} at day 7 in LNCaP cells for CV706 and radiation was 0.028 MOI and 7.57 Gy, respectively. Fig. 1*B* shows isobologram representation of the statistical modeling used to analyze the interaction between CV706 and radiation. The combined data points fell to the left of the envelope of additivity, indicating sequential exposure to CV706 followed by radiation produced synergistic cytotoxicity. The enhanced cytotoxicity was also observed in LNCaP cells when CV787, a second prostate-specific adenovirus variant, was combined with radiation (data not shown). Taken together, our *in vitro* data demonstrate that prostate-specific adenovirus variants in combination with radiation produce synergistic cell cytotoxicity in prostate carcinoma LNCaP cells.

Radiation Increases CV706 Burst Size in LNCaP Cells. To examine the effect of radiation on virus replication, we performed a one-step growth curve experiment. LNCaP cells were infected with CV706 at an MOI of 0.1 for 24 h, followed by radiation at a dose of 10 Gy. Cells were harvested at various times after infection, and the number of infectious virus particles was determined on 293 cells by standard plaque assay (14). As shown in Fig. 2, cells treated with CV706 plus radiation produced a larger burst size, although the initial rate of increase of CV706 in cells treated with combined CV706 and radiation was similar to that of cells treated with CV706 alone; *e.g.*, cells treated with CV706 plus radiation produced 8000 PFU/cell 9 days after infection, whereas cells infected with CV706 alone generated about 500 PFU/cell at this time point (Fig. 2). Combination treatment with radiation and CV706 at MOIs of 0.01 or 1 also resulted in larger virus burst sizes. Cells treated with CV706 alone at MOIs of 0.01 and 1 produced 15 and 3500 PFU/cell, respectively, whereas cells treated with the same doses of CV706 combined with radiation produced 4750 and 8700 PFU/cell, respectively, 9 days after virus infection (data not shown). This observation was confirmed by quantitative PCR, which determines the number of copies of CV706 genome (data not shown). Thus, rather than inhibiting CV706 replication, the addition of radiation significantly increased virus propagation.

Cytotoxicity of CV706 in Combination with Radiation Does Not Alter Viral Specificity to Prostate Cancer Cells. To evaluate whether the addition of radiation could change the specificity of CV706-mediated cytotoxicity, we assessed the specificity of the combination treatment of CV706 and radiation by measuring the viability of various infected cell lines using the MTT assay. LNCaP, HBL-100, and OVCAR-3 cells were infected with CV706 at an MOI of 0.01 for 24 h, followed by a single dose of radiation at 10 Gy. The percentage of cell viability *versus* time after treatment was plotted in Fig. 3. The combination of CV706 and radiation was toxic to LNCaP cells but not to HBL-100 and OVCAR-3 cells. There were few surviving LNCaP cells 9 days after infection. In contrast, the viability of HBL-100 and OVCAR-3 cells treated with CV706 and radiation remained at >90% throughout the course of the experiment, similar to that of cells treated with radiation alone. These data demonstrate that combination with radiation does not alter the specificity of CV706 for PSA(+) cells.

Synergistic Efficacy of CV706 in Combination with Radiation *in Vivo*. The *in vivo* antitumor efficacy of CV706 in combination with radiation was assessed in the LNCaP mouse xenograft model. We have shown previously (12) that a single intratumoral administration of CV706 at 5×10^8 particles/mm^3 of tumor can eliminate s.c. xenograft tumors in 6 weeks. Established human prostate cancer xenografts (LNCaP cells) were treated with either vehicle, CV706 (1×10^7 particles/mm^3; a 50-fold lower dose), radiation (10 Gy), or both CV706 and radiation. For the combination treatment, animals were i.t. injected with CV706, and 24 h later, animals received a single dose of radiation. In this study, a single dose of 10 Gy was used because it caused a tumor growth delay in a previous pilot study. The dose of 1×10^7 CV706 particles/mm^3 of tumor was selected to produce a modest antitumor effect, based on our previous studies of antitumor efficacy (14).

The tumor volume data presented in Fig. 4*A* shows that there was a significant decrease in tumor volume between control and all of the treatment groups. In all of the cases, although a single dose of CV706 or radiation was effective in producing tumor growth inhibition, the combination of the two showed significantly greater tumor regression; *e.g.*, tumor volume of the group treated with radiation (10 Gy) was 120% of baseline 6 weeks after treatment, and the tumor volume of the group treated with CV706 was 97% of baseline at this time point. However, when the same dose of CV706 was followed 24 h later with the same dose of radiation, a statistically significant drop in the relative tumor volume to 4% of baseline was observed ($P < 0.01$; Fig. 4*A*). Twelve weeks after treatment, no visual tumors were observed in the group of animals that received a combination treatment of CV706 plus radiation, whereas tumor volume of the group treated with

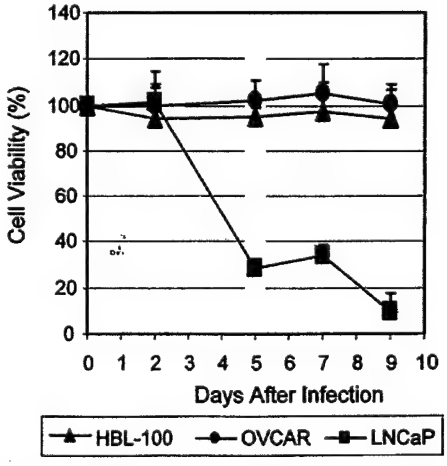

Fig. 3. Effect of radiation on the replication-mediated cytotoxicity of CV706. LNCaP, HBL-100, and OVCAR-3 cells were infected with CV706 (MOI, 0.01) 24 h before exposure to radiation (10 Gy). Cell viability was determined by MTT assay; *error bars* equal the SE.

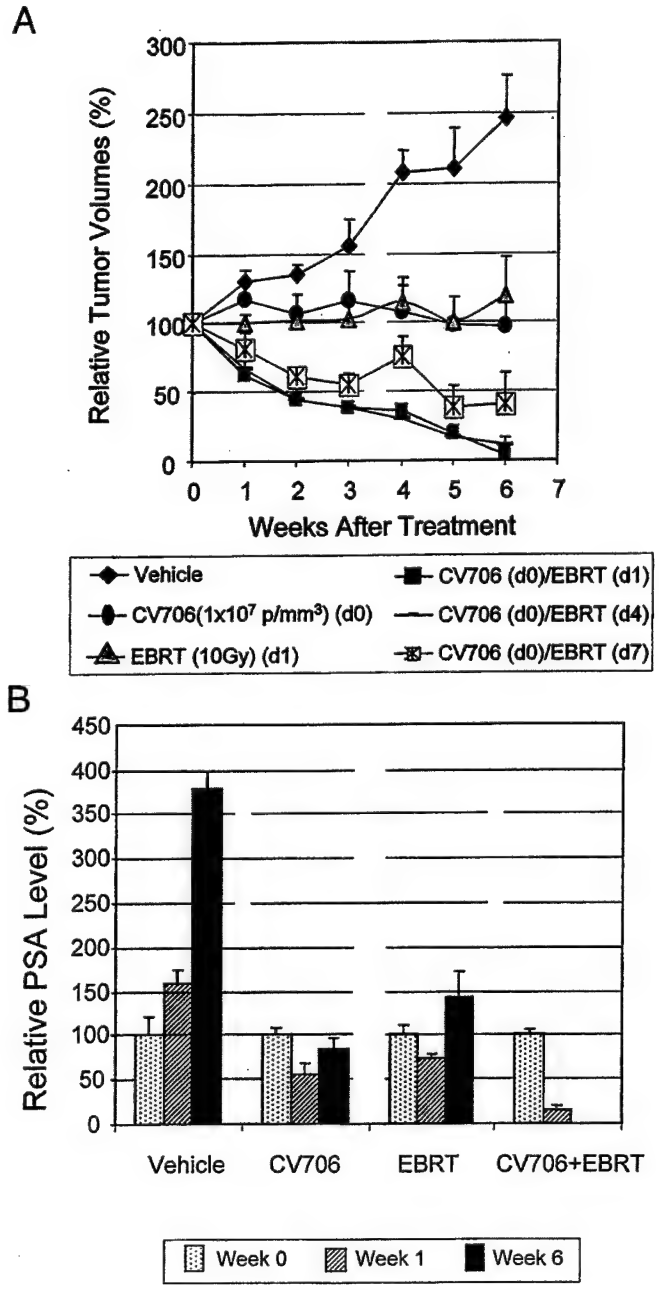

Fig. 4. *In vivo* efficacy of i.t. administered CV706 and radiation against nude mouse LNCaP xenografts. *A*, tumor volume of LNCaP xenografts treated with either vehicle (◆), CV706 alone (1×10^7 particles/mm^3 of tumor; ●), radiation alone (10 Gy; △), CV706 (1×10^7 particles/mm^3 of tumor) on day 0 plus radiation (10 Gy) on day 1 (■), CV706 on day 0 plus radiation on day 4 (*line*), or CV706 on day 0 plus radiation on day 7 (*cross line*). *B*, serum PSA values in the mice treated with either vehicle, CV706 (1×10^7 particles/mm^3 of tumor), radiation (10 Gy), or CV706 (1×10^7 particles/mm^3 of tumor) on day 0 plus radiation (10 Gy) on day 1. Groups consisted of eight mice each.

radiation was 510% of baseline and the tumor volume of the group treated with CV706 was 86% of baseline at this time point (data not shown). Serum PSA levels were also monitored in the mice to assess antitumor efficacy. The mean PSA level in mice receiving vehicle treatment increased to 370% of baseline after 6 weeks. In mice treated with radiation (10 Gy) alone, PSA increased only to 139% of baseline after 6 weeks, and PSA was reduced to 84% of baseline 6 weeks after treatment with CV706 (1×10^7 particles/mm^3) alone. In contrast, PSA levels in mice treated with CV706 plus radiation decreased substantially by 1 week after treatment and reached less than 1% of baseline within 6 weeks.

Table 1 summarizes the relative tumor volume of control and treated groups at six different time points. Combination treatment demonstrated greater than an additive effect on tumor growth inhibition at all of the time points studied after day 7. On day 21, there was a 2-fold improvement in antitumor activity in the combination group when compared with the expected additive effect. At this time point, CV706 and radiation (10 Gy) individually inhibited tumor growth by 26% and 34%, respectively (fractional tumor volumes of 0.7419 and 0.6645, respectively) when compared with the control group. A simple additive effect would predict a fractional tumor volume of 0.4930 from combination treatment (51% tumor inhibition), whereas treatment with CV706 plus radiation resulted in an average measured fractional volume of 0.2452, representing a 75% inhibition. This antitumor activity further improved with time. On day 42, the group treated with the combination of CV706 and radiation showed a 6.7-fold greater inhibition of tumor growth over that expected from an additive effect alone (Table 1). These observations further support the conclusion of synergy between CV706 and radiation in the eradication of LNCaP xenografts.

Enhanced antitumor efficacy was also observed in the animal model in which the prostate cancer tumors are implanted in hind limb of mice. In this study, tumors were produced by inoculation of 1×10^6 cells into limb muscle. When the tumors attained a volume of 200 mm^3 to 300 mm^3, the mice were randomized into four groups and treated as described above for back tumors. As before, the weekly tumor volume measurements showed that combination treatment with CV706 plus radiation led to significant antitumor activity in comparison with either CV706 or radiation alone. Tumor volume of the group treated only with radiation (20 Gy) was 70% of baseline 4 weeks after treatment, whereas the tumor volume of the group treated solely with CV706 (5×10^7 particle/mm^3 of tumor) was 75% of baseline at this time point. However, when CV706 was combined with radiation at these dose levels, the tumor volume dropped to 8% of baseline (data not shown).

A series of experiments was then designed to examine the effects of various factors, including the temporal sequence of the two agents, the timing of radiation after virus administration, and radiation fractionation. The effect of order of administration for the tested agents was examined in an *in vivo* study using the back tumor xenograft model. LNCaP xenografts were irradiated either 24 h before or after CV706 administration. Tumor volume (measured weekly) indicated that treatment with CV706 before radiation was superior to radiation followed by CV706 within the first 6 weeks; however, the difference became insignificant 8 weeks after treatment (data not shown).

The second study was designed to evaluate the timing of radiation after virus administration. Tumors were treated with CV706 at day 0 and followed by radiation at various time points. The results indicated similar antitumor efficacy when tumors treated with CV706 at day 0

Table 1 *Combination treatment with CV706 and radiation*

	FTV relative to untreated controls[a]				
			Combination treatment		
Day[b]	CV706	Irradiation	Expected[c]	Observed	Ratio of expected FTV/observed FTV[d]
7	0.9070	0.7752	0.7031	0.4806	1.46
14	0.7910	0.7537	0.5962	0.3280	1.82
21	0.7419	0.6645	0.4930	0.2452	2.01
28	0.5144	0.5481	0.2819	0.1683	1.66
35	0.4667	0.4762	0.2222	0.0905	2.46
42	0.3943	0.4837	0.1907	0.0285	6.69

[a] FTV (mean tumor volume experimental)/(mean tumor volume control).
[b] Day after tumors treated with agents.
[c] (mean FTV of CV706) × (mean FTV of radiation).
[d] Obtained by dividing the expected FTV by the observed FTV. A ratio of >1 indicates a synergistic effect, and a ratio of <1 indicates a less than additive effect.

were followed by radiation either 1 day or 4 days after virus administration; both treatments eliminated tumors within 6 weeks of treatment (Fig. 4*A*). However, the antitumor activity was decreased when the tumors were treated with radiation 7 days after CV706 administration (Fig. 4*A*).

The third study was designed to assess the effect of radiation fractionation on antitumor efficacy. Animals with human prostate cancer tumors on their backs were randomized into five groups. Two groups were treated with either CV706 on day 0, followed by a single dose of radiation at 10 Gy on day 1, or CV706 on day 0, followed by four fractional doses of radiation at 2.5 Gy on days 1, 3, 6, and 8, to provide a cumulative dose of 10 Gy. Tumor volume data, measured weekly, indicated that both treatments eliminated preexisting tumors 6 weeks after treatment and produced comparable synergistic antitumor activity when compared with either agent alone. No significant difference in antitumor efficacy was observed between these two virus/radiation combination groups as long as the total doses of radiation were comparable (data not shown).

Synergistic antitumor efficacy of CV706 in combination with radiation was further documented by histological analysis of the tumors. More necrotic cells were observed in the tumors treated with CV706 plus radiation than those treated with either agent alone (Table 2; and Fig. 5, *A* and *B*). The amount of necrosis in tumors treated with CV706 alone was higher than that seen in the control tumors or in the tumors treated with radiation alone. Evidence of necrosis and multifocal inflammation was observed in a small portion of tumors treated with radiation. In the tumors treated with both CV706 and radiation, only a few virus-infected cells were detected (Fig. 5*A*, *Panel R*). Most of the cells in the sections were empty and virtually devoid of cellular content. A significant increase in the extent of necrosis was the dominant histological feature, which involved about 95% of the tumor mass in this treatment group (Fig. 5*A*, *Panel R*). The average necrosis scores in a 400× magnification of the tumors treated with vehicle, radiation, CV706, or CV706 plus radiation were 5.4 ± 2.2, 67.0 ± 48.2, 258.2 ± 80.8, and 461.6 ± 37.9, respectively (Table 2). The presence of mass necrosis in the tumors treated with CV706 or CV706 plus radiation verifies the *in vivo* antitumor efficacy based on tumor volume analysis. Analysis of the necrosis data by a Student *t* test revealed that tumor cell necrosis induced by CV706 in combination with radiation was significantly greater than by CV706 ($P < 0.03$) or radiation alone ($P < 0.0001$). Likewise, a significantly greater number of apoptotic cells were observed in the treated tumors (Table 2). The number of apoptotic cells detected using TUNEL assay (22, 23) in the tumors treated with CV706 and radiation was 16.7-fold higher than with vehicle, 8.8-fold higher than with radiation alone, and 3.2-fold higher than with CV706 alone (Table 2).

Additionally, we observed a significant reduction in the number of blood vessels in the tumors treated with CV706 in combination with radiation, as shown in Fig. 5*B*. The average number of blood vessels observed at a magnification of 400× in tumors treated with vehicle, CV706, radiation, or the combination of CV706 and radiation was 87.5 ± 6.3, 27.5 ± 8.9, 58.5 ± 3.1, and 4.5 ± 1.9, respectively (Table 2). Significantly reduced numbers of blood vessels in tumors treated with combination in comparison with CV706 alone or radiation alone ($P < 0.01$) suggest that the reduction of tumor vascularization may contribute to enhanced tumor regression. It is unclear at this time as to the precise mechanism by which this reduction in blood vessel number is achieved. This can result either through direct damage of endothelial cells or through the destruction of tumor vasculature by extensive necrosis indirectly. CD31 is expressed constitutively on the surface of adult and embryonic endothelial cells and has been used as a marker to detect angiogenesis (24, 25). Immunohistochemical staining was performed to examine the effect of virus and radiation treatment on tumor angiogenesis by using a monoclonal antibody against CD31 (26). Tumors treated with CV706 followed by radiation showed a significantly lower level of CD31-positive cells when compared with tumors treated with either radiation ($P = 0.003$) or CV706 alone ($P = 0.03$; Table 2). When compared with untreated mice, CV706/radiation treated mice exhibited significantly lower (4.0-fold) CD31-positive blood cells ($P < 0.0001$), whereas radiation-treated or CV706-treated mice displayed 1.6-fold ($P = 0.03$) or 2.3-fold ($P = 0.004$) lower CD31-positive blood vessels. These observations suggest that CV706 in combination with radiation may be inhibiting tumor angiogenesis to a significant extent.

Finally, combination treatment of virus and radiation does not seem to impair the general health of the treated animals in comparison to the treatment with either virus or radiation alone. The quality of life of the animals seemed to be greatly improved, as evidenced by both general appearance and a significant gain in body weight. Indeed, animals treated with both CV706 and radiation gained 38% more weight than untreated control animals, 22% more than CV706-treated animals, and 25% more than radiation-treated animals (Table 3). The combination treatment was also found to protect the animals from the transient weight loss observed in the case of animals treated with radiation alone (Table 3).

Table 2 *Effect of CV706, radiation, or both on necrosis, apoptosis, and vascularization in LNCaP tumor xenografts*

LNCaP tumor-bearing animals were treated with CV706 (i.t. administration of 1×10^7 particles/mm^3 of tumor), radiation (local tumor radiation at a dose of 10 Gy), or both as described in "Materials and Methods." Tumor samples were harvested 14 days after treatment and analyzed by histological staining (H&E for necrosis and blood vessel and immunohistochemical staining with anti-CD31 antibody for angiogenesis) and TUNEL assay (for apoptotic cells). Groups consisted of six mice each.

Treatment	Necrosis	Blood vessel	CD31$^+$ cells	Apoptosis
Vehicle	5.4 ± 2.2	87.5 ± 6.3	33.7 ± 8.2	4.7 ± 1.2
CV706	258.2 ± 80.8	58.5 ± 3.1	14.8 ± 3.9	24.6 ± 7.2
Radiation	67.1 ± 48.2	27.5 ± 8.9	20.6 ± 7.3	8.9 ± 2.2
CV706 + Radiation	461.6 ± 37.9	4.5 ± 1.9	8.4 ± 2.7	78.3 ± 12.2

DISCUSSION

Although radiation is capable of permanently eradicating localized prostate tumors, as many as 40% of patients with clinically localized prostate cancer treated with potentially curative doses of standard, external beam radiation relapse at the site of the irradiated tumors within 5 years (3, 6, 8). Specifically, the eradication of locally advanced or high-risk prostate cancer with radiation has proven more difficult than believed previously (5). A modest increase in efficacy can be achieved by increasing the radiation dose, but this approach is limited by a concomitant increase in toxicity (5). Thus, a relatively nontoxic means of enhancing radiosensitivity could represent a useful clinical approach. The results presented above demonstrate that substantial synergy can be achieved when radiation treatment is complemented with a tumor-specific oncolytic virus.

Initial *in vitro* experiments in LNCaP prostate cancer cells demonstrated synergistic cytotoxicity when CV706 was combined with radiation. LNCaP cells treated with CV706 plus radiation had significantly decreased viability compared to cells treated with either agent alone. Surprisingly, LNCaP cells treated with CV706 plus radiation exhibited a greater burst size, suggesting that radiation treatment enhanced viral replication. Importantly, the addition of radiation to the cells treated with CV706 did not alter the specificity of replication-mediated cytotoxicity for PSA(+) cells. Thus, the CV706-radiation treatment retains the inherent high selectivity of the CV706 virus.

The *in vitro* demonstration of synergistic antitumor efficacy of combination therapy with CV706 and radiation was supported by

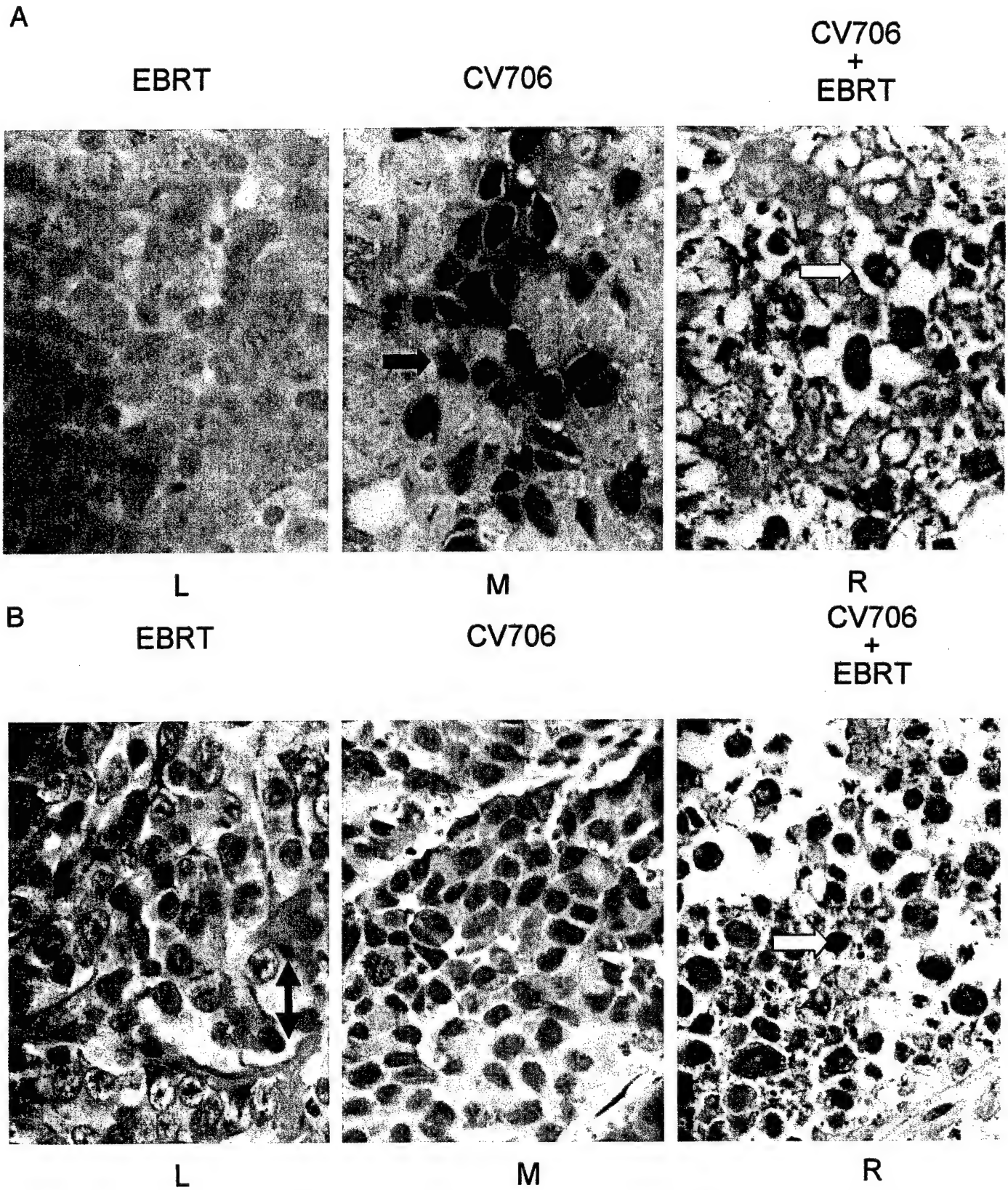

Fig. 5. Histological analysis of LNCaP tumors. LNCaP xenografts were treated with vehicle, CV706 alone (1×10^7 particles/mm^3 of tumor), radiation (10 Gy), or CV706 on day 0 plus radiation on day 1 and harvested on day 14 for histological analysis. *A*, immunohistochemical staining with anti-adenovirus polyclonal antibodies. *B*, H&E staining for blood vessels and necrotic cells. Representative histological features of LNCaP tumors at 400× magnification were documented. Adenovirus-infected cells stain dark blue as indicated by a *filled arrow*, blood vessels as indicated by a *double arrow*, and necrotic cells as indicated by the *open arrow*.

Table 3 *Relative body weight of animals bearing LNCaP tumor xenografts*

Groups consisted of eight animals treated with either vehicle, CV706 (1×10^7 particles/mm^3 of tumor), radiation (10 Gy), or CV706 plus radiation as described in the legend of Figure 4.

Treatment	Week 0	Week 1	Week 4	Week 6
Vehicle	100	97.2	92.4	96.3
CV706	100	101.3	106.5	112.9
Radiation	100	96.9	105.7	109.2
CV706 + Radiation	100	105.7	126.4	134.7

comparable synergy in the *in vivo* LNCaP xenograft model. Previous *in vivo* studies have demonstrated that large prostate tumors were completely eliminated within 6 weeks by a single i.t. administration of CV706 at a dose 5×10^8 particles/mm^3 of tumor (12, 14, 27). When combined with radiation (10 Gy), comparable eradication of tumors was observed with a 50-fold lower dose of virus (1×10^7 particles/mm^3). Under similar conditions, this dose of CV706 or radiation alone could only inhibit further tumor growth, but neither agent resulted in tumor eradication. Statistical analysis of the *in vivo* studies indicated that the CV706 and radiation combination resulted in significant antitumor synergy, with a 1.5–6.7-fold greater inhibition of tumor growth than expected from a simple additive effect during whole treatment period (Table 1). Subsequent studies have shown that similar synergistic antitumor efficacy can be achieved when 1×10^7 particles of CV706 are combined with only 5-Gy radiation (data not shown). Additional *in vivo* studies are in progress to determine the effective minimum dose of CV706 in combination with radiation required for complete regression of tumors in this xenotransplant model.

The timing of radiation after virus administration was found to be critical. The antitumor activity was decreased when the tumors were treated with radiation 7 days after CV706 administration, although no difference in antitumor effect was observed when the radiation was given 1 day or 4 days after CV706 injection. Conventional radiation therapy for localized prostate cancer in the clinic is delivered by a fractionated radiation schema. This is one fraction of radiation/day, 5 days/week. Our *in vivo* study indicated that no significant difference in antitumor efficacy was observed when tumors were treated with CV706 and a single dose of radiation or four doses of radiation as long as the total dose of radiation was the same. This is particularly interesting because the fractionated radiation protocol used in this study is actually less biologically effective in killing tumor clones than the single radiation dose fraction, yet it provided similar tumor control. In addition, fractionated radiation therapy is known to cause less damage to normal tissues when compared with radiation given in only one or several large fractions. The data from this study suggest that it may be possible to use less total radiation to control tumors if CV706 is given concomitantly, demising the risk of radiation-induced injury to normal tissues and thereby improving the therapeutic ratio. This hypothesis will require further study to verify.

A preliminary assessment of the synergistic activity of CV706 plus radiation treatment reveals several mechanistic possibilities. First, as mentioned above, radiation at the synergistic dose significantly increases virus replication. A one-step growth curve study showed that radiation significantly increased the burst size of CV706 in LNCaP cells without altering the kinetics of virus replication (Fig. 2). The burst size of CV706 in LNCaP cells treated with CV706 for 24 h followed by radiation was 500-fold higher than that in cells treated with CV706 (0.01 MOI) alone (Fig. 2; and data not shown). Radiation kills mammalian cells by inducing a reproductive (also known as mitotic) cell death, apoptotic death pathways, and by breaking DNA strands. Most radiation-induced DNA double-stranded breaks are rapidly repaired by constitutively expressed DNA repair mechanisms (28). DNA repair becomes more active in irradiated cells, potentially allowing for greater replication/multiplication of the episomal adenoviral DNA. Because of its small target size, the adenoviral genome (36 kb) is far less likely to sustain radiation-induced damage because it is 10^5-fold smaller than that of the DNA in human cells (3×10^6 kb). Therefore, the more active cellular DNA synthesis machinery in the irradiated cells may facilitate viral DNA synthesis and virus replication. Secondly, CV706 may be augmenting the antitumor activity of radiation. The adenovirus *E1A* gene is the only viral gene expressed during the first 2.5 h of infection and encodes a multifunctional transcriptional factor also known to induce apoptosis (29, 30). It is believed that the adenovirus E1A gene product represents a potent inducer of chemosensitivity and radiosensitivity through both p53-dependent and independent mechanisms. Malignant tumors, when expressing adenovirus E1A, are very sensitive to treatment with DNA-damaging agents *in vivo,* including radiation (17, 31–33). The histological features, which included intravascular thrombosis and massive necrosis positioned more centrally within tumors (data not shown), support the involvement of the vascular effect on tumor reduction. This seems to be in agreement with a recent finding (34) that inhibition of angiogenesis leads to increased tumor radioresponse. Indeed, CV706 in combination with radiation induced a significant reduction of CD31-positive cells in blood vessels, indicating a potential antiangiogenic effect of the combination treatment (24, 25).

Recently, a similar effect of radiation was reported when a colon cancer-specific replication competent adenovirus variant was combined with radiation in colon tumor cells (Dr. William Wold, CapCure Gene Therapy Summit 2001). Additionally, a replication-selective adenovirus, ONYX-015, in combination with radiation was also shown to have a greater effect than either individual modality (35). Thus, it is suggesting that the combination of adenovirus-based therapy with radiation for the cancer treatment appears to be promising.

Combination therapy using cytotoxic agents with differing mechanisms of action is a mainstay of oncology treatment, because it affords several important advantages not achievable with single-agent treatment, including: maximal cell kill within the range of toxicity tolerated by the patient for each agent (assuming dosing is not compromised); a broader range of interactions between the therapeutic modalities and tumor cells with different genetic abnormalities (in a heterogeneous tumor population); and the potential for preventing or slowing the development of treatment resistance (36). As demonstrated here, radiation can be successfully combined with cytolytic adenoviral therapy because it increases virus replication. In addition, the damaging effects are primarily limited to the irradiated host cell. In human prostate tumor xenografts, at least 50 times less CV706 is required to eliminate preexisting tumors in the combination treatment compared with single treatment. Moreover, combination treatment leads to significantly increased necrosis and a significant decrease in tumoral blood vessels and angiogenesis. Finally, no additional toxicities were noted from the combined treatment. In fact, the animals receiving combination treatment appeared healthier than those treated with radiation alone, as judged by a significant weight gain compared with the groups treated with either agent alone. If these results are replicated in human studies, it opens the potential of improved treatments for localized prostate cancer, offering enhanced efficacy while minimizing toxicity.

ACKNOWLEDGMENTS

We thank Natalie Nguyen, Heini Ilves, Eric Memarzaden, Joseph Oh, Pinky Amin, Mike McGlothlen, and Tina Le for technical help and Dr. Albert Owens, Dr. W. K. Joklik, and Gary Brouwer for thoughtful discussion.

REFERENCES

1. Kurth, K. H., Altwein, J. E., Skoluda, D., and Hohenfellner, R. Follow-up of irradiated prostatic carcinoma by aspiration biopsy. J. Urol., *117:* 615–617, 1977.
2. Pollack, A., and Zagars, G. K. External beam radiotherapy dose response of prostate cancer. Int. J. Radiat. Oncol. Biol. Phys., *39:* 1011–1018, 1997.
3. Hanks, G. E., Hanlon, A., Schulthess, T. E., Pinover, W. H., Movsas, B., Epstein, B. E., and Hunt, M. A. Dose escalation with 3D conformal treatment: five year outcomes, treatment optimization, and future directions. Int. J. Radiat. Oncol. Biol. Phys., *41:* 501–510, 1998.
4. Stamey, T. A., Kabalin, J. N., and Ferrari, M. Prostate specific antigen in the diagnosis and treatment of adenocarcinoma of the prostate. III. Radiation treated patients. J. Urol., *141:* 1084–1087, 1989.
5. Zelefsky, M. J., Leibel, S. A., Gaudin, P. B., Kutcher, G. J., Fleshner, N. E., Venkatramen, E. S., Reiter, V. E., Fair, W. R., Ling, C. C., and Fuks, V. Dose escalation with three-dimensional conformal radiation therapy affects the outcome in prostate cancer. Int. J. Radiat. Oncol. Biol. Phys., *41:* 491–500, 1998.
6. Horwitz, E. M., and Hanks, G. E. External beam radiation therapy for prostate cancer. CA Cancer J. Clin., *50:* 349–375, 2000.
7. Cowen, D., Salem, N., Ashoori, F., Meyn, R., Meistrich, M. L., Roth, J. A., and Pollack, A. Prostate cancer radiosensitization *in vivo* with adenovirus-mediated p53 gene therapy. Clin. Cancer Res., *6:* 4402–4408, 2000.
8. Zerati, M., and Pontes, J. E. Treatment of local failure of prostate cancer after radiotherapy and surgery. *In:* D. Raghavan, H. I. Scher, S. A. Leibel, and P. Lange (eds.), Principles and Practice of Genitourinary Oncology, pp. 567–571. Philadelphia: Lippincott-Raven Publishers, 1997.
9. Bolla, M., Gonzalez, D., Warde, P., Dubois, J. B., Mirimanoff, R. O., Storme, G., Bernier, J., Kuten, A., Steinberg, C., Gil, T., Collette, L., and Pierart, M. Improved survival in patients with locally advanced prostate cancer treated with radiotherapy and goserelin. N. Engl. J. Med., *337:* 295–300, 1997.
10. Joon, D. L., Hasegawa, M., Sikes, C., Khoo, U. S., Terry, N. H., Zagars, G. K., Meistrich, M. L., and Pollack, A. Supraadditive apoptotic response of R3327-G rat prostate tumors to androgen ablation and radiation. Int. J. Radiat. Oncol. Biol. Phys., *38:* 1071–1077, 1997.
11. Pilepich, M. V., Caplan, R., Byhardt, R. W., Lawton, C. A., Gallagher, M. J., Mepic, J. B., Hanus, G. E., Coughlin, C. T., Porter, A., Shipley, W. U., and Grignon, D. Phase III trial of androgen suppression using goserelin in unfavorable-prognosis carcinoma of the prostate treated with definitive radiotherapy: report of Radiation Therapy Oncology Group Protocol 85–31. J. Clin. Oncol., *15:* 1013–1021, 1997.
12. Rodriguez, R., Schuur, E. R., Lim, H. Y., Henderson, G. A., Simons, J. W., and Henderson, D. R. Prostate-attenuated replication competent adenovirus (ARCA) CN706: a selective cytotoxic for prostate-specific antigen positive prostate cancer cells. Cancer Res., *57:* 2559–2563, 1997.
13. Yu, D. C., Sakamoto, G. T., and Henderson, D. R. Identification of the transcriptional regulatory sequences of human kallikrein 2 and their use in the construction of Calydon virus 764, an attenuated replication competent adenovirus for prostate cancer therapy. Cancer Res., *59:* 1498–1504, 1999.
14. Yu, D-C., Chen, Y., Seng, M., Dilley, J., and Henderson, D. R. The addition of the Ad5 Region E3 enables Calydon virus 787 to eliminate distant prostate tumor xenografts. Cancer Res., *59:* 4200–4203, 1999.
15. DeWeese, T. L., Rioseco-Camacho, N., Ramakrishna, N. R., Henderson, D., Sawyers, C. L., and Simons, J. W. Results of a Phase I study of CN706, a replication-competent cytolytic adenovirus, for the treatment of adenocarcinoma of the prostate which is locally recurrent following radiation therapy. Int. J. Radiat. Oncol. Biol. Phys., *48:* 172, 2000.
16. Yu, D-C., Chen, Y., Dilley, J., Li, Y., Embry, M., Zhang, H., Nguyen, N., Amin, P., Oh, J., and Henderson, D. R. Antitumor synergy of CV787, a prostate cancer-specific adenovirus, and paclitaxel and docetaxel. Cancer Res., *61:* 517–525, 2001.
17. Martin-Duque, P., Sanchez-Prieto, R., Romero, J., Martinez-Lamparero, A., Cebrian-Sagarriga, S., Guinea-Viniegra, J., Dominguez, C., Lleonart, M., Cano, A., Quintanilla, M., Ramon, Y., and Cajal, S. *In vivo* radiosensitizing effect of the adenovirus *E1A* gene in murine and human malignant tumors. Int. J. Oncol., *15:* 1163–1168, 1999.
18. Steel, G. G., and Peckham, M. J. Exploitable mechanisms in combined radiotherapy-chemotherapy: the concept of additivity. Int. J. Radiat. Oncol. Biol. Phys., *5:* 85–91, 1993.
19. Aoe, K., Kiura, K., Ueoka, H., Tabata, M., Matsumura, T., Chikamor, I. M., Matsushita, A., Kohara, H., and Harada, M. Effect of docetaxel with cisplatin or vinorelbine on lung cancer cell lines. Anticancer Res., *19:* 291–299, 1999.
20. Yokoyama, Y., Dhanabal, M., Griffioen, A. W., Sukhatme, V. P., and Ramakrishnan, S. Synergy between angiostatin and endostatin: inhibition of ovarian cancer growth. Cancer Res., *60:* 2190–2196, 2000.
21. Alfieri, A. A., and Hahn, E. W. An *in situ* method for estimating cell survival in a solid tumor. Cancer Res., *38:* 3006–3011, 1978.
22. Milross, C. G., Tucker, S. L., Mason, K. A., Hunter, N. R., Peters, L. J., and Milas, L. The effect of tumor size on necrosis and polarographically measured pO2. Acta Oncol., *36:* 183–189, 1997.
23. Milas, L., Mason, K., Hunter, N., Petersen, S., Yamakawa, M., Ang, K., Mendelsohn, J., and Fan, Z. *In vivo* enhancement of tumor radioresponse by C225 antiepidermal growth factor receptor antibody. Clin. Cancer Res., *6:* 701–708, 2000.
24. Giatromanolaki, A., Sivridis, E., Koukourakis, M. I., Georgoulias, V., Gatter, K. C., and Harris, A. L. Intratumoral angiogenesis: a new prognostic indicator for stage I endometrial adenocarcinomas? Oncol. Res., *11:* 205–212, 1999.
25. Giatromanolaki, A., Koukourakis, M. I., Theodossiou, D., Barbatis, K., O'Byrne, K., Harris, A. L., and Gatter, K. C. Comparative evaluation of angiogenesis assessment with anti-factor-VIII and anti-CD31 immunostaining in non-small cell lung cancer. Clin. Cancer Res., *3:* 2485–2492, 1997.
26. Horak, E. R., Leek, R., Klenk, N., LeJeune, S., Smith, K., Stuart, N., Greenall, M., Stepniewska, K., and Harris, A. L. Angiogenesis, assessed by platelet/endothelial cell adhesion molecule antibodies, as indicator of node metastases and survival in breast cancer. Lancet, *340:* 1120–1124, 1992.
27. Chen, Y., Yu, D-C., Charlton, D., and Henderson, D. R. Pre-existent adenovirus antibody inhibits systemic toxicity and antitumor activity of CN706 in the nude mouse LNCaP xenograft model: implications and proposals for human therapy. Hum. Gene Ther., *11:* 1153–1167, 2000.
28. Garzotto, M., Haimovitz-Friedman, A., Liao, W-C., Whit-Jones, M., Huryk, R., Heston, W. D., Cardon-Cardo, C., Kolesnick, R., and Fuks, Z. Reversal of radiation resistance in LNCaP cells by targeting apoptosis through ceramide synthase. Cancer Res., *59:* 5194–5201, 1999.
29. Jones, N., and Shenk, T. An adenovirus type 5 early gene function regulates expression of other early viral genes. Proc. Natl. Acad. Sci. USA, *76:* 3665–3669, 1979.
30. Horwitz, M. S. Adenovirus and their replication. *In:* B. N. Fields and D. M. Knipe (eds.), Virology, Ed. 2, pp. 1679–1721. New York: Raven Press, Ltd., 1990.
31. Sanchez-Prieto, R., Lleonart, M., and Ramon y Cajal, S. Lack of correlation between p53 protein level and sensitivity of DNA-damaging agents in keratinocytes carrying adenovirus E1a mutants. Oncogene, *11:* 675–682, 1995.
32. Sanchez-Prieto, R., Lleonart, M., and Ramon y Cajal, S. Carcinoma cell lines become sensitive to DNA-damaging agents by the expression of the adenovirus *E1A* gene. Oncogene, *13:* 1083–1092, 1996.
33. Sanchez-Prieto, R., Quintanilla, M., Martin, P., Lleonart, M., Cano, A., Dotto, G. P., and Ramon y Cajal, S. *In vivo* antitumor effect of retrovirus-mediated gene transfer of the adenovirus *E1a* gene. Cancer Gene Ther., *5:* 215–224, 1998.
34. Gorski, D. H., Beckett, M. A., Jaskowiak, N. T., Calvin, D. P., Mauceri, H. J., Salloum, R. M., Seetharam, S., Koons, A., Hari, D. M., Kufe, D. W., and Weichselbaum, R. R. Blockage of the vascular endothelial growth factor stress response increases the antitumor effects of ionizing radiation. Cancer Res., *59:* 3374–3378, 1999.
35. Rogulski, K. R., Freytag, S. O., Zhang, K., Gilbert, J. D., Paielli, D. L., Kim, J. H., Heise, C. C., and Kirn, D. H. *In vivo* antitumor activity of ONYX-015 is influenced by p53 status and is augmented by radiotherapy. Cancer Res., *60:* 1193–1196, 2000.
36. Chu, E., and DeVita, V. T., Jr. Principles of cancer management: chemotherapy. *In:* J. Vincent, T. DeVita, S. Hellman, S. A. Rosenberg (ed.), Cancer: Principles and Practice of Oncology, pp. 289–306. Philadelphia: Lippincott Williams & Wilkins, 2001.

[CANCER RESEARCH 61, 7464–7472, October 15, 2001]

A Phase I Trial of CV706, a Replication-competent, PSA Selective Oncolytic Adenovirus, for the Treatment of Locally Recurrent Prostate Cancer following Radiation Therapy[1]

Theodore L. DeWeese,[2] Henk van der Poel, Shidong Li, Bahar Mikhak, Renee Drew, Marti Goemann, Ulrike Hamper, Robert DeJong, Nicholas Detorie, Ronald Rodriguez, Thomas Haulk, Angelo M. DeMarzo, Steven Piantadosi, D. C. Yu, Yu Chen, Daniel R. Henderson, Michael A. Carducci, William G. Nelson, and Jonathan W. Simons

Divisions of Radiation Oncology [T. L. D., S. L., R. D., N. D., T. H.], Medical Oncology [H. v. d. P., B. M., M. G., M. A. C., W. G. N., J. W. S.], and Biostatistics [S. P.], The Johns Hopkins Oncology Center, Baltimore, Maryland 21231-1000; Departments of Urology [T. L. D., R. R., M. A. C., W. G. N., J. W. S.], Radiology [U. H., R. D.], and Pathology [A. M. D.], The Johns Hopkins Hospital, The Johns Hopkins University School of Medicine, Baltimore, Maryland 21231-1000, and Calydon, Inc., Sunnyvale, California [D. C. Y., Y. C., D. R. H.]

ABSTRACT

CV706 is a prostate-specific antigen (PSA)-selective, replication-competent adenovirus that has been shown to selectively kill human prostate cancer xenografts in preclinical models. To study the safety and activity of intraprostatic delivery of CV706, a Phase I dose-ranging study for the treatment of patients with locally recurrent prostate cancer after radiation therapy was conducted. Twenty patients in five groups were treated with between 1×10^{11} and 1×10^{13} viral particles delivered by a real-time, transrectal ultrasound-guided transperineal technique using a three-dimensional plan. The primary end point was the determination of treatment-related toxicity. Secondary objectives included evaluation of the antitumor activity of CV706 and monitoring for other correlates of antineoplastic action. In this study, CV706 was found to be safe and was not associated with irreversible grade 3 or any grade 4 toxicity. No grade >1 alterations in liver function tests associated with CV706 administration were observed. Posttreatment prostatic biopsies and detection of a delayed "peak" of circulating copies of virus provided evidence of intraprostatic replication of CV706. The study defined the timing of CV706 shedding into blood and urine as well as the appearance of circulating Ad5 neutralizing antibodies. Finally, this study documents the serum PSA response of treated patients and reveals a dose response showing that all five patients who achieved a ≥50% reduction in PSA were treated with the highest two doses of CV706. This study represents the first clinical translation of a prostate-specific, replication-restricted adenovirus for the treatment of prostate cancer. Taken together, this study documents that intraprostatic delivery of CV706 can be safely administered to patients, even at high doses, and the data also suggest that CV706 possesses enough clinical activity, as reflected by changes in serum PSA, to warrant additional clinical and laboratory investigation.

INTRODUCTION

Radiation therapy is frequently used in the definitive management of patients with clinically localized PCa.[3] For men with PCa at an early stage, of a low to moderate grade, and associated with a serum PSA <10 ng/ml, a 7-year disease-free survival of 75–85% can be expected (1, 2). Men with PCa of a higher stage and/or grade, and/or cancer associated with a serum PSA >10 ng/ml, have a lower disease-free survival regardless of the treatment modality. For patients treated with radiation therapy, ~10–50% of men whose cancer recurs have a local recurrence as the first site of treatment failure, depending on pretreatment risk factors (3). Not surprisingly, men who do not suffer local recurrence are less likely to develop subsequent distant metastatic disease (3, 4). Given these facts, the development of novel therapies that can minimize the risk of tumor recurrence and extend disease-free survival is logical and appropriate. Ideally, these novel therapies should have the potential for disease eradication and not be associated with a significant risk of toxicity and long-term complications.

One new antineoplastic approach involves exploitation of the cytolytic capacity of adenovirus. It is well known that the adenoviruses can induce cell death by cytolysis as part of their normal life cycle (5). Importantly, adenoviruses possess several important characteristics that make them attractive agents for PCa gene therapy, including a relatively high transduction efficiency (6, 7) and the ability to transduce and lyse nonreplicating cells (7). The latter point is particularly important, as PCa typically possesses a very low S-phase fraction of about 5% or less (8, 9). Several investigators have attempted to achieve intratumoral cell killing with oncolytic viruses, including adenoviruses (10, 11). In fact, some of the earliest work included treatment of patients with intratumoral injection of wild-type adenovirus into cervical cancer that was locally recurrent after radiation therapy (12). Antitumor effects were clinically documented and provided a foundation for future studies. More recently, molecular biological techniques have allowed for genetic manipulation of the adenovirus, providing the ability to restrict its replication to unique genetic profiles of the tumor type to be treated (13, 14). These techniques include the production of replication-restricted adenoviruses that use heterologous tissue-specific promoters to control viral genes critical to replication (15)

In 1997, Rodriguez *et al.* (14), reported on the development of a replication-competent, E3-deleted, cytolytic Ad5 adenovirus called CN706 (subsequently renamed CV706), with replication that was restricted to PSA-producing cells. This restricted replication was achieved by the insertion of a minimal promoter-enhancer construct of the human PSA gene (*PSE*) 5′ of E1A, 3′ of the E1A promoter, resulting in PSA-regulated expression of E1A. This E1A regulation, in turn, resulted in the restriction of CV706 replication primarily to cells expressing PSA. Single, intratumoral, injections of CV706 into PSA-producing human PCa xenografts (LNCaP) resulted in rapid regression of those established tumors with a concomitant decrement in serum PSA. These data and others provided a strong rationale for clinical testing of CV706 in a manner analogous to the preclinical models: *i.e.*, by directed, intratumoral injections into the prostates of men with PCa.

PCa tends to be a multifocal disease. In fact, even clinically localized PCa typically has, on average, seven separate foci of cancer

Received 5/15/01; accepted 8/16/01.

The costs of publication of this article were defrayed in part by the payment of page charges. This article must therefore be hereby marked *advertisement* in accordance with 18 U.S.C. Section 1734 solely to indicate this fact.

[1] Supported, in part, by the Johns Hopkins General Clinical Research Center (NIH/National Center for Research Resources M01RR00052), CaPCURE, and NIH/National Cancer Institute Grant CA58236

[2] To whom requests for reprints should be addressed, at Radiation Biology Program, The Johns Hopkins Oncology Center, 1650 Orleans Street, Room 1-144, Baltimore, MD 21231-1000.

[3] The abbreviations used are: PCa, adenocarcinoma of the prostate; PSA, prostate-specific antigen; MTD, maximal tolerated dose; DLT, dose-limiting toxicity; AE, adverse event; PR, partial response; PFU, plaque-forming units; AST, aspartate aminotransferase.

in the prostate, and these foci are frequently bilobar (16). Therefore, any intraprostatic delivery of virus would, ideally, need to cover the entirety of the prostate to adequately treat this multifocal disease. Intratumoral injections of virus into the prostate can be performed several ways, including delivery by transrectal and transperineal routes. Intraprostatic delivery of radioactive sources, termed prostate brachytherapy, used in the definitive management of early-stage PCa, is a routine, outpatient procedure performed via the transperineal route (17). This stereotactically guided approach generally allows for complete coverage of the prostate volume by the radioactive sources. Translation of this technique to *in vivo* PCa gene therapy is a logical extension of this well-proven technology, particularly when combined with a highly tissue-specific, replication-competent oncolytic adenoviral therapeutic. Together, these considerations formed the preclinical rationale for translation of replication-competent cytolytic viral therapy to the clinic. For men who experience a local recurrence of cancer after radiation therapy, there are no standard salvage therapies available. In addition, the presently available options for salvage (prostatectomy, brachytherapy, and cryotherapy; Refs. 18–21) are associated with high rates of side effects, including impotence, incontinence, and rectal injury. Therefore, we designed a Phase I, dose-escalation study to determine the MTD and DLTs of CV706 when delivered by stereotactically guided intraprostatic injections in this group of patients.

MATERIALS AND METHODS

Study Design. The primary objective of this study was to determine the MTD of CV706 when administered by transrectal ultrasound-guided transperineal injections into the prostate of men whose PCa was locally recurrent after radiation therapy, who also had an associated rising serum PSA. This was a single-institution study. All men were treated with CV706 in the NIH General Clinical Research Center of The Johns Hopkins Hospital by one physician (T. L. D.). Five cohorts of three to six men received treatment with one dose of CV706. Cohorts were treated sequentially with CV706 at dose levels of 1×10^{11}, 3×10^{11}, 1×10^{12}, 3×10^{12}, or 1×10^{13} viral particles/patient (Table 1). All patients completed 3 weeks of observation after treatment before dose escalation to the next cohort. If none of the men experienced any DLT, the study proceeded. The MTD was defined as the dose below the one at which 2 or more of 6 men experienced a DLT. A DLT was defined as any irreversible grade 3 or any grade 4 toxicity (National Cancer Institute-Common Toxicity Criteria) or a prostate symptom score >>28, considered potentially related to study treatment. Secondary objectives included the evaluation of antitumor activity of CV706 and monitoring for other molecular correlates of antineoplastic action.

Patient Selection. All men were required to have biopsy-proven, locally recurrent PCa, to have been previously treated with definitive external beam radiation therapy, and to provide informed consent (Joint Committee on Clinical Investigation-approved). Initially, men were required to have a serum PSA >10 ng/ml and rising. Approximately halfway through the protocol, this criteria was amended to conform to the American Society for Therapeutic Radiology and Oncology (ASTRO) criteria of biochemical failure after definitive radiation therapy, which is defined as three consecutive increases in PSA after the postradiotherapy nadir (22). Patients were free of detectable metastatic disease as determined by routine whole-body bone scan as well as computed tomography scan of the abdomen and pelvis at study entry. Additional eligibility criteria included: The Eastern Cooperative Oncology Group (ECOG) performance status of 0–1; normal liver and renal function; a normal serum testosterone level (>200 ng/dl); normal hematological and coagulation profiles; and absence of immunosuppression or concomitant systemic immunosuppressive agents. Table 2 outlines the demographic features of each study subject, including age, race, preradiation prognostic factors, dose of radiation received, and interval between radiation and treatment with CV706.

Three-Dimensional Treatment Planning and Delivery of CV706. Planning and delivery of CV706 was performed by a modified, transperineal prostate brachytherapy technique. Transrectal ultrasound was performed with the men in the extended dorsal lithotomy position. Transverse images of the prostate were obtained at 5-mm intervals from the base to the apex. Sagittal images of the prostate were also obtained. Three-dimensional reconstruction of the prostate was performed using a MMS Therapac Plus 6.6 prostate brachytherapy planning system (Varian Medical Systems, Palo Alto, CA).

Table 1 *Number of viral particles administered, maximum number of needles, and maximum number of intraprostatic viral deposits used for each dose level of CV706*

Dose level	No. patients treated	No. viral particles injected	Maximum no. needles	Maximum no. deposits
1	3	1×10^{11}	10	20
2	3	3×10^{11}	10	20
3	3	1×10^{12}	10	20
4A	2	3×10^{12}	30	40
4B	2	3×10^{12}	40	60
4C	2	3×10^{12}	40	80
5A	2	1×10^{13}	30	40
5B	2	1×10^{13}	40	60
5C	1	1×10^{13}	40	80

Preclinical data suggested that a single, intratumoral injection of CV706 would result in ~1 ml of tumor killing in an LNCaP xenograft model (14). Using this information, a "viral dosimetric" algorithm was devised and entered into the MMS Therapac treatment planning system.[4] This viral dosimetry was used to determine the most optimal sites for CV706 injection so as to effect the most homogenous coverage of the prostate within the confines of the protocol restrictions. Table 1 outlines the number of needles and viral depositions allowed in each portion of the protocol. On the day of treatment, a Foley catheter was placed into the patient's bladder, and was maintained for 14 days. In the operating room, under spinal anesthesia, the patient was repositioned in the extended dorsal lithotomy position. The real-time, transrectal ultrasound was used to guide each 18-gauge Zebra needle (Mick Radio-Nuclear Instruments, New York, NY) through the perineum, into the prostate via a template to the predetermined positions for delivery of each 0.1-ml injection.

Patient Monitoring. Patients were hospitalized for observation for 24 h after CV706 administration. Vital signs were monitored closely and blood and urine samples were obtained at predetermined intervals. Laboratory studies included: hematology, liver and renal functions, coagulation profiles, serum PSA and acid phosphatase, analysis for circulating CV706 in the blood and excreted in the urine, as well as neutralizing antibody titers. Physical exams were performed on subsequent days in the outpatient clinic, and patients completed a Functional Assessment of Cancer Treatment—Prostate (FACT-P) quality-of-life assessment. On days 4 and 22 and at month 3 posttreatment, transrectal prostate biopsies were obtained.

Manufacturing and Preparation of CV706. CV706 was supplied by Calydon, Inc., as a sterile, clear, frozen liquid in vials containing 0.5 ml of virus at a concentration of 1×10^{12} viral particles/ml. CV706 was formulated in PBS with 10% glycerol and 1 mM $MgCl_2$ and stored at −80°C until needed. On the day of the procedure, the CV706 was thawed and resuspended in sterile 0.9% saline immediately before administration. In the operating room, CV706 was drawn into a sterile syringe, and the air was expelled to insure accurate delivery.

Neutralizing Antibody Titers in Blood. The neutralization assay used in this study was performed as described previously (23). Briefly, serial dilutions of heat-inactivated patient serum (56°C for 30 min) was mixed for 1 h with adenovirus (1 PFU/cell). The virus-antibody mixture was then plated onto 293 cells (10,000 cells/well; 96-well plates) for 1 h. After incubation, the mixture was removed, RPMI 1640 was added, and the 293 cells were cultured for 5–7 days at 37°C. Cytopathic effect was then monitored at the time when control samples revealed 100% cytopathic effect after incubation.

Quantitative PCR for CV706 in Plasma. Plasma samples (2–4 ml) were analyzed from all available samples obtained before treatment, as well as at 30 min, 1 h, 4 h, 8 h, 12 h, 18 h, and 24 h and at days 3, 8, 14, and 28 after treatment. Samples were frozen at −20°C or below immediately after plasma separation. One-ml aliquots of plasma were centrifuged and guanidinium thiocyanate solution was added to the pellet. DNA was extracted from samples with phenol/chloroform/isoamyl alcohol and precipitated in isopropyl alcohol. DNA was washed, dried, and resuspended in Tris-EDTA buffer. A PCR master

[4] T. L. DeWeese, J. W. Simons, R. Rodriquez, and A. Baccala, unpublished data.

Table 2 *Demographics of all 20 men treated with intraprostatic CV706*

Patient no.	Race	Stage	Gleason score	Pre-radiation therapy serum PSA (ng/ml)	Radiation dose (cGy)	Interval (mo) between radiation therapy and CV706	Pre-CV706 serum PSA (ng/ml)	CV706 dose level
1	AA[a]	T_{2C}	7	9.4	7020	24	58.7	1
2	W	T_{2B}	7	6.6	6660	39	59.7	1
3	W	T_{3A}	7	7.7	6840	74	17.6	1
4	W	T_{3A}	8	14.7	7020	39	10.9	2
5	W	T_{2C}	5	20.8	6480	56	11.8	2
6	W	T_{2B}	6	9.3	7020	35	20.9	2
7	W	T_{3A}	7	17.0	7020	27	14.6	3
8	W	T_{3A}	7	9.7	6840	90	54.8	3
9	W	T_{1C}	8	16.1	6840	33	13.0	3
10	W	T_{3C}	5	2.7	7000	76	12.4	4A
11	W	T_{2C}	8	13.2	7020	36	7.6	4A
12	W	T_{2C}	6	16.5	7020	41	7.5	4B
13	W	T_{1C}	4	14.3	6840	35	6.4	4B
14	W	T_{2C}	6	11.0	6840	84	44.8	4C
15	W	T_{1C}	5	8.3	N/A	50	8.6	4C
16	W	T_{1C}	6	8.9	6840	56	9.1	5A
17	W	T_{2A}	6	24	7020	39	7.4	5A
18	W	T_{2A}	7	8.3	6300	92	13.2	5B
19	W	T_{1C}	6	6.5	6696	41	4.2	5B
20	W	T_{1C}	6	5.6	6660	50	1.4	5C

[a] AA, African American; W, white; N/A, data not available.

mix containing the following HPLC-purified primers and fluorescent probe were added:

Forward: 5′ CCCCAGCCCCAAGCTT 3′

Reverse: 5′ GCGGCCATTTCTTCGGTAATA 3′

Probe: 5′ FAMCCGGTGACTGAAAATGAGACATATTATCTGCCAT-AMRA 3′

PCR with real-time detection was performed in a Perkin-Elmer/ABI Prism 7700 Sequence Detection System (Applied Biosystems, Foster City, CA) with the following cycling profile: 95°C for 10 min then 40 cycles of 95°C for 15 s, 60°C for 30 s, and 72°C for 1 min. Assay performance was monitored by spiking eight control plasma samples with known amounts of CV706 (either 2,500 or 75,000 CV706 particles/ml of plasma), interspersed with patient samples as "unknowns." Insufficient plasma or insufficiently separated plasma could not be analyzed.

Determination of CV706 Viral Shedding in Urine. Sterile urine samples from postinjection days 1, 8, 15, and 29 were collected, immediately centrifuged, and stored at −20°C until assayed. A plaque assay procedure on HEK-293 cell monolayers was used to screen and quantitate infectious CV706 viral particles. The urine samples were diluted 100-fold with DMEM (BioWhittaker, Walkersville, MD) supplemented with 5% fetal bovine serum (HyClone Laboratories, Logan, UT) to overcome the cytotoxicity of urine and run in duplicate or six-replicate wells. Plaques were counted on days 12, 13, and 14 after infection. In addition, where significant cytopathic effect was observed, the samples were repeatedly assayed with a 10-fold serial dilution in duplicate to accurately quantify PFU. Repeat assays were performed on both HEK-293 and nonpermissive HBL-100 cells to test for tissue selectivity of the isolated virus.

Electron Microscopy of Prostatic Biopsy Material. Electron microscopy was performed on prostatic tissue obtained from transrectal needle biopsies of the prostate 4 days after CV706 treatment. Tissue samples were prepared as described previously (24). Briefly, prostate biopsy material was fixed in 2.5% glutaraldehyde and cut into thin sections. Sections were exposed to 1% osmium tetroxide and then dehydrated in ethanol. Next, a propylene oxide/embedding medium mixture was applied and, subsequently, a 100% embedding medium for 24 h. Sections were then polymerized and stained. Transmission electron microscopic images were analyzed for evidence of intranuclear viral particles.

Immunohistochemistry. After paraffin removal and hydration, slides were immersed in 0.1% Tween 20, preheated in Protease Type VIII (Sigma Chemical Co., St. Louis, MO), and then treated with 3% hydrogen peroxide to quench endogenous peroxidases. Protein Blocker (Ventana Medical Systems, Tucson, AZ) was then applied, slides were washed, and the primary antibody, Adenovirus (Chemicon, Temecula, CA), was applied at 1:20,000 dilution in PBS for 45 min. The secondary biotin-labeled antibody was applied for 30 min (goat antimouse; 1:50), and localization was accomplished by exposure to an avidin-biotin complex horseradish peroxidase solution for 30 min. A diaminobenzidine substrate was used according to the manufacturer's instructions (ChemMate; Ventana Medical Systems, Tucson, AZ), and the slides were counterstained with hematoxylin. Hexon staining was evaluated by a pathologist using an Olympus BX-40 light microscope without knowledge of the timing of the biopsy specimen, dose level, or patient identification.

Statistical Considerations. The PSA velocity was evaluated by the method of Piantadosi, *et al.*[5] to quantify the CV706 treatment effect. Using this method, the log of the pre- and posttreatment serum PSA values were calculated. The slope of the log PSA *versus* time trends was calculated before and after treatment using linear regression. If the mean change in log serum PSA (comparing pre- and posttreatment PSA slopes) is positive or zero, then the treatment had no effect. If the mean change is negative, then the treatment had an antitumor effect, as evidenced by reducing PSA velocity.

RESULTS

Patient Characteristics

A total of 24 men were enrolled, and 20 men were treated with CV706 between September 1998 and May 2000. The reasons for no treatment in four patients included: (*a*) an inability to tolerate the transrectal ultrasound (three patients); and (*b*) no evidence of recurrent cancer on biopsy of the prostate (one patient). The demographics for the treatment cohorts are listed in Table 2. The median age of treated men was 70 years, with a range of 60–83 years. The preradiation clinical T stages (1992, American Joint Committee on Cancer) ranged from T_{1C}-T_{3C}. The median preradiation Gleason score was 6 (range, 4–8). The median time from the end of radiation to treatment with CV706 was 41 months (range, 24–92 months). The median dose of radiation used in the initial management of these men was 68.4 Gy. Four of the 20 treated men were initially managed with neoadjuvant and/or concomitant androgen suppression and radiation therapy, but they had normal serum testosterone levels at time of treatment. The median pre-CV706 serum PSA was 12.1 ng/ml (range, 1.4–59.7 ng/ml). The Eastern Cooperative Oncology Group performance status of 20 of 20 patients was "0." The median follow-up time in the 20 treated men is 17 months.

CV706 Treatment-Related Toxicity

Patient Reported AEs. Table 3 summarizes all AEs reported in two or more men. The majority (74%) of the AEs noted were mild in

[5] S. P., B. M., and J. W. S., unpublished data.

severity and/or grade 1 toxicity. Only 24% of the AEs were considered to be moderate in severity and/or grade 2 toxicity. The majority of men (15 of 20) experienced a grade ≤2 fever approximately 3–8 h after injection that was either self-limited or responded to treatment with acetaminophen. Half of the men with fever had associated shaking chills and received acetaminophen (7 of 20). The majority of men (15 of 20) also experienced local pain at the injection site (perineum) and/or pelvic pain in the immediate postoperative period, 10 of whom were treated with acetaminophen and/or oxycodone. Approximately one-half of these men (9 of 20) had local pain with associated inflammation noted by examination. Hematuria was noted in all men, with 20 of 20 patients experiencing microscopic hematuria. Urinary irritative symptoms were frequently documented, including urethral pain, urinary urgency, and frequency. Patients consistently noted that the indwelling Foley catheter they were required to maintain for 14 days after CV706 administration was, in large part, related to these irritative urinary symptoms. Postprocedure nausea and vomiting was occasionally seen and was thought to be related to use of oxycodone in the immediate postprocedure setting. Two men each were noted to develop transient hypertension and hypotension, respectively. These episodes occurred in the immediate postprocedure setting and were most likely related to the anesthesia. One of the patients with hypertension was treated with hydralazine and the other with atenolol. No specific treatment was required for the patients with mild hypotension. Postprocedure amnesia was also thought to be related to the anesthesia. Several men complained of skin rashes (torso and arms) with or without pruritis, three of which were thought to be possibly related to the study drug.

Table 3 *Patient-reported toxicity noted in two or more men treated with intraprostatic CV706*

Body system	Costart term	Cohort 1 1×10^{11}	Cohort 2 3×10^{11}	Cohort 3 1×10^{12}	Cohort 4 3×10^{12}	Cohort 5 1×10^{13}	Overall
No. of patients treated		3	3	3	6	5	20
No. of patients with any AE		3 (100%)	3 (100%)	3 (100%)	6 (100%)	5 (100%)	20 (100%)
No. of all AEs		41	37	34	100	47	259
No. of related AEs		15	13	12	34	12	86
Body as a whole	Total	3 (100%)	3 (100%)	3 (100%)	6 (100%)	5 (100%)	20 (100%)
	Fever	1 (33%)	1 (33%)	2 (67%)	6 (100%)	5 (100%)	15 (75%)
	Chills	0 (0%)	2 (67%)	1 (33%)	3 (50%)	3 (60%)	9 (45%)
	Asthenia	1 (33%)	0 (0%)	0 (0%)	4 (67%)	1 (20%)	6 (30%)
	Back pain	0 (0%)	1 (33%)	1 (33%)	1 (17%)	0 (0%)	3 (15%)
	Headache	0 (0%)	0 (0%)	0 (0%)	1 (17%)	1 (20%)	2 (10%)
	Pain	0 (0%)	0 (0%)	0 (0%)	1 (17%)	1 (20%)	2 (10%)
	Injection site pain	2 (67%)	1 (33%)	3 (100%)	6 (100%)	2 (40%)	14 (70%)
	Injection site inflammation	1 (33%)	0 (0%)	2 (67%)	3 (50%)	3 (60%)	9 (45%)
	Injection site hemorrhage	0 (0%)	0 (0%)	1 (33%)	1 (17%)	3 (60%)	5 (25%)
	Pelvic pain	1 (33%)	2 (67%)	1 (33%)	4 (67%)	1 (20%)	9 (45%)
Digestive system	Total	3 (100%)	3 (100%)	2 (67%)	5 (83%)	2 (40%)	15 (75%)
	Vomiting	1 (33%)	2 (67%)	0 (0%)	2 (33%)	0 (0%)	5 (25%)
	Nausea	1 (33%)	2 (67%)	0 (0%)	2 (33%)	1 (20%)	6 (30%)
	Anorexia	0 (0%)	0 (0%)	0 (0%)	2 (33%)	1 (20%)	3 (15%)
	Constipation	1 (33%)	0 (0%)	0 (0%)	1 (17%)	0 (0%)	2 (10%)
	Diarrhea	1 (33%)	0 (0%)	0 (0%)	1 (17%)	0 (0%)	2 (10%)
	Rectal disorder	0 (0%)	1 (33%)	1 (33%)	0 (0%)	0 (0%)	2 (10%)
	Rectal hemorrhage	1 (33%)	1 (33%)	1 (33%)	1 (17%)	0 (0%)	4 (20%)
Cardiovascular system	Total	1 (33%)	2 (67%)	0 (0%)	3 (50%)	0 (0%)	6 (30%)
	Hypertension	1 (33%)	1 (33%)	0 (0%)	0 (0%)	0 (0%)	2 (10%)
	Hypotension	0 (0%)	0 (0%)	0 (0%)	2 (33%)	0 (0%)	2 (10%)
Hemic and lymphatic system	Total	2 (67%)	1 (33%)	0 (0%)	2 (33%)	0 (0%)	5 (25%)
	Ecchymosis	0 (0%)	1 (33%)	0 (0%)	2 (33%)	0 (0%)	3 (15%)
	Lymphadenopathy	2 (67%)	0 (0%)	0 (0%)	0 (0%)	0 (0%)	2 (10%)
	Total	3 (100%)	1 (33%)	3 (100%)	6 (100%)	2 (40%)	15 (75%)
	Amnesia	0 (0%)	0 (0%)	1 (33%)	5 (83%)	2 (40%)	8 (40%)
	Dizziness	2 (67%)	0 (0%)	0 (0%)	1 (17%)	0 (0%)	3 (15%)
	Hypertonia	0 (0%)	1 (33%)	0 (0%)	4 (67%)	1 (20%)	6 (30%)
	Insomnia	1 (33%)	0 (0%)	0 (0%)	1 (17%)	0 (0%)	2 (10%)
	Paresthesia	1 (33%)	0 (0%)	2 (67%)	1 (17%)	2 (40%)	6 (30%)
Respiratory system	Total	2 (67%)	1 (33%)	0 (0%)	2 (33%)	1 (20%)	6 (30%)
	Cough increased	0 (0%)	1 (33%)	0 (0%)	1 (17%)	0 (0%)	2 (10%)
	Lung disorder	1 (33%)	0 (0%)	0 (0%)	1 (17%)	1 (20%)	3 (15%)
	Pharyngitis	1 (33%)	0 (0%)	0 (0%)	0 (0%)	1 (20%)	2 (10%)
	Rhinitis	1 (33%)	1 (33%)	0 (0%)	0 (0%)	0 (0%)	2 (10%)
Skin and appendages	Total	3 (100%)	1 (33%)	1 (33%)	3 (50%)	0 (0%)	8 (40%)
	Pruritus	3 (100%)	0 (0%)	0 (0%)	0 (0%)	0 (0%)	3 (15%)
	Rash	1 (33%)	1 (33%)	1 (33%)	1 (16.7%)	0 (0%)	4 (20%)
	Sweating	1 (33%)	1 (33%)	0 (0%)	2 (33%)	0 (0%)	4 (20%)
Urogenital system	Total	3 (100%)	3 (100%)	3 (100%)	6 (100%)	5 (100%)	20 (100%)
	Dysuria	1 (33%)	2 (67%)	1 (33%)	2 (33%)	1 (20%)	7 (35%)
	Hematuria	3 (100%)	3 (100%)	3 (100%)	6 (100%)	5 (100%)	20 (100%)
	Urethral pain	2 (67%)	1 (33%)	1 (33%)	4 (67%)	1 (20%)	9 (45%)
	Urinary retention	0 (0%)	0 (0%)	1 (33%)	1 (17%)	1 (20%)	3 (15%)
	Urinary frequency	1 (33%)	0 (0%)	1 (33%)	2 (33%)	3 (60%)	7 (35%)
	Nocturia	1 (33%)	0 (0%)	0 (0%)	0 (0%)	2 (40%)	3 (15%)
	Urination impaired	0 (0%)	1 (33%)	2 (67%)	1 (17%)	0 (0%)	4 (20%)

There were no serious AEs. However, there were five reports of severe AEs and/or grade 3 toxicity occurring in five men. All of these were considered to be reversible grade 3 toxicities and were not considered related to the study drug. One event was a short episode of hypertension (in a patient noted above), which occurred immediately postoperatively in a man with underlying hypertension. Another event was a short episode of psychosis, which occurred immediately postoperatively, in a patient with a history of postanesthesia psychosis. No specific intervention was required for either patient. The remaining events were hematuria with clots thought most likely to be secondary to the extended prophylactic indwelling Foley catheter. One man who reported grade 3 hematuria also reported the onset of erectile dysfunction, occurring at least 9 days after CV706 administration, that has persisted and was thought probably related to treatment. A second man experienced severe myalgias the day of treatment with CV706 that resolved with conservative management within 24 h. There have been no long-term toxicities in any of the patients.

Laboratory Data. Clinical laboratory safety data were assessed for 1 month after treatment. Posttreatment liver transaminase levels have been generally normal. Minor transient elevations in AST to just above the upper limit of normal (grade 1) were seen in three men in cohort 4 1 week after treatment. In all cases, AST returned to normal at the next time point, 1 week later. Three men showed comparable minor elevations of alanine aminotransferase at the same time point that resolved spontaneously within 1–2 weeks. Two patients in the highest dose level experienced mild increases in AST to just above the upper limit of normal (grade 1), one of whom also had a very slight, transient elevation in alanine aminotransferase to just above normal values. These values returned to baseline levels within 30 days. Thus, there were no National Cancer Institute grade 2 toxicities for hepatotoxicity.

Hematological studies disclosed a transient, small and clinically nonsignificant decrease in platelets (average decrement of 22%), seen consistently two days following treatment, with levels returning to baseline by one week after treatment. Even smaller changes were seen in RBCs in most patients, also transient, returning to normal by day fourteen. These decrements in RBC were not associated with fibrin split products, D-dimer levels or clinical signs of disseminated intravascular coagulopathy (DIC) and were reversible without intervention. A transient, clinically nonsignificant decrease in absolute lymphocyte levels was observed in 90% of patients and was found to be maximal one or two days posttreatment, with an average drop of 66%. Lymphocyte levels returned to within 25% of baseline in the majority of patients by day 7 posttreatment. No specific subset analysis of lymphocytes was performed. These hematological findings are consistent with an acute phase response, not marrow suppression and were asymptomatic.

PSA

There were statistically significant differences between cohorts in mean pretreatment PSA levels ($P = 0.04$): dose level 1, 45.3 ng/ml; dose level 2, 14.5 ng/ml; dose level 3, 27.5 ng/ml; dose level 4, 14.5 ng/ml; and dose level 5, 7.1 ng/ml The variance in pretreatment PSA between groups was significantly greater than the variance within groups. These differences were, in part, related to modification of the PSA entry criteria instituted approximately halfway through the trial.

There were immediate alterations in serum PSA levels in all patients after treatment. These alterations were an expected consequence of the frequent, invasive, prostatic manipulations performed within the first month, including the intraprostatic delivery of CV706 and the transrectal biopsies performed at days 4 and 22 posttreatment. Table 4 outlines the PSA changes seen in the 20 treated patients. Thirteen of 20 patients (65%) experienced a reduction in serum PSA of ≥30% from pretreatment levels. Five of 20 patients (25%) experienced a reduction in serum PSA of ≥50%. All five patients with a reduction in serum PSA of ≥50% were in dose levels 4 and 5 (5 of 11). Of these patients, four patients achieved a PR, defined as a reduction in serum PSA by ≥50% from pretreatment levels, sustained for at least 4 weeks. The maximum duration of this PSA response was 11.3 months.

When PSA data from this trial were subjected to analysis to determine the change in velocity (Fig. 1), it seems that treatment with CV706 at the two highest dose levels resulted in the largest net negative posttreatment log PSA slope (*i.e.*, greatest treatment effect). In fact, 14 of 20 men exhibited a net negative change in log PSA slope, with 10 of 14 occurring in dose levels 4 and 5.

Post-CV706 Treatment Prostate Biopsies

After CV706 administration, patients underwent repeat sextant biopsy of their prostate on posttreatment days 4 and 22 and at month 3. Adenoviral infection was demonstrable in the higher dose levels as documented by routine light microscopy. This analysis revealed morphologically identifiable intranuclear inclusions characteristic of adenovirus (data not shown). This finding was confirmed by immunohistochemistry for adenoviral hexon protein (Fig. 2*C*). Positive hexon staining was confined to prostatic epithelial cells only and was most striking in samples from patients treated in dose level 5. Positive and negative staining controls for immunohistochemistry against hexon protein were performed (Fig. 2, *A* and *B*, respectively). Day 4 biopsy material from several patients was fixed in gluteraldehyde and analyzed by transmission electron microscopy. Fig. 2*D* represents one of these analyses and reveals obvious virion within the nucleus of a prostatic epithelial cell, consistent with Ad5 replication.

Neutralizing Antibodies

A determination of anti-CV706 antibody titers was performed on blood samples from patients before and after treatment. The results of this analysis are shown in Table 5. This analysis demonstrates that anti-CV706 antibody levels increased after treatment in all patients. There was no evident correlation between baseline antibody titer and subsequent PSA response.

Table 4 *Change in serum PSA after intraprostatic delivery of CV706*

Patient no.	Dose level	Pre-CV706 serum PSA (ng/ml)	Post-CV706 serum PSA (ng/ml) nadir	Change in serum PSA
1	1	58.7	37.1	−37%
2	1	59.7	N/C[a]	N/C
3	1	17.6	12.1	−31%
4	2	10.9	N/C	N/C
5	2	11.8	8.0	−32%
6	2	20.9	11.0	−47%
7	3	14.6	N/C	N/C
8	3	54.8	46.6	−15%
9	3	13.0	N/C	N/C
10	4A	12.4	7.6	−39%
11	4A	7.6	4.2	−45%
12	4B	7.5	N/C	N/C
13	4B	6.4	1.2	−81%[b]
14	4C	44.8	28.3	−37%
15	4C	8.6	3.9	−55%[b]
16	5A	9.1	N/C	N/C
17	5A	7.4	2.5	−66%[b]
18	5B	13.2	3.6	−73%[b]
19	5B	4.2	2.6	−38%
20	5C	1.4	0.7	−50%

[a] N/C, no change.
[b] Patients who meet criteria for PR.

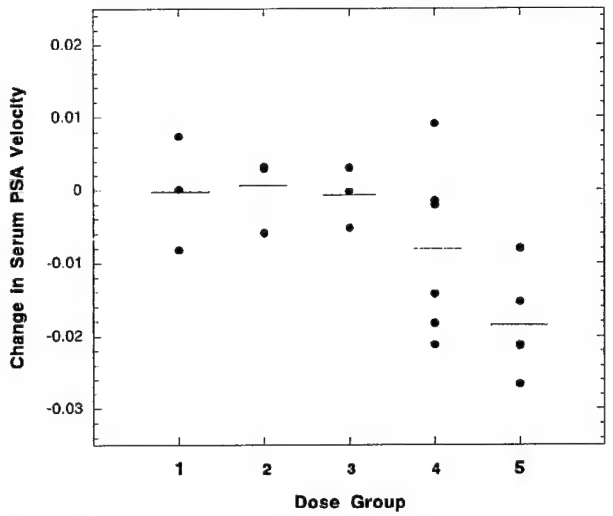

Fig. 1. Mean change in the slope of log serum PSA for each treated patient. This parameter provides information as to change in PSA velocity. The change in the log PSA slope (pretreatment *versus* posttreatment slopes) was determined for each patient and is presented here (some symbols overlap). The mean change in the log PSA within each dose group was also determined and is represented by the *horizontal bar*. The mean change in log PSA slope and SD, respectively, for each dose group: dose level 1, −0.0002 and 0.0078; dose level 2, 0.00007 and 0.0052; dose level 3, −0.0008 and 0.0041; dose level 4, −0.0080 and 0.0117; dose level 5, −0.0184 and 0.0071. Dose levels 4 and 5 had greatest negative change in log serum PSA slope. Larger negative values indicate greater treatment effect using reduction in PSA velocity as an end point. F-test of overall heterogeneity among the dose group means reveals them to be statistically different at $P < 0.004$.

Circulating and Excreted CV706

Circulating CV706. A quantitative PCR technique was used to determine the amount of CV706 in circulation after viral instillation. This technique detects viral DNA only, likely from intact virus particles, but does not necessarily correlate with infectious virus titer. At baseline (pretreatment), the average number of CV706 copies/ml was 168 ± 385, representing background in the assay. The cutoff for a potentially significant number above background was set at 1300 copies/ml (approximately the average baseline value + 3 SDs). Copies of CV706 were detected in the earliest plasma sample taken after virus administration (*i.e.*, 30 min posttreatment) in all but 2 of 16 tested patients (both patients from dose level 5A). Plasma from these two patients contained no CV706 at this time point, although virus was identified in plasma at subsequent time points. The amount of CV706 viral genome in circulation 30 min after treatment varied significantly between patients, with between 0.007% and 0.129% of the total dose of virus administered being detected. This initial peak in circulating virus subsided to near-baseline levels in all patients tested within 12–24 h after treatment. Elimination of the virus appeared biphasic, with a sharp decline between 30 and 60 min after treatment and then a slower elimination over the next 12 h by first-order kinetics. On the basis of the 30- and 60-min time points, the average initial half-life of virus in circulation was 23 min (range, 11–170 min).

A single productive infectious cycle of adenovirus takes ~24–36 h before the release of newly formed virus from infected cells occurs (25). Interestingly, a second peak of detectable CV706 genome found in the circulation in all patients tested except three (one patient each from dose levels 3, 4A, and 4B) between 2 and 8 days after treatment. The viral load associated with this secondary peak varied between patients, and in at least four patients, it exceeded the load detected in circulation shortly after treatment. This secondary peak had a longer duration in most patients (median of 5 days) and, therefore, the total amount of systemic virus was substantially larger than that from the initial treatment in at least 10 of 16 tested patients. An example of this time course, from one patient treated in dose level 5A (1×10^{13} viral particles), is provided in Fig. 3. For all patients tested, circulating CV706 levels returned to values indistinguishable from baseline (≤1300 copies/ml) by day 15 after treatment.

Ad5-neutralizing antibody titers were measured in patients as described above. All patients that had a significant secondary virus peak

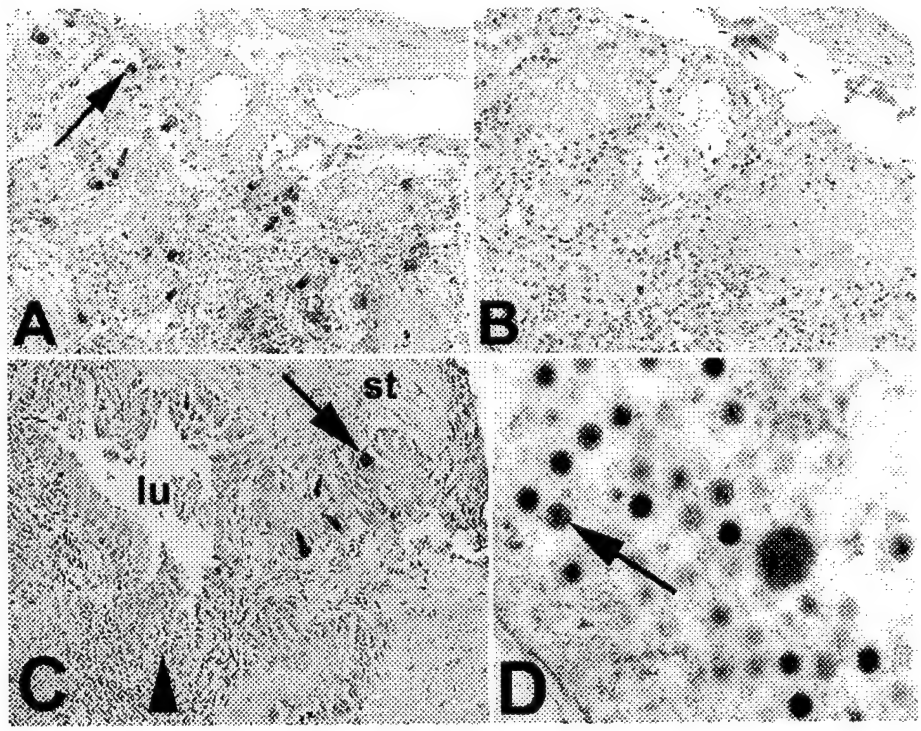

Fig. 2. Day 4 posttreatment prostatic needle biopsies for detection of adenovirus. *A*, positive control for immunohistochemistry against hexon protein. Lung tissue from an autopsy case of a patient with disseminated adenoviral infection (patient was not part of this study). *Arrow*, infected alveolar cell. *B*, negative control for immunohistochemistry against hexon protein. Adjacent section lung tissue from autopsy case of patient with disseminated adenoviral infection. *C*, immunohistochemistry against hexon protein from patient treated with CV706. *Arrow*, prostatic epithelial cells staining positive. *Arrowhead*, mononuclear inflammatory infiltrate involving the edge of a prostatic acinus. *st*, stromal tissue; *lu*, luminal tissue. *D*, transmission electron microscopy. *Arrow*, example of mature adenovirus within nucleus of prostatic epithelial cell.

Table 5 *Neutralizing antibody titers to CV706 before and after intraprostatic administration*

Patient	Baseline	Day 3	Day 8	Day 15	Day 30
001	1:256	1:256	1:6400	1:6400	1:6400
002	1:32	1:32	1:1024	1:2048	1:2048
003	1:1024	1:1024	1:4000	1:4000	1:4000
004	<1:4	<1:4	1:256	1:256	1:512
005	<1:4	<1:4	1:128		1:256
006	<1:4	<1:4	1:256	1:256	1:128
007	1:128	1:64	1:1024	1:2048	1:2048
008	0	0	0	1:256	1:128
009	0	0	1:16	1:32	1:64
010	1:8	1:32	1:250	1:2048	1:1024
011	0	0	0	1:16	1:128
012	ND	1:8	1:1024	1:4056	>1:128
013	0	0	0	1:16	>1:128
014	<1:4	<1:4	>1:256	>1:256	>1:256
015	<1:4	<1:4	>1:256	ND	>1:256
016	1:8	1:8	>1:256	>1:256	>1:256
017	>1:128	>1:128	>1:128	>1:128	>1:128
018	1:2	1:4	>1:128	>1:128	>1:128

also had low levels or undetectable anti-Ad5 antibodies at baseline. However, one patient with no anti-Ad5 antibodies at baseline did not produce a significant secondary peak of circulating CV706 genome. There seemed to be an inverse relationship between neutralizing antibody titer at baseline and the amount of viral genome seen in the secondary peak. Levels of anti-Ad5 antibodies at baseline did not seem to correlate with systemic levels of CV706 immediately after treatment.

Excreted CV706. Urine was collected from all patients at specified times before and after treatment with CV706. Standard plaque assays were performed to determine the amount of virus shedding in the urine. At baseline (pretreatment), urine from all tested patients failed to induce plaque formation. By day 2 posttreatment, urine from 11 of 19 treated patients was positive for viral shedding as determined by plaque formation at >50 plaque-forming units/ml. Urine from only two patients continued to induce plaque formation at day 8, and by days 15 and 29, urine from all tested patients failed to induce plaques. No plaques were observed from urine samples in the tissue selectivity assay using HBL-100 cells, which are permissive for wild-type virus but nonpermissive for CV706 replication. A control assay using an equivalent Ad5 vector containing a wild-type *E1A* region was able to infect HBL-100 cells efficiently, suggesting that the virus in the urine of treated patients was not likely a wild-type recombinant.

DISCUSSION

This study represents the first clinical translation of a prostate-specific, replication-restricted adenovirus for the treatment of PCa. In addition, it is one of the first studies to document therapeutic viral replication in specific cells of the target organ in the human. More importantly, the data presented in this manuscript showed intraprostatic CV706 to be safe and not associated with irreversible grade 3 or any grade 4 toxicity. The most common side effects noted were genitourinary symptoms, likely worsened by the prophylactic insertion of an indwelling Foley catheter that the patients were required under the protocol to maintain for 14 days. Systemic toxicity was minimal, with the majority of these side effects limited to a brief grade 1 or 2 fever with or with out an associated shaking chill. These episodes were self-limited and responded to routine antipyretics, and no patient required antibiotics. This phenomenon is consistent with previously reported series using intratumoral injections of replication-competent adenovirus (Onyx-015; Refs. 10, 26, 27) and may represent a cytokine release in response to the adenovirus (28–30).

A transient lymphopenia, which was not clinically significant, was noted in a majority of patients within 48 h of viral instillation with recovery of counts to within 25% of baseline in the majority of patients by 7 days posttreatment. The timing of this decrement combined with the quick recovery is most suggestive of an acute-phase reaction with associated leukocyte margination, and not bone marrow suppression (31). Importantly, treatment with CV706 was not associated with significant hepatic or coagulation abnormalities. Specifically, no patient experienced greater than grade 1 elevation of liver transaminases, and no patient had evidence of alteration in prothrombin time or partial thromboplastin time or a decrement in fibrinogen. This safety was evident even at the highest dose level of 1×10^{13} viral particles and with evidence of viral shedding into the blood. Although the quantitative PCR for CV706 is likely detecting intact virus but not necessarily only viable virus, it is consistent with *in vivo* viral replication. The MTD of intraprostatic CV706 was not reached in this study, even at the highest administered dose of 1×10^{13}. Significantly higher doses could not be delivered given manufacturing limitations in concentrating the virus further. Taken together, these data reveal the safety of CV706 when administered by intraprostatic injection and are critical to the future development of similar tissue-specific replication-competent adenoviruses.

The analysis of secondary study end points provides compelling evidence of CV706 activity. Serum PSA is well known to be a marker of both disease activity as well as disease burden (32–36). In this study, all patients achieving a PSA reduction ≥50% and/or who achieved a PR occurred in the highest two dose levels, suggesting a dose response for CV706. Moreover, there was a statistically significant reduction in the PSA velocity after treatment with CV706, again most pronounced for patients in dose levels 4 and 5, also suggestive of a dose-response relationship. The mean and median duration of PR was just over 6 months (6.6 months), suggesting the potential for disease stabilization by CV706 treatment. Biopsy of the prostate results in significant elevations in serum PSA for >2 weeks (37). Although the design of this study, with frequent posttreatment biopsies, aided in the documentation of viral replication, these same invasive procedures prevented a full analysis of the PSA-response to therapy with CV706. Thus, it is possible that substantial reductions in serum PSA could have been obscured by these frequent prostatic manipulations. Despite this possibility, the evidence gathered on PSA levels subsequent to treatment with CV706 are encouraging and

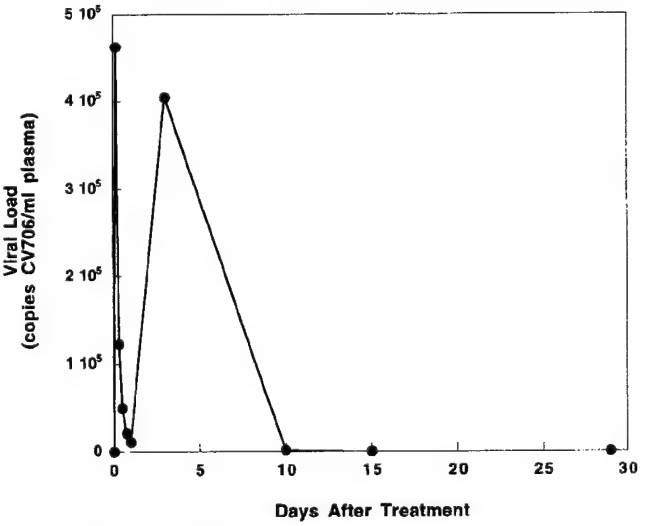

Fig. 3. CV706 viral load/ml of plasma from day of treatment to month 1 in a patient treated with 1×10^{13} viral particles. The peak height 30 min after treatment in this patient is equivalent to 0.014% of the injected dose, assuming 3 liters of plasma.

suggest that at the higher dose levels, a clinically meaningful treatment effect may be achievable.

This treatment effect at higher doses is associated with clear histological and molecular evidence of viral replication. The viral inclusions seen on electron microscopy and the positive staining for hexon protein seen on immunohistochemistry from day 4 biopsy materials was confined to prostatic epithelial cells. Of note, hexon staining was most prominent in the highest dose levels and, like the electron microscopy, highly suggestive of intraprostatic replication of CV706 in these patients. At the highest dose level, Phase II trials estimating efficacy seem fully warranted.

Importantly, we were able to rigorously document CV706 shedding in the blood after intraprostatic delivery without significant associated clinical sequelae. The quantitative PCR assay is very specific for CV706 and is capable of detecting 1300 copies/ml of plasma. These results confirm that a small but significant amount of the intraprostatically administered virus reached the circulation. These experiments were not, however, designed to quantitatively assess the proportion of detectable genome derived from only viable CV706. The amount of virus released in the first "peak" varied between patients, did not seem to be related to the dose level or neutralizing antibody titer, and may represent leakage of virus during the administration procedure. The highest total amount of virus detected was in two patients (patients 12 and 14), with an estimate of <2% of the dose being detected. A significant secondary peak of circulating CV706 genome was observed in most patients ~3 days after treatment, suggestive of viral replication. The appearance and size of the secondary peak seemed to depend on a low anti-Ad5 antibody titer at the time of treatment. These data are consistent with those derived from electron microscopy and immunohistochemistry and support the *in vivo* observations of CV706 replication in the human prostate.

Response to CV706 was not correlated with the presence of preexisting Ad5 neutralizing antibodies. After administration, most patients developed Ad5 neutralizing antibodies. These new antibodies did not block clinical response to treatment. Moreover, our data also reveal that the presence of preexisting anti-Ad5 antibodies is not obviously correlated with treatment-related toxicity. These data extend the previously reported work on intratumoral delivery of replication-competent adenovirus by revealing a lack of association between neutralizing antibody levels and treatment toxicity (10). Whereas circulating anti-Ad5 antibody may significantly impact on the efficacy and toxicity of systemically administered adenovirus (38), it is not clear that these antibodies have the same access to the tumor-bearing prostate, and thus they may have a limited impact on direct intratumoral injections (39).

In summary, CV706 seems safe when delivered by intraprostatic injection using a planned, stereotactic approach. This trial also suggests that CV706 replicates selectively in prostatic epithelial cells, *i.e.,* those prostate cells that make PSA, and does so in a time frame consistent with an adenoviral replicative cycle. To our knowledge, this is the first report of oncolytic viral vectors showing molecular and clinical activity in humans with PCa. Finally, these data suggest that CV706 possess biological activity, as evidenced by significant decreases in serum PSA, which seem to be dose-related. This was evident despite the frequent prostatic manipulations experienced by patients in this study, which could have significantly obscured full interpretation of these results. Thus, continued development of prostate-specific adenoviral vectors is compelling. In fact, concomitant treatment of carcinoma cells with oncolytic adenoviruses and DNA-damaging agents like radiation or certain chemotherapeutic agents can result in supra-additive cell killing (40–43). Thus, when considering the safety and activity of CV706, a strong rationale exists for additional laboratory and clinical investigation of CV706 in conjunction with radiation therapy for the treatment of human PCa.

ACKNOWLEDGMENTS

We thank Drs. Donald Coffey, Martin Abeloff, Albert Owens, and David Karpf for their thoughtful review of this manuscript and Jurg Sömmer for performing assays for circulating CV706.

REFERENCES

1. Shipley, W. U., Thames, H. D., Sandler, H. M., Hanks, G. E., Zietman, A. L., Perez. C. A., Kuban, D. A., Hancock, S. L., and Smith, C. D. Radiation therapy for clinically localized prostate cancer: a multi-institutional pooled analysis. JAMA, *281:* 1598–1604, 1999.
2. Hanlon, A. L., and Hanks, G. E. Scrutiny of the ASTRO consensus definition of biochemical failure in irradiated prostate cancer patients demonstrates its usefulness and robustness. Int. J. Radiat. Oncol. Biol. Phys., *46:* 559–566, 2000.
3. Kuban, D. A., el-Mahdi, A. M., and Schellhammer, P. The significance of post-irradiation prostate biopsy with long-term follow-up. Int. J. Radiat. Oncol. Biol. Phys., *24:* 409–414, 1992.
4. Fuks, Z., Leibel, S. A., Wallner, K. E., Begg, C. B., Fair, W. R., Anderson, L. L., Hilaris, B. S., and Whitmore, W. F. The effect of local control on metastatic dissemination in carcinoma of the prostate: long-term results in patients treated with ^{125}I implantation. Int. J. Radiat. Oncol. Biol. Phys., *21:* 537–547, 1991.
5. Webb, H. E., and Smith, C. E. Viruses in the treatment of cancer. Lancet, *1:* 1206–1208, 1970.
6. Ilan, Y., Droguett, G., Chowdhury, N. R., Li, Y., Sengupta, K., Thummala, N. R., Davidson, A., Chowdhury, J. R., and Horwitz, M. S. Insertion of the adenoviral E3 region into a recombinant viral vector prevents antiviral humoral and cellular immune responses and permits long-term gene expression. Proc. Natl. Acad. Sci. USA, *94:* 2587–2592, 1997.
7. Ali, M., Lemoine, N. R., and Ring, C. J. The use of DNA viruses as vectors for gene therapy. Gene Ther., *1:* 367–384, 1994.
8. Visakorpi, T., Kallioniemi, O. P., Paronen, I. Y., Isola, J. J., Heikkinen, A. I., and Koivula, T. A. Flow cytometric analysis of DNA ploidy and S-phase fraction from prostatic carcinomas: implications for prognosis and response to endocrine therapy. Br. J. Cancer, *64:* 578–782, 1991.
9. Kallioniemi, O. P., Visakorpi, T., Holli, K., Heikkinen, A., Isola, J., and Koivula, T. Improved prognostic impact of S-phase values from paraffin-embedded breast and prostate carcinomas after correcting for nuclear slicing. Cytometry, *12:* 413–421, 1991.
10. Ganly, I., Eckhardt, S. G., Rodriguez, G. I., Soutar, D. S., Otto, R., Robertson, A. G., Park, O., Gulley, M. L., Heise, C., Von Hoff, D. D., and Kaye, S. B. A Phase I study of Onyx-015, an E1B attenuated adenovirus, administered intratumorally to patients with recurrent head and neck cancer. Clin. Cancer Res., *6:* 798–806, 2000.
11. Nemunaitis, J., Ganly, I., Khuri, F. Arseneau, J., Kuhn, J., McCarty, T., Landers, S., Maples, P., Romel, L., Randlev, B., Reid, T., Kaye, S., and Kirn, D. Selective replication and oncolysis in p53 mutant tumors with ONYX-015, an E1B–55kD gene-deleted adenovirus, in patients with advanced head and neck cancer: a Phase II trial. Cancer Res., *60:* 6359–6366, 2000.
12. Smith, R. R., Huebner, R. J., Rowe, W. P., Schatten, W., and Thomas, L. Studies on the use of viruses in the treatment of carcinoma of the cervix. Cancer (Phila.), *9:* 1211–1218, 1956.
13. Bischoff, J. R., Kirn, D. H., Williams, A., Heise, C., Horn, S., Muna, M., Ng, L., Nye, J. A., Sampson-Johannes, A., Fattaey, A., and McCormick, F. An adenovirus mutant that replicates selectively in p53-deficient human tumor cells. Science (Wash. DC), *274:* 373–376, 1996.
14. Rodriguez, R., Schuur, E. R., Lim, H. Y., Henderson, G. A., Simons, J. W., and Henderson, D. R. Prostate attenuated replication competent adenovirus (ARCA) CN706: a selective cytotoxic for prostate-specific antigen-positive prostate cancer cells. Cancer Res., *57:* 2559–2563, 1997.
15. Curiel, D. T. The development of conditionally replicative adenoviruses for cancer therapy. Clin. Cancer Res., *6:* 3395–3399, 2000.
16. Bastacky, S. I., Wojno, K. J., Walsh, P. C., Carmichael, M. J., and Epstein, J. I. Pathological features of hereditary prostate cancer. J. Urol., *153:* 987–992, 1995.
17. Ragde, H., Blasko, J. C., Grimm, P. D., Kenny, G. M., Sylvester, J. E., Hoak, D. C., Landin, K., and Cavanagh, W. Interstitial iodine-125 radiation without adjuvant therapy in the treatment of clinically localized prostate carcinoma. Cancer (Phila.), *80:* 442–453, 1997.
18. de la Taille, A., Hayek, O., Benson, M. C., Bagiella, E., Olsson, C. A., Fatal, M., and Katz, A. E. Salvage cryotherapy for recurrent prostate cancer after radiation therapy: the Columbia experience. Urology, *55:* 79–84, 2000.
19. Rogers, E., Ohori, M., Kassabian, V. S., Wheeler, T. M., and Scardino, P. T. Salvage radical prostatectomy: outcome measured by serum prostate specific antigen levels. J. Urol., *153:* 104–110, 1995.
20. Beyer, D. C. Permanent brachytherapy as salvage treatment for recurrent prostate cancer. Urology, *54:* 880–883, 1999.
21. Grado, G. L., Collins, J. M., Kriegshauser, J. S., Balch, C. S., Grado, M. M., Swanson, G. P., Larson, T. R., Wilkes, M. M., and Navickis, R. J. Salvage brachytherapy for localized prostate cancer after radiotherapy failure. Urology, *53:* 2–10, 1999.
22. Consensus statement: guidelines for PSA following radiation therapy. American Society for Therapeutic Radiology and Oncology Consensus Panel. Int. J. Radiat. Oncol. Biol. Phys., *37:* 1035–1041, 1997.

23. Mastrangeli, A., Harvey, B. G., Yao, J., Wolff, G., Kovesdi, I., Crystal, R. G., and Falck-Pedersen, E. "Sero-switch" adenovirus-mediated *in vivo* gene transfer: circumvention of anti-adenovirus humoral immune defenses against repeat adenovirus vector administration by changing the adenovirus serotype. Hum. Gene Ther., *7:* 79–87, 1996.
24. Doane, F. W., and Anderson, N. Electron Microscopy in Diagnostic Virology, a Practical Guide and Atlas. Cambridge: Cambridge University Press, 1987.
25. Fields, B., Knipe, D. M., and Howley, P. M. Fields Virology. Philadelphia: Lippincott-Raven, 1996.
26. Khuri, F. R., Nemunaitis, J., Ganly, I., Arseneau, J., Tannock, I. F., Romel, L., Gore, M., Ironside, J., MacDougall, R. H., Heise, C., Randlev, B., Gillenwater, A. M., Bruso, P., Kaye, S. B., Hong, W. K., and Kirn, D. H. A controlled trial of intratumoral ONYX-015, a selectively-replicating adenovirus, in combination with cisplatin and 5-fluorouracil in patients with recurrent head and neck cancer. Nat. Med., *6:* 879–885, 2000.
27. Kirn, D., Nemunaitis, J., Gainley, I., Posner, M., Vokes, E., Kuhn, J., Heise, C., Maack, C., and Kaye, S. A Phase II trial of intratumoral injection with an E1B-deleted adenovirus, onyx-015, in patients with recurrent, refractory head and neck cancer. Proc. of Am. Soc. Clin. Oncol., *17:* 391A, 1998.
28. Benihoud, K., Salone, B., Esselin, S., Opolon, P., Poli, V., DiGiovine, M., Perricaudet, M., and Saggio, I. The role of IL-6 in the inflammatory and humoral response to adenoviral vectors. J. Gene Med., *2:* 194–203, 2000.
29. Cartmell, T., Southgate, T., Rees, G. S., Castro, M. G., Lowenstein, P. R., and Luheshi, G. N. Interleukin-1 mediates a rapid inflammatory response after injection of adenoviral vectors into the brain. J. Neurosci., *19:* 1517–1523, 1999.
30. Mistchenko, A. S., Diez, R. A., Mariani, A. L., Robaldo, J., Maffey, A. F., Bayley-Bustamante, G., and Grinstein, S. Cytokines in adenoviral disease in children: association of interleukin-6, interleukin-8, and tumor necrosis factor α levels with clinical outcome. J. Pediatr., *124:* 714–720, 1994.
31. Lee, G. R., Foerster, J., and Lukens, J. Wintrobe's Clinical Hematology, pp. 1836–1861. Baltimore, MD: Williams & Wilkins, 1999.
32. Polascik, T. J., Oesterling, J. E., and Partin, A. W. Prostate specific antigen: a decade of discovery—what we have learned and where we are going. J. Urol., *162:* 293–306, 1999.
33. Kelly, W. K., Scher, H. I., Mazumdar, M., Vlamis, V., Schwartz, M., and Fossa, S. D. Prostate-specific antigen as a measure of disease outcome in metastatic hormone-refractory prostate cancer. J. Clin. Oncol., *11:* 607–615, 1993.
34. Smith, D. C., Dunn, R. L., Strawderman, M. S., and Pienta, K. J. Change in serum prostate-specific antigen as a marker of response to cytotoxic therapy for hormone-refractory prostate cancer. J. Clin. Oncol., *16:* 1835–1843, 1998.
35. Zagars, G. K., and Pollack, A. Kinetics of serum prostate-specific antigen after external beam radiation for clinically localized prostate cancer. Radiother. Oncol., *44:* 213–221, 1997.
36. Pound, C. R., Partin, A. W., Eisenberger, M. A., Chan, D. W., Pearson, J. D., and Walsh, P. C. Natural history of progression after PSA elevation following radical prostatectomy. JAMA, *281:* 1591–1597, 1999.
37. Yuan, J. J., Coplen, D. E., Petros, J. A., Figenshau, R. S., Ratliff, T. L., Smith, D. S., and Catalona, W. J. Effects of rectal examination, prostatic massage, ultrasonography and needle biopsy on serum prostate specific antigen levels. J. Urol., *147:* 810–814, 1992.
38. Chen, Y., Yu, D. C., Charlton, D., and Henderson, D. R. Pre-existent adenovirus antibody inhibits systemic toxicity and antitumor activity of CN706 in the nude mouse LNCaP xenograft model: implications and proposals for human therapy. Hum. Gene Ther., *11:* 1553–1567, 2000.
39. Baxter, L. T., Zhu, H., Mackensen, D. G., Butler, W. F., and Jain, R. K. Biodistribution of monoclonal antibodies: scale-up from mouse to human using a physiologically based pharmacokinetic model. Cancer Res., *55:* 4611–4622, 1995.
40. Sanchez-Prieto, R., Quintanilla, M., Cano, A., Leonart, M. L., Martin, P., Anaya, A., and Ramon y Cajal, S. Carcinoma cell lines become sensitive to DNA-damaging agents by the expression of the adenovirus *E1A* gene. Oncogene, *13:* 1083–1092, 1996.
41. Rogulski, K. R., Freytag, S. O., Zhang, K., Gilbert, J. D., Paielli, D. L., Kim, J. H., Heise, C. C., and Kirn, D. H. *In vivo* antitumor activity of ONYX-015 is influenced by p53 status and is augmented by radiotherapy. Cancer Res., *60:* 1193–1196, 2000.
42. Yu, D-C., Chen, Y., Dilley, J., Li, Y., Embry, M., Zhang, H., Nguygen, N., Amin, P., Oh, J., and Henderson, D. R. Antitumor synergy of CV787, a prostate cancer-specific adenovirus, and paclitaxel and docetaxel. Cancer Res., *61:* 517–525, 2001.
43. Chen, Y., DeWeese, T. L., Dilley, J., Zhang, Y., Li, Y., Ramesh, N., Lee, J., Pennathur-Das, R., Radzyminski, J., Wypych, J., Brignetti, D., Scott, S., Stephens, J., Karpf, D. B., Henderson, D. R., and Yu, D-C. CV706, a prostate cancer-specific adenovirus variant, in combination with radiotherapy produces synergistic antitumor efficacy without increasing toxicity. Cancer Res., *61:* 5453–5460, 2001.

Expression of adenovirus E4orf6 as a potential radiation sensitization strategy

Spencer J. Collis, Ph.D.[1], Gary W. Ketner, Ph.D.[2], Jessica L. Hicks, BS. [3], Angelo M. DeMarzo, M.D. Ph.D. [3] and Theodore L. DeWeese, M.D.[1 4 †]

Departments of Oncology[1], Urology[4] and Pathology[3], Johns Hopkins University School of Medicine, Baltimore, Maryland 21231, USA.

[2]Department of Molecular Microbiology and Immunology, Johns Hopkins University School of Public Health, Baltimore, Maryland 21205, USA.

[†]Corresponding author:-

Theodore L. DeWeese, M.D.
Assistant Professor of Oncology and Urology
Director, Radiation Research Program
The Sidney Kimmel Comprehensive Cancer Center at Johns Hopkins
Bunting-Blaustein Cancer Research Building
1650 Orleans Street
Baltimore
MD 21231-1000
Phone: (410) 614 3979
Fax: (410) 502 7234
E-mail: DeWeete@jhmi.edu

Supported in part by NCI/NIH CA.58236 and DAMD 17-981-1-8475 grants.

Abstract

Purpose: The adenovirus E4orf6 34kDa protein (E4-34k) is known to disrupt V(D)J recombination as a result of its interaction with the catalytic sub-unit of cellular DNA-dependent protein kinase (DNA-PK_{cs}), a major factor in the repair of DNA double-strand breaks (dsb). Previous studies have shown that cells with disrupted dsb repair and V(D)J recombination due to attenuation of DNA-PK_{cs} activity exhibit a radiation sensitive phenotype. It is not known at present whether the E4-34k protein can also modify cellular response to ionising radiation. In an attempt to develop a novel gene therapy strategy to modify cellular radiation response, we sought to determine if expression of the adenovirus E4-34k protein results in sensitization to clinically relevant doses of ionizing radiation.

Methods and Materials: Clonogenic survival assays were carried out on Du145, RKO and 293 cells following transient transfection of E4-34k and/or E1B-55k expressing plasmids. Western blots and immunohistochemical analyses were used to demonstrate E4-34k expression within transfected cells. FACS sorting was carried out to enrich cells transfected with a plasmid which expresses both E4-34k and enhanced green fluorescent protein (EGFP).

Results: We show that E4-34k expression does not affect cellular radiosensitivity of transiently transfected populations of prostate or colon cancer cell lines. Similar results were obtained using both human embryonic kidney 293 cells, which constitutively expresses the E1B-55k protein, and Du145 cells co-transfected with separate E4-34k and E1-55K-expressing plasmids, demonstrating that the adenovirus E1B-55k protein does not augment any effects E4-34k might have on DNA-PK_{cs} activity.

Conclusions: This finding is quite intriguing, as it is known that E4-34k interaction with DNA-PK_{cs} causes disruption of V(D)J recombination, a process dependent on dsb re-joining. These data clearly suggest that the V(D)J recombination and the dsb repair activities of DNA-PK_{cs}

can be separated and that preferential targeting of certain components of DNA-PK$_{cs}$ will be required to influence cellular radiosensitivity.

Keywords: DNA-PK, adenovius, radiosensitizing, gene therapy

Introduction

The adenovirus type 5 E4orf6 region encodes a 34 kDa protein, which plays an important role in viral infection. During early infection, it facilitates the inactivation of p53 via direct binding and/or forming a complex with E1B-55kDa, which leads to rapid turnover of p53 (1, 2, 3). This activity is necessary in order to prevent p53-mediated cell-cycle arrest and subsequent apoptosis that results from E1A expression (4). During late stages of viral infection, E4-34k in combination with E1B-55k shuttles between the nucleus and cytoplasm in order to accumulate viral late mRNA within the cytoplasm and simultaneously inhibit export of cellular mRNAs (5, 6, 7).

DNA-PK is a trimeric protein comprised of the DNA-binding Ku heterodimer and 450 kDa phosphatidylinositol 3 (PI-3)-kinase sub-unit DNA-PK$_{cs}$ (8). As DNA-PK$_{cs}$ is fundamental in the processes of DNA dsb repair and V(D)J recombination (9, 10), linear double-stranded viral DNA are likely to provide a substrate for DNA-PK-mediated recombination. Indeed, previous work has shown that E4-34k interacts with DNA-PK$_{cs}$ and inhibits V(D)J recombination within infected cells to prevent concatemerisation of viral DNA and aid infection (11). The inhibition of DNA-PK activity may also be advantageous to the propagation of viral infection as recent work has shown that DNA-PK$_{cs}$ is required for p53

DNA binding (12). Thus, inhibition of DNA-PK_{cs} by E4-34k may highlight another mechanism by which the virus can prevent p53-mediated apoptosis of infected cells.

Defective DNA-PK_{cs} in rodent models leads to a 'severe combined immune deficiency' (SCID) phenotype, which is associated with defective V(D)J recombination and hypersensitivity to ionising radiation (9, 13, 14). Furthermore, non-specific inhibition of cellular DNA-PK_{cs} kinase activity using the PI-3-kinase inhibitor wortmannin leads to a dramatic increase in radiosensitivity (15). It has shown that cells deficient in DNA-PK activity are also more sensitive to various DNA-damaging agents (16, 17, 18). Recent work has demonstrated that although DNA-PK is may be involved in the sensing of DNA damage caused by nucleoside analogues such as Gemcitabine (19), its activity does not appear to be critical for the radiosensitizing effect of these drugs (20).

We were therefore interested in the potential use of exogenously delivered E4-34k expression as a novel mechanism for radiosensitization. However, we show in the present study that E4-34k is incapable of causing any increase in radiation sensitivity either independently or in conjunction with E1B-55k expression. These data demonstrate that E4-34k inhibition of DNA-PK_{cs}-mediated V(D)J recombination must not be a consequence of reduced kinase activity and thus, the two functions of DNA-PK_{cs} which appear inter-related, can be separated.

Methods and Materials

Cell culture

DU145, RKO and 293 cell were obtained from the American Type Culture Collection and maintained as adherent monolayer cultures in RPMI (Du145 and RKO) or MEM (293) culture medium (GibcoBRL), supplemented with 10% foetal bovine serum (GibcoBRL). All cultures were grown at 37°C in a humidified atmosphere of 5% carbon dioxide, fed every 5 days with complete medium and sub-cultured when confluence was reached.

Plasmids

The plasmid pCMV6.9 has been previously described (21). The plasmid pREV-E4orf6 was constructed by excising the E4orf6 sequence from pCMV6.9 and inserted it into the multiple cloning site (REO site) of pREV (22). Diagnostic digestion, PCR and sequencing were used to confirm correct orientation/sequence of E4orf6 within this plasmid. pREV-E4orf6 encodes EGFP and E4orf6 under the control of separate CMV promoters. Previous work has demonstrated that both CMV promoters function equally within the pREV construct (22, 23).

Transfection of cells

A total of 1 x 10^5 cells were seeded into each well of a 6-well tissue culture plate (Falcon). The following day (when the cells were 70-80% confluent) the culture medium was aspirated and the cell monolayer was washed with pre-warmed sterile phosphate-buffered saline (PBS). Cells were transfected with the appropriate construct using LipofectaminePlus™ reagent (GibcoBRL) according to the manufacturer's protocol. Green fluorescence of pREV-transfected cells was quantified at each time point by FACS analysis and used to ascertain transfection efficiencies for cells transiently transfected with pCI, pCMV6.9 and pCMV-55k.

For RKO cells, replica wells transfected with pREV and pREV-E4orf6 were analysed by FACS to obtain an average transfection efficiency for each plasmid in individual experiments.

FACS analysis

For each sample 1x 10^4 cells were analysed on a Becton Dickinson FACScan flow cytometer with an excitation wavelength of 488nm and fluorescein isothiocyanate (FITC) collection wavelength using a band-pass filter at 530± 15nm. Dead cells were gated out of the samples by forward and side scatter. The level of EGFP fluorescence in live cells was determined using the Becton Dickinson CellQuest program. These settings were also used for cell sorting at ≥ 10^2 fluorescence (four-log scale).

Clonogenic survival

Cell survival was carried out as previously described (24). Briefly, cells were trypsinised and diluted to the appropriate cell density in 100mm culture dishes to give at least 50 colonies per dish following irradiation and then irradiated at 0.78 Gy/min to the desired dose using an aerated ^{137}Caesium source. Ten or 14 days after irradiation (Du145 or 293 cells respectively), colonies comprising of at least fifty cells were counted after staining with Crystal Violet (Sigma-Aldridge). Cell survival was plotted as a function of dose.

Immunoblots and Immunohistochemistry

The orf6 antibody used for immunohistochemistry has been previously described (25). Cytospin preparations were made from aliquots of FACS sorted Du145 cells used for clonogenic survival assays and fixed for 10mins in 4% paraformaldehyde. Slides were stained using a previously published protocol and reagents (26). The E4-34k antibody was diluted to

1:100, and protein expression was visualised by DAB staining. For immunoblots, standard protein extraction and Western blot procedures were used. A total of 10μg of protein extracted from each transfected cell population was used per blot. Blots were probed with anti-DNA-PK antibody (Oncogene, 1:1000), E4-34k antisera (25, 1:500) and an anti-actin antibody (Sigma, 1:1000), and then incubated with the appropriate secondary antibody (respectively diluted to 1:5000, 1:1000 and 1:000). Protein expression was visualised using an ECL kit (Amersham-Pharmacia). All Western blot experimental procedures and antibody concentrations were optimised for each protein/antibody.

Results

Radiosensitivity of Du145 and RKO cells transfected with E4-34k-expressing plasmids

In order to assess the effects of E4-34k expression on cellular radiosensitivity, the prostate cancer cell line Du145 was transfected with either an empty vector control (pCI; Promega) or pCMV6.9, which encodes E4-34k under the control of a CMV promoter (11, 21). Clonogenic survival assays were carried out 48hrs post-transfection and cellular radiosensitivity was assessed (Figure 1). The 48hr time point was used as this is when E4-34k has been shown to bind DNA-PK and disrupt V(D)J recombination (11). Over the range of radiation doses used (0-6Gy), expression of E4-34k did not result in significant radiation sensitization when compared to empty vector-transfected or untransfected cells. No difference in radiosensitizing effect was seen at 24hrs or 72hrs post-transfection (data not shown). However, the average plating efficiency of the pCMV6.9-transfected cells was 64 ± 6 % with corresponding transfection efficiencies of 41 ± 8% (mean plating efficiency of untransfected cells was 75 ± 8

%). It is theoretically possible, although unlikely, that the majority of pCMV6.9-transfected cells failed to seed. This could therefore explain why pCMV6.9-transfected cells show the same radiation response as untransfected and pCI-transfected cells.

In order to enrich the transfected population, the E4-34k-encoding sequence was cloned into the multiple cloning site of the plasmid pREV (22) to create the plasmid pREV-E4orf6. This places E4orf6-34k under the control of a CMV promoter with EGFP expression being controlled by a separate CMV promoter. Both CMV promoters within the pREV plasmid are equally active (22, 23). Du145 cells were transfected with either a control plasmid pREV or pREV-E4orf6 and FACS sorted 48 hours post-transfection. Radiosensitivity of FACS sorted cells was then assessed by clonogenic survival (Figure 2). Again, no significant increase in radiosensitivity was observed in cells transfected with pREV-E4orf6 compared to pREV-transfected or untransfected cells. Also, RKO colon carcinoma cells were transfected with the pREV or pREV-E4orf6 (average transfection efficiency of 80% from two repeat experiments) and subjected to clonogenic survival assays 48hrs post-transfection to assess cellular radiosensitivity (Figure 2). Transfected RKO ells were not FACS sorted due to the high transfection efficiency. As with Du145 cells, no increased radiation sensitivity was seen in pREV-E4orf6-transfected RKO cells compared to controls, demonstrating that the result seen in Du145 cells was not cell type specific. Likewise, no E4-34k-mediated radiosensitization was seen in the prostate cancer cell line LNCaP (data not shown).

To confirm that FACS sorted Du145 cells and unsorted RKO cells transfected with pREV-E4orf6 express the E4-34k protein, cytospin preparations and protein extracts were respectively made from a sample of FACS sorted Du145 cells and unsorted transfected RKO cells used for clonogenic survival assays. Cytospins of Du145 cells were immunostained and

RKO extracts were probed by Western blot to determine E4-34k expression (Figure 3). Only Du145 cells transfected with pREV-E4orf6 stained for E4-34k (Figure 3, panel A). Furthermore, it was shown that RKO cells transfected with pREV-E4orf6 produced an expected protein band at 34kDa on Western blots (Figure 3, panel B). Consistent with previous data (11), DNA-PK expression was not altered in cells expressing E4-34k (Figure 3, panel B). Also evident in pREV-E4orf6 transfected RKO cells was a less defined band above 220 kDa, which may be indicative of binding of E4-34k to DNA-PK_{cs} (data not shown). This data confirms that although E4-34k is expressed within transfected cells, it does not modulate cellular radiosensitivity of the prostate cancer cell line Du145 or the colon carcinoma cell line RKO.

Effects on radiosensitivity of E4-34k expression in the presence of E1B-55k

As mentioned previously, the E4orf6 product E4-34k functions as a complex with E1B-55k during stages of adenoviral infection. We therefore were interested to see if expression of E1B-55k is critical for any effects E4-34k may have on attenuation of DNA-PK_{cs} function and subsequent modulation of radiation response. We therefore repeated the procedure outlined in figure 1 but used the transformed human embryonic kidney (HEK) cell line 293 which constituatively expresses high levels of the adenoviral E1B-55k protein (27). HEK 293 cells were transfected with either pCI or pCMV6.9 and clonogenic survival was carried out 48hrs post-transfection (Figure 4). No modulation of cellular radiosensitivity was observed in pCMV6.9-transfected cells compared to either pCI-transfected or untransfected cells. However, it must be noted that the plating efficiency of pCMV6.9-transfected cells was 27% with a corresponding transfection efficiency of 22%. It is therefore possible that all transfected cells did not seed which would account for similarity of the survival curves between pCMV6.9 transfected and pCI or untransfected cells.

Because the transfection procedure was relatively toxic to 293 cells we further attempted to assess the effects of E4-34k expression on DNA-PK in the presence of E1B-55k by co-transfecting Du145 cells (which have higher plating and transfection efficiencies compared to 293 cells) with the E4-34k expressing plasmid pCMV6.9 and with the E1B-55k expressing plasmid pCMV-55k (21). Clonogenic survival was then assessed 48hrs post-transfection (Figure 5). There was no significant increase in radiosensitivity of cells transfected with pCMV6.9 or pCMV-55k alone or together compared to empty vector-transfected and untransfected cells. However, as with the studies on 293 cells, the plating efficiency of pCMV6.9 + pCMV-55k co-transfected cells was drastically lower compared to untransfected cells or cells transfected with either of the plasmids alone (transfection efficiency = 35 ± 10% with corresponding plating efficiency of 26 ± 11%). This increased toxicity was evident by a high number of detached cells present within the cultures 48hrs post-transfection. Similarly, a high level of expression of E4-34k in 293 cells appears toxic (see above). This is consistent with the finding that it is extremely difficult to produce 293 cell lines with stably integrated E4orf6 (Ketner *et al*, unpublished data).

Discussion

In an attempt to modify cellular radiosensitivity by specifically targeting the DNA double-strand break repair pathway, we have exogenously delivered adenovirus E4-34k-encoding plasmids into cultured cells as a means of attenuating DNA-PK_{cs} function. Transient transfections were used for all experiments for two main reasons; firstly, if such an approach is to be made applicable to a clinical gene therapy situation then the effect of E4-34k expression on radiation response in stable cell lines would not be as relevant. Secondly, we and others

have previously shown that stable integration of exogenous DNA gives both varying amounts of protein expression and clonal variation as much as 1 log of cell kill difference at 6Gy for RKO cells (28) in radiation survival curves.

Following 48hrs transient transfection of the prostate cancer cell line Du145 with the E4-34k-encoding plasmid pCMV6.9, we showed no difference in radiation response of these populations compared to untransfected or empty vector-transfected cells (Figure 1). Also, no difference in radiosensitivity was seen at 24hrs or 72hrs post-transfection (data not shown). Similar results were obtained using transiently transfected RKO colorectal tumour cells (Figure 2) and LNCaP prostate cancer cells (data not shown), which shows that this finding was not cell type specific. Enrichment of the transfected population using FACS sorting of pREV-E4orf6 transfected Du145 cells gave similar results (Figure 2), thus demonstrating the inability of transiently-transfected E4-34k-encoding plasmids to modulate radiation response was not simply due to a loss of transfected cells within the mixed population. Immunohistochemical and Western blot analyses carried out respectively on FACS sorted Du145 cells and unsorted RKO cells clearly showed that transfected cells expressed relatively high levels of E4-34k (Figure 3). Interestingly, the E4-34k antisera used for Western blots also bound to a protein product greater that 220kDa which may be indicative of E4-34k binding to DNA-PK_{cs} (data not shown).

During viral infection, E4-34k binds with E1B-55k (1-3, 5-7), thus we were interested to see if the E4-34k binding partner E1B-55k could augment any E4-34k-mediated modulation of radiation response. Using pCMV6.9-transfected 293 cells which constituatively express E1B-55k and co-transfecting E4-34k and E1B-55k-encoding plasmids into Du145 cells, we showed no significant difference in radiosensitivity compared with cells transfected with either an

empty plasmid, with each plasmid alone or untransfected cells (Figures 4 & 5). It must be noted that due to the high toxicity observed from the combined expression of these proteins, the survival curves shown in figures 4 and 5 may not represent the radiation response of the transiently transfected cell population within these experiments.

The lack of E4-34k-mediated modulation of radiation response may initially seem surprising as previous work has shown that E4-34k interacts with DNA-PK_{cs} and attenuates V(D)J recombination (11) would expect that this interaction would also have a similar inhibitory effect on DNA-PK_{cs}-mediated dsb repair. However, Boyer *et al.* (11) also reported that the interaction between E4-34k and DNA-PK_{cs} did not lead to decreased DNA-PK_{cs} kinase activity, which is essential for the re-joining of DNA strands (29, 30). This may explain why the interaction between E4-34k and DNA-PK_{cs} does not increase cellular sensitivity to radiation. How E4-34k can specifically inhibit the V(D)J recombination activity of DNA-PK_{cs} without affecting the repair of radiation-mediated DNA dsb repair is presently not understood. One possibility is that interaction between E4-34k and DNA-PK_{cs} physically prevents DNA-PK_{cs} interacting with other factors essential for V(D)J recombination without affecting its association with single and double-stranded DNA, which is believed to be important in initiating its kinase activity (31). The recent elucidation of the protein structures of both DNA-PK_{cs} and E4-34k may aid the study of such an interaction (31, 32, 33).

In summary, the expression of the adenovirus E4orf6 protein product E4-34k does not modulate the cellular response to ionising radiation of the prostate cancer cell lines Du145 and LNCaP (data not shown), colorectal tumour cell line RKO or the transformed human embryonic kidney cell line 293. We also report that the co-expression of E1B-55k did not alter radiation sensitivity within these cells, although this was somewhat difficult to assess due to

the high toxicity resulting from the expression of these two proteins. Previous data has shown that E4-34k interacts with DNA-PK_{cs} leading to attenuation of V(D)J recombination (11). Thus, the data presented here extends this work and suggests that the dsb repair and V(D)J recombination functions of DNA-PK_{cs} may be individually targeted.

References

1. Dobner T, Horikoshi N, Rubenwolf S, *et al.* Blockage by adenovirus E4orf6 of transcriptional activation by the p53 tumor suppressor. *Science* 1996;272 (5267):1470-1473.

2. Querido E, Marcellus RC, Lai A, *et al.* Regulation of p53 levels by the E1B 55-kilodalton protein and E4orf6 in adenovirus-infected cells. *J Virol* 1997;71 (5):3788-3798.

3. Steegenga WT, Riteco N, Jochemsen AG, *et al.* The large E1B protein together with the E4orf6 protein target p53 for active degradation in adenovirus infected cells. *Oncogene* 1998;16 (3):349-357.

4. Debbas M & White E. Wild-type p53 mediates apoptosis by E1A, which is inhibited by E1B. *Genes Dev* 1993;7 (4):546-554.

5. Bridge E. & Ketner G. Interaction of adenoviral E4 and E1b products in late gene expression. *Virology* 1990;174 (2):345-353.

6. Dobbelstein M., Roth J, Kimberly WT, *et al.* Nuclear export of the E1B 55-kDa and E4 34-kDa adenoviral oncoproteins mediated by a rev-like signal sequence. *EMBO J* 1997;16 (14):4276-4284.

7. Weigel S & Dobbelstein M The nuclear export signal within the E4orf6 protein of adenovirus type 5 supports virus replicationand cytoplasmic accumulation of viral mRNA. *J Virol* 2000;74 (2):764-772.

8. Gottlieb TM. & Jackson SP The DNA-dependent protein kinase: requirement for DNA ends and association with Ku antigen. *Cell* 1993;72 (1):131-142.

9. Finnie NJ, Gottlieb TM, Blunt T, *et al.* DNA-dependent protein kinase defects are linked to deficiencies in DNA repair and V(D)J recombination. *Philos Trans R Soc Lond B Biol Sci* 1996;351 (1336):173-179.

10. Jackson SP. DNA-dependent protein kinase. *Int J Biochem Cell Biol* 1997;29 (7): 935-938.

11. Boyer J, Rohleder K & Ketner G. Adenovirus E4 34k and E4 11k inhibit double strand break repair and are physically associated with the cellular DNA-dependent protein kinase. *Virology* 1999;263 (2):307-312.

12. Woo RA., McLure KG, Lees-Miller SP, *et al.* DNA-dependent protein kinase acts upstream of p53 in response to DNA damage. *Nature* 1998;394 (6694):700-704.

13. Blunt T, Finnie NJ, Taccioli GE, *et al.* Defective DNA-dependent protein kinase activity is linked to V(D)J recombination and DNA repair defects associated with the murine scid mutation. *Cell* 1995;80 (5):813-823.

14. Taccioli GE, Amatucci AG, Beamish HJ, *et al.* Targeted disruption of the catalytic subunit of the DNA-PK gene in mice confers severe combined immunodeficiency and radiosensitivity. *Immunity* 1998;9 (3):355-366.

15. Chernikova SB, Wells RL. & Elkind MM. Wortmannin sensitizes mammalian cells to radiation by inhibiting the DNA-dependent protein kinase-mediated rejoining of double-strand breaks. *Radiat Res.* 1999;151 (2):159-166.

16. Caldecott K & Jeggo P. Cross-sensitivity of gamma-ray-sensitive hamster mutants to cross-linking agents. *Mut Res* 1991;255 (2):111-121.

17. Muller C, Christodoulopoulos G, Salles B, *et al.* DNA-dependent protein kinase activity correlates with clinical in vitro sensitivity of chronic lymphocytic leukemia lymphocytes to nitrogen mustards. *Am Soc Hematol* 1998;92 (7):2213-2219.

18. Damia G, Silvestri S, Carrassa L, *et al.* Unique patter of ET-743 activity in different cellular systems with defined deficiencies in DNA-repair pathways. *Int J Cancer* 2001;92 (4):583-588.

19. Achanta G, Pelicano H, Feng L, *et al.* Interaction of p53 and DNA-PK in response to nucleoside analogues: Potential role as a sensor complex for DNA damage. *Cancer Res* 2001;61 (24):8723-8729.

20. van Putten JWG, Groen HJM, Smid K, *et al*, End-joining deficiency and radiosensitization induced by gemcitabine. *CancerRes* 2001;61 (4):1585-1591.

21. Boyer JL & Ketner G. Genetic analysis of a potential zinc-binding domain of the adenovirus E4 34k protein. *J Biol Chem* 2000;275 (20):14969-14978.

22. Collis SJ, Tighe A, Scott SD, *et al*, Ribozyme minigene-mediated RAD51 down-regulation increases radiosensitivity of human prostate cancer cells. *Nucleic Acids Res* 2001;29 (7):1534-1538.

23. Collis SJ, Sangar VK, Tighe A, *et al*, Development of a novel rapid assay to assess the fidelity of double-strand break repair in human tumour cells. *Nucleic Acids Res* 2002;30 (2): E1-E1.

24. DeWeese TL, Shipman JM, Dillehay LE, *et al*, Sensitivity of human prostatic carcinoma cell lines to low dose rate radiation exposure. *J Urol* 1998;159 (2):591-598.

25. Boivin D, Morrison MR, Marcellus RC, *et al*, Analysis of synthesis, stability, phosphorylation, and interacting polypeptides of the 34-kilodalton product of open reading frame 6 of the early region 4 protein of human adenovirus type 5. *J Virol* 1999;73 (2):1245-1253.

26. DeWeese TL, van der Poel H, Li S, *et al*, A phase I trial of CV706, a replication-competent, PSA selective oncolytic adenovirus, for the treatment of locally recurrent prostate cancer following radiation therapy. *Cancer Res* 2001;61(20): 7464-7472.

27. Graham FL, Smiley J, Russell WC, *et al*, Characteristics of a human cell line transformed by DNA from human adenovirus type 5. *J Gen Virol* 1977;36 (1):59-74.

28. DeWeese TL, Walsh JC, Dillehay LE, *et al*, Human papillomavirus E6 and E7 oncoproteins alter cell cycle progression but not radiosensitivity of carcinoma cells treated with low-dose-rate radiation. *Int J Radiat Biol Phys* 1997;37 (1):145-154.

29. Kurimasa A, Kumano S, Boubnov NV, *et al*, Requirement for the kinase activity of human DNA-dependent protein kinase catalytic subunit in DNA strand break rejoining. *Mol Cell Biol* 1999;19 (5):3877-3884.

30. Kienker LJ, Shin EK & Meek K Both V(D)J recombination and radioresistance require DNA-PK kinase activity, though minimal levels suffice for V(D)J recombination. *Nucleic Acids Res* 2000;28 (14):2752-2761.

31. Leuther KK, Hammarsten O, Kornberg RD, *et al*, Structure of DNA-dependent protein kinase: implications for its regulation by DNA. *EMBO J* 1999;18 (5):1114-1123.

32. Fujimori A, Araki R, Fukumura R, *et al*, Identification of four highly conserved regions in DNA-PKcs. *Immunogenetics* 2000;51 (11):965-973.

33. Brown LM, Gonzalez RA, Novotny J, *et al*, Structure of the adenovirus E4 Orf6 protein predicted by fold recognition and comparative protein modeling. *Proteins* 2001;44 (2):97-109.

Figure legends

Figure 1. Clonogenic survival curves for Du145 cells 48 hrs post-transfection. Each survival curve represents the mean of three independent experiments. Transfection efficiencies were obtained for each experiment using identical cell populations transfected with a construct (pREV) encoding EGFP under the control of a CMV promoter and analyzed by FACS. The mean transfection efficiency of pCMV6.9-transfected cells for the three experiments was 41 ± 8 %.

Figure 2. Clonogenic survival of transiently transfected RKO cells and FACS sorted transfected Du145 cells. RKO transfection efficiencies for pREV and pREV-E4orf6 were 80% (average of two repeat experiments). Both pREV and pREV-E4orf6-transfected cells were FACS sorted 48 hrs post-transfection. Untransfected cells were run through the FACS machine and collected using the same procedure.

Figure 3. Immunohistochemical and Western blot analyses for E4-34k expression in FACS-sorted transfected Du145 cells and transiently transfected RKO cells respectively. A; Stained cytospin preparations of untransfected, pREV transfected, pREV-E4orf6 transfected; no primary antibody added, or pREV-E4orf6 transfected; primary antibody added. FACS-sorted Du145 cells visualized at x400 magnification. All cells viewed at x400 magnification. B; Western blots of transiently transfected RKO cells probed for DNA-PK_{cs}, E4-34k and Actin expression (loading control). Lanes: 1; untransfected, 2; pREV, 3; pREV-orf6. Only Du145 and RKO cells transfected with pREV-E4orf6 express E4-34k.

Figure 4. Clonogenic survival curves for 293 cells 48 hrs post-transfection. Transfection efficiency for pCMV6.9 transfected cells was 22 ± 1 %. With a corresponding plating efficiency of 27 %.

Figure 5. Clonogenic survival curves for Du145 cells 48 hrs post-transfection. Each survival curve represents the mean of two independent experiments. The mean transfection efficiency of pCMV6.9 + pCMV-55k transfected cells for the two experiments was 35 ± 10 % with a corresponding plating efficiency of 26 ± 11 %. The plating efficiency of untransfected cells was 70 ± 12.

Figure 1

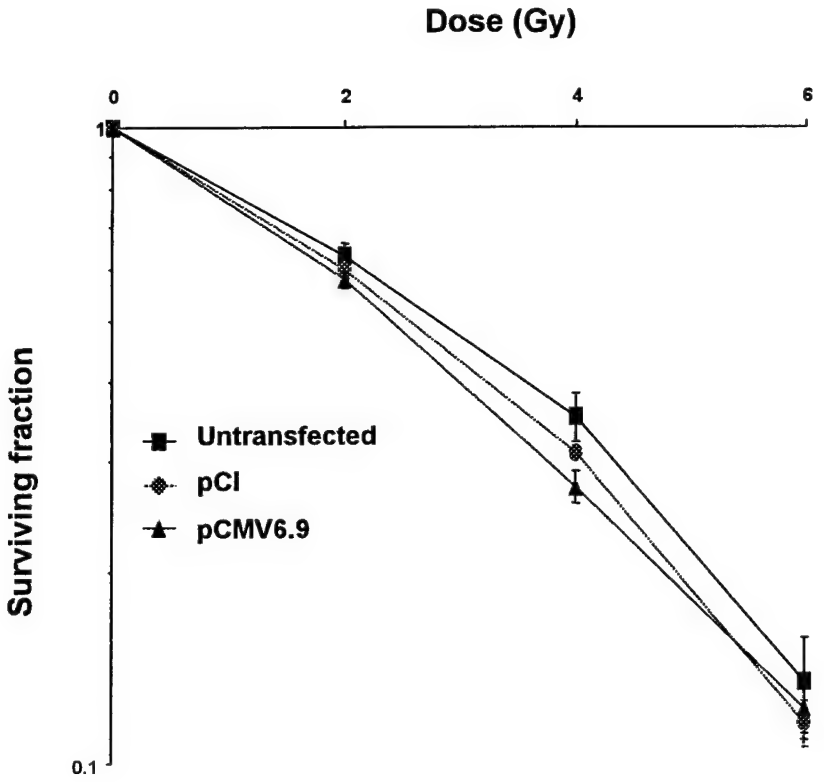
Dose (Gy)
0
2
4
6
1
0.1
Surviving fraction
Untransfected
pCI
pCMV6.9

Figure 2

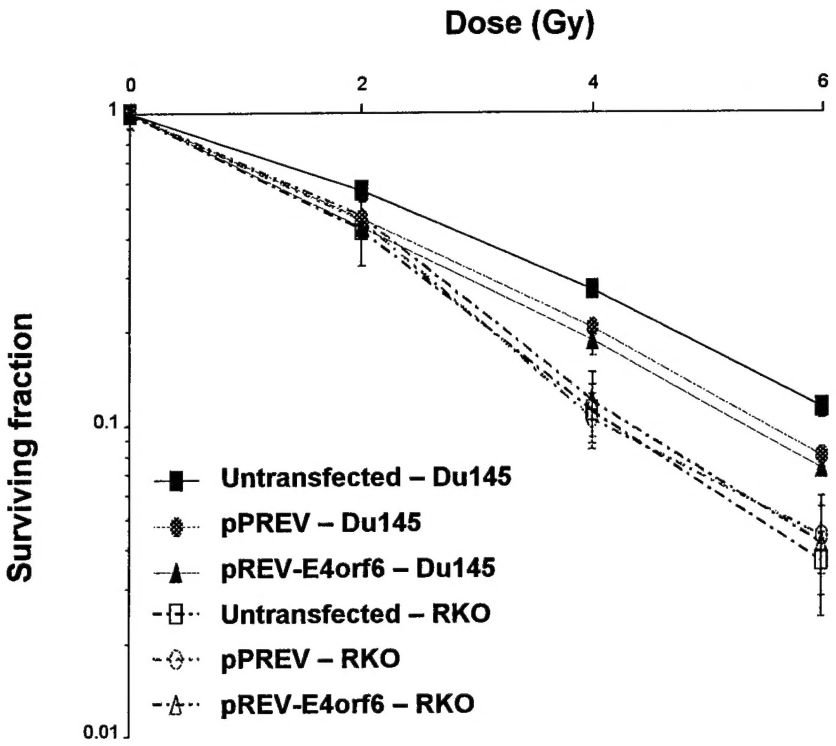
Dose (Gy)
0
2
4
6
1
0.1
0.01
Surviving fraction
Untransfected – Du145
pPREV – Du145
pREV-E4orf6 – Du145
Untransfected – RKO
pPREV – RKO
pREV-E4orf6 – RKO

Figure 3

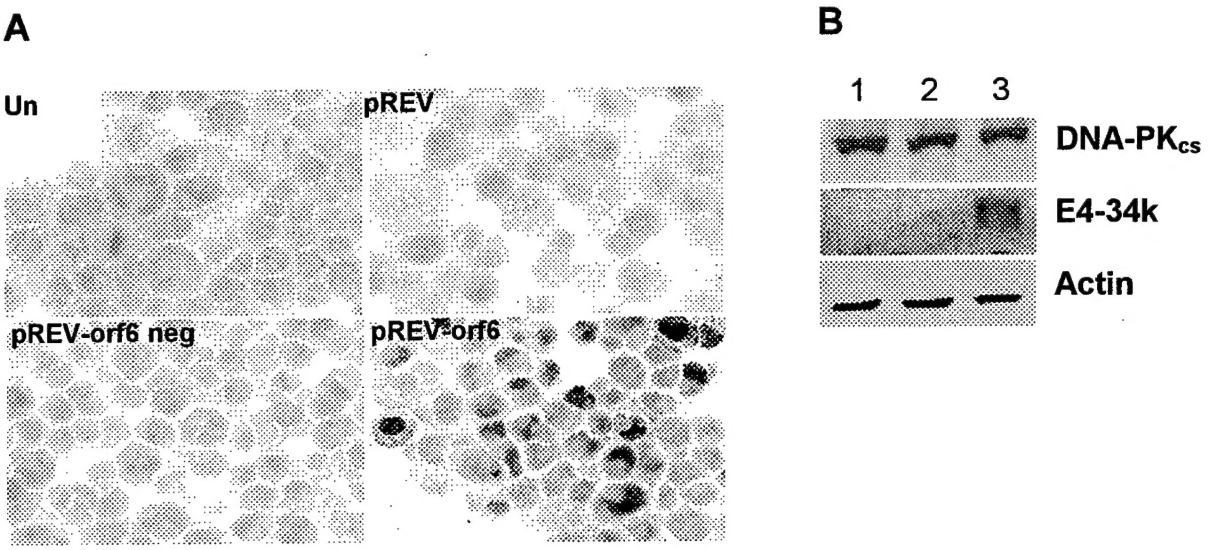

Figure 4

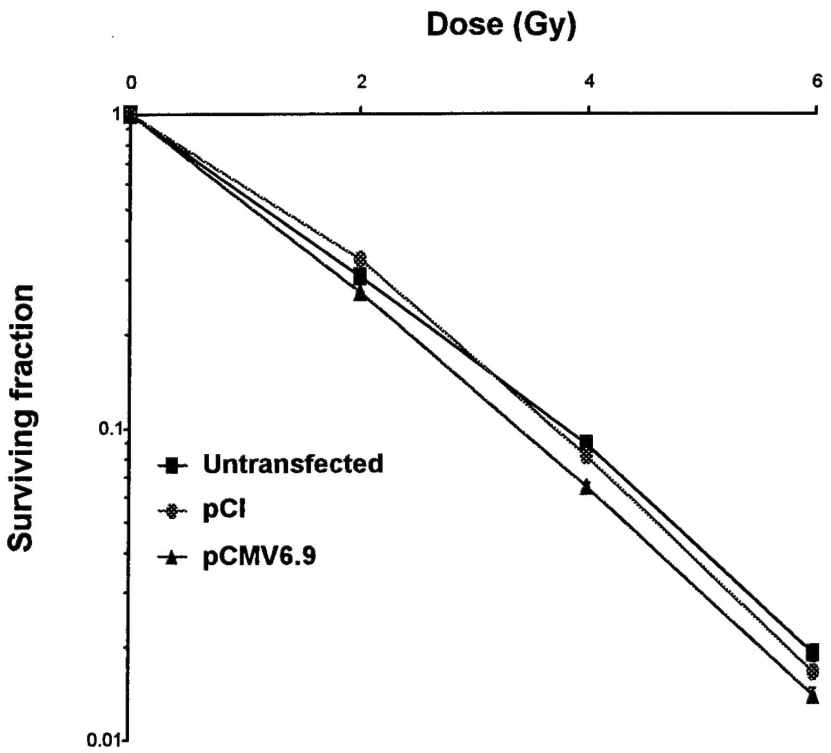
Dose (Gy)
0
2
4
6
1
0.1
0.01
Surviving fraction
Untransfected
pCI
pCMV6.9

Figure 5

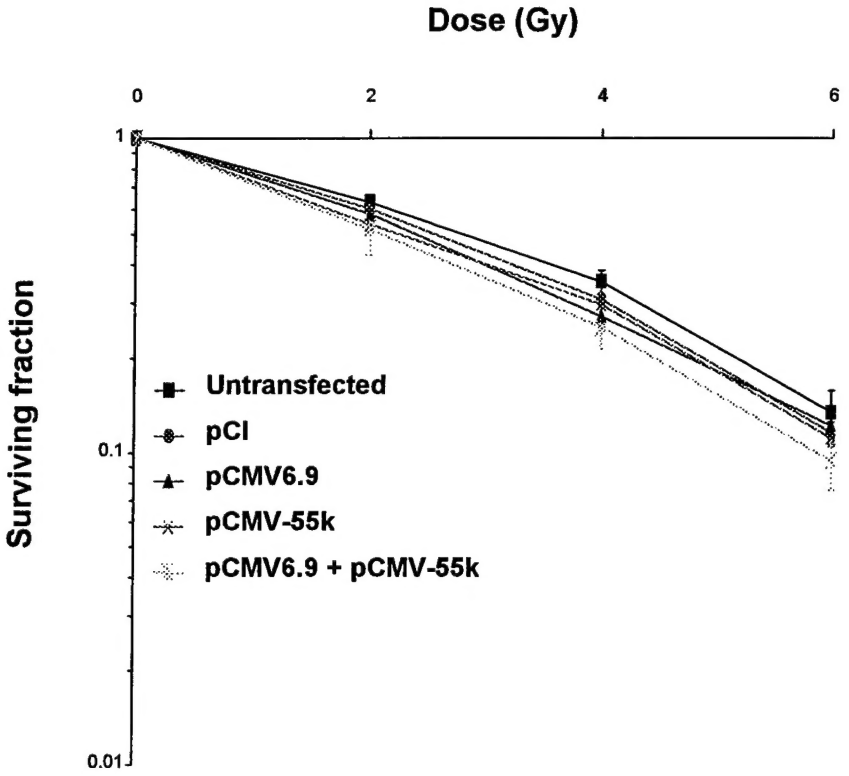
Dose (Gy)
0
2
4
6
1
0.1
0.01
Surviving fraction
Untransfected
pCI
pCMV6.9
pCMV-55k
pCMV6.9 + pCMV-55k